



Universidad de Burgos

ESCUELA POLITÉCNICA SUPERIOR

DEPARTAMENTO DE CONSTRUCCIONES ARQUITECTÓNICAS E  
INGENIERÍA DE LA CONSTRUCCIÓN Y DEL TERRENO

## TESIS DOCTORAL

# Addition of new polymer-based and mineral-based fillers in mortar: influences of polyurethane and afwillite on the microstructure and final properties

Burgos, 2017

AUTOR A:  
Raquel Arroyo Sanz

DIRECTOR AS:  
Dra. Verónica Calderón Carpintero  
Dra. Sara Gutiérrez González  
TUTOR EMPRESARIAL:  
Matthieu Hognies





**Dña. Verónica Calderón Carpintero**, Profesora Doctora y **Dña. Sara Gutiérrez González**, Profesora Doctora, del Área de Construcciones Arquitectónicas del Departamento de Construcciones Arquitectónicas e Ingeniería de la Construcción y del Terreno de la Escuela Politécnica Superior de la Universidad de Burgos,

**INFORMAN DE:**

Que la presente Memoria titulada "**Addition of new polymer-based and mineral-based fillers in mortar: influences of polyurethane and afwillite on the microstructure and final properties**" se ha realizado en el Departamento de Construcciones Arquitectónicas e Ingeniería de la Construcción y del Terreno de la Universidad de Burgos, bajo su dirección, y en el Departamento Innovación Group del Centro de Investigación de Lafarge Holcim R&D en Saint Quentin-Fallavier en Lyon, Francia, por la Ingeniera de Caminos, Canales y Puertos Dña. **Raquel Arroyo Sanz** y autorizan su presentación para que sea calificada como TESIS DOCTORAL.

Burgos, Junio de 2017

Fdo.: Dra. Verónica Calderón  
Carpintero

Fdo.: Dra. Sara Gutiérrez  
González



A Alfonso, Carlota y Alfonso

A mi madre y mis hermanas



# Agradecimientos

---

Gracias a todo el equipo del departamento de Construcciones Arquitectónicas de la Universidad de Burgos, sobre todo a Verónica y Sara.

A todo el equipo del Centre de Reserche de LafargeHolcim, al Innovation Group, a Matthieu y a los compañeros de Lafarge.

A toda mi familia, en especial a mi marido, a mi madre y a mis hermanas.

Muchas gracias a todos.



## Resumen

---

El hormigón es el material manufacturado más utilizado en la Tierra. Con la ayuda de cementos hidráulicos a base de clinker de cemento Portland, mezclados con áridos gruesos, finos y agua, se pueden moldear de la manera deseada, procediendo a un proceso de fraguado y curado posterior.

Por otro lado, y acorde con la política europea de reducir la cantidad de plásticos y polímeros que se depositan en vertederos, la inclusión de compuestos tales como residuos de espuma de poliuretano como material reciclado y reutilizable en sustitución de cantidades variables de áridos es de gran interés en la producción de nuevos materiales de construcción debido a sus características físicas y químicas. Con la intención de eliminar la limitación de resistencia mecánica derivada del empleo de polímero, y en un intento de ir más lejos en este campo de investigación, se han modificado las propiedades químicas de los aglutinantes con tensioactivos no iónicos que aumentan el efecto sobre la hidratación del clínker. Esta alteración produce un cambio importante en la resistencia mecánica para lograr materiales estructurales reciclados con una baja densidad con respecto a los morteros ligeros convencionales. Además, estos aditivos mejoran otras propiedades incluyendo la trabajabilidad, compactación de la matriz, evitan la disgregación de las partículas de poliuretano y ayudan a mejorar las resistencias mecánicas a la flexión, compresión, ductilidad, resistencia térmica y durabilidad frente a agentes como el fuego para reforzar los materiales. Se consideran productos con capacidades estructurales ya que las resistencias a compresión son mayores en los morteros con sustitución de árido por poliuretano y surfactantes que en los materiales de referencia, llegando a alcanzar valores mayores a 30 MPa, pero con la ventaja añadida de tener densidades mucho menores.

Sin embargo, los morteros y hormigones son propensos a agrietarse debido en gran parte a la fragilidad de la pasta de cemento la cual pierde agua por evaporación. Este efecto se hace más evidente en este tipo de morteros reciclados, donde el requerimiento de agua por la presencia de poliuretano es mayor de lo habitual debido al carácter hidrofóbico del residuo. Aunque a menudo es simplemente un efecto estético, puede afectar a la durabilidad estructural del material.

Esta retracción puede limitarse al menos de dos maneras diferentes, ya sea añadiendo aditivos que disminuyen la tensión superficial del agua, o reduciendo el volumen de poros pequeños. El trabajo presentado se centra en el segundo enfoque, que implica la modificación de la hidratación del cemento a través de los poros más pequeños.

La principal fase de unión en prácticamente todos los morteros y hormigones es el silicato de calcio amorfó altamente nanoporoso, de composición variable, denominada gel C-S-H. La porosidad más pequeña siempre viene dada por los nanoporos en este gel, que producen una retracción de secado relativamente alta. Así que una forma de abordar este problema, consiste en formar diferentes hidratos con una porosidad inherentemente mucho menos ultrafina. Esto se consigue a partir del empleo de fases cristalinas de afwillita ( $\text{Ca}_3(\text{SiO}_3\text{OH})_2 \cdot 2\text{H}_2\text{O}$ ; o en su forma oxidada  $(\text{C}_3\text{S}_2\text{H}_3)$ , cuya obtención se ha optimizado en un proceso de siembra y posterior implantación, en proporción de 1% a 4% en peso respecto a pastas puras de  $\text{C}_3\text{S}$ . Los superplastificantes comerciales a base de poliacrilato permiten que las pastas requieran una relación agua/pasta baja.

Se siembran pastas de  $\text{C}_3\text{S}$  con semillas de afwillita para comprobar, mediante diferentes métodos de caracterización, el aumento de la tasa de afwillita con el tiempo. Se estudian las propiedades de las pastas sembradas para llegar a la conclusión de que la afwillita acelera de forma significativa la tasa de hidratación, aumenta en gran medida la porosidad total y el tamaño medio de poro, tiende a reducir la resistencia a compresión a 28 días y reduce la retracción por secado en 2,5 veces empleando una relación agua/ $\text{C}_3\text{S}$  de 0,5.

Por último se analiza la viabilidad del uso de estos morteros en construcción, considerando que los morteros aligerados con propiedades estructurales son una buena opción y aptos para su uso en edificación.

# Abstract

---

Concrete is the most widely used material in the world. With the help of hydraulic cements based on Portland cement clinker, mixed with coarse aggregate, fines and water, it may be molded as desired, before it undergoes a setting process and subsequent curing.

Moreover, in line with European policy, to reduce the amount of plastics and polymers that are dumped in landfill sites, the inclusion of compounds such as polymer foam waste as a recycled and reusable material in substitution of variable amounts of aggregate is of great interest in the production of new construction materials, due to their physical and chemical properties.

With the intention of eliminating the limitation of mechanical strength arising from the use of polymers, and in an effort to study this field of investigation in greater depth, the chemical properties of the binders were modified with non-ionic surfactants that increased the effect on the hydration of the clinker. This alteration produced an important change in mechanical strength to achieve recycled structural materials of low density with regard to lightweight conventional mortars. In addition, these additives improved other properties including workability, compaction of the matrix, and avoided polyurethane particle disaggregation, helping to improve the mechanical strength of the matrix under flexion, compression, ductility, thermal strength and durability, reinforcing the materials against such agents as fire. They are considered products with structural capabilities, because the compressive strengths in the mortars containing polyurethane and surfactants in substitution of fines were higher than the values of over 30 MPa reached by the reference materials, but with the added advantage of much lower densities.

However, mortars and concretes are susceptible to cracking due in great part to the fragility of the cement paste. This fragility is due to shrinkage that occurs within the cement paste, because water is lost by evaporation, and especially so in these recycled mortars, where the need for water due to the presence of polyurethane is higher than usual, due to the hydrophobic properties of the waste. Although simply an esthetic effect, it can affect the structural durability of the material.

Drying shrinkage can be reduced in at least two different ways, either by adding additives that reduce the surface tension of the water, or by reducing the volume of small pores. The work presented in this thesis centers on the second approach, which implies the modification, through the smallest pores sizes, of the hydration process of the cement.

The physical bonds in the principal binding phase of practically all mortars and concretes, known as C-S-H gels, are highly nanoporous amorphous calcium silicates, of variable compositions. The smallest porosity is always given by the nanopores of this gel, which produces a relatively high drying shrinkage. Thus, one way of approaching this problem consists in forming different hydrates with a porosity that is inherently far less ultrafine. This objective is achieved in this study by using crystalline phases of afwillite ( $\text{Ca}_3(\text{SiO}_3\text{OH})_2 \cdot 2\text{H}_2\text{O}$ ; or in its oxidized form ( $\text{C}_3\text{S}_2\text{H}_3$ ), the production of which was optimized in a seeding process and subsequent addition of the seeds, in proportions of 1% to 4% in weight with regard to pure pastes of  $\text{C}_3\text{S}$ . Commercial superplasticizers based on polyacrylate give the pastes a low water/paste ratio.

$\text{C}_3\text{S}$  pastes were seeded with afwillite to confirm (through different characterization methods) the increase in the afwillite growth rate over time. The properties of the seeded pastes were studied to arrive at the conclusion that afwillite accelerates the hydration rate in a significant way, increasing total porosity and the average pore size to a great extent, and tending to reduce the compressive strength at 28 days and to reduce the drying shrinkage by 2.5 times employing a water/ $\text{C}_3\text{S}$  ratio of 0.5.

Finally, the viability of the use of these construction mortars was analyzed, considering that the light-weight mortars with structural properties are a good option and suitable for use in building.



# Índice

<b>Chapter 1. Introduction .....</b>	<b>1</b>
1.1 Background .....	3
1.2 Polyurethane foam wastes.....	6
1.3 Recycled lightweight polyurethane materials foam wastes .....	9
1.4 New additives and fillers to improve the properties of ightweight polymer mortars .....	18
<b>Capítulo 2. Objetivos .....</b>	<b>23</b>
2.1 Objetivos generales .....	25
2.2 Objetivos específicos .....	25
<b>Chapter 3. Use of C<sub>3</sub>S paste as a model to add afwillite-based filler (or seeds).....</b>	<b>29</b>
3.1. Introduction .....	31
3.2. Synthesis of afwillite germs using C <sub>3</sub> S-based slurries.....	32
3.2.1. Preparation of the germs specimens .....	32
3.2.2. Granulometry Blaine of C <sub>3</sub> S.....	34
3.2.3. Superplasticizer-based admixtures .....	35
3.2.4. "Pre-seeding" of C <sub>3</sub> S slurry with afwillite germs .....	35
3.2.5. Combine afwillite-based germ pre-seeding and superplasticizer.....	35
3.2.6. Influences of granulometry, balls/C <sub>3</sub> S weight ratio and ball-mill hydration time .....	36
3.2.7. Influence of the superplasticizer-based admixtures .....	38
3.2.8. Seeding of C <sub>3</sub> S slurry with afwillite germs.....	39
3.2.9. Seeding of C <sub>3</sub> S slurry with afwillite germs and superplasticizer.....	42
3.3. Microstructure of C <sub>3</sub> S pastes seeded with afwillite germs .....	44
3.3.1. Preparation of the specimens to investigate microstructural properties .....	44
3.3.2. Growth of afwillite into C <sub>3</sub> S pastes seeded with germs .....	44
3.3.3. Rate oh hydration .....	47

**Chapter 4. Influence of the addition of afwillite on cement paste..... 63**

4.1. Introduction.....	65
4.2 Reactivity of different cement-based diluted slurries .....	66
4.2.1 Use of slurry to synthesize afwillite germs: preparation of the specimens .....	66
4.2.2 Granulometry (Blaine) of cements.....	68
4.2.3 Superplasticizer-based admixtures .....	68
4.2.4 "Pre-seeding" of slurry with afwillite germs .....	68
4.2.5 Combine afwillite-based pre-seeding and superplasticizer.....	69
4.2.6 Effects of the type of cement and granulometry(Blaine) ..	69
4.2.7 Influence of the superplasticizer-based admixtures.....	70
4.2.8 Seeding of cement-based slurries with afwillite germs .....	71
4.2.9 Seeding of slurries with afwillite germs and superplasticizer.....	72
4.3 Growth of afwillite in seeded cement-based pastes .....	73
4.3.1 Seeding of cement-based pastes: Preparation of the specimens .....	73
4.3.2 Growth of afwillite in seeded cement-based pastes .....	75
4.4 Growth of afwillite in alite-based diluted slurry and C <sub>3</sub> S/C <sub>3</sub> A pastes..	78
4.4.1 Maximum C <sub>3</sub> A percentage allowable to obtain afwillite	78
4.4.2 Different C <sub>3</sub> S ratios vs amount of afwillite .....	79
4.5 Drying shrinkage properties and porosity of seeded cement pastes.....	80

**Capítulo 5. Obtención y caracterización de morteros aligerados estructurales fabricados con poliuretano reciclado..... 85**

5.1 Introducción.....	88
5.2 Caracterización de las materias primas .....	90
5.2.1 Cemento .....	91
5.2.2 Áridos .....	91
5.2.3 Agua .....	94
5.2.4 Espuma triturada de poliuretano .....	95



5.2.5 Aditivos .....	97
5.3 Dosificación .....	98
5.4 Caracterización en estado fresco y en estado endurecido.....	102
5.4.1 Densidad aparente del mortero fresco .....	102
5.4.2 Determinación del contenido de aire del mortero fresco.....	108
5.4.3 Densidad aparente en seco del mortero endurecido .....	114
5.5 Resistencias mecánicas .....	117
5.5.1 Resistencias mecánicas a flexión .....	117
5.5.2 Resistencias mecánicas a compresión.....	117
5.6. Retracción.....	133
<b>Capítulo 6. Otras propiedades de los morteros aligerados con capacidades estructurales.....</b>	<b>138</b>
6.1 Microscopía electrónica de barrido (SEM) .....	140
6.2 Porosidad .....	148
6.2.1 Porosimetría de intrusión de mercurio (MIP) .....	148
6.2.2 Tomografía axial computerizada (TAC) .....	150
6.3 Termogravimetría .....	153
6.4 Reacción al fuego .....	155
6.5 Carbonatación.....	158
<b>Chapter 7. Conclusions .....</b>	<b>164</b>
<b>Capítulo 8. Lineas futuras de investigación.....</b>	<b>172</b>
<b>Anexo 1. Bibliografía .....</b>	<b>177</b>
<b>Anexo 2. Producción científica .....</b>	<b>190</b>



# **Chapter 1**

---

## **Introduction**





## 1.1 Background

The European Union has introduced management policies oriented toward sustainable development within the framework of the Horizon 2020 plan, with a commitment to the introduction of specific changes, including the reuse and recycling of waste in large amounts.<sup>1</sup> Such attitudes in time become real and favourable economic data referring to the material generation rate, space and cost savings at the warehousing/waste removal stages, reduced demand for natural resource construction materials and the availability of technical support systems which can tackle environmental requirements.<sup>2</sup>

In spite of the uncertainty of the available references and estimations, the world polymer and plastic industry has produced 322 million tonnes of materials in 2015, including thermoplastics and polyurethanes. China is the largest producer with almost 90 million tonnes followed by Europe that reaches 58 million tonnes each year.<sup>3</sup> This field generates significant amounts of waste in the form of different by-products, of which only 7.7 million tons are recycled, 10.2 million tonnes was recovered through recycling and energy recovery processes while landfill is still the first option in many countries. As a rough estimate, polyurethane amount is the 7.7% of the global demand since is manufactured for building insulation, automotive industry, insulating foams for fridges, etc. (Figure 1.1).

---

<sup>1</sup> Communication from the commission to the European Parliament, the Council, the European Economic and Social Committee and the Committee of the Regions. "A resource-efficient Europe – Flagship initiative under the Europe 2020 Strategy".

<sup>2</sup> Directive 2008/98/CE of European Parliament and Council of 19th November 2008 about wastes.

<sup>3</sup> Plastics The facts 2016. An analysis of European plastics production, demand and waste data. Brussels, Belgium.

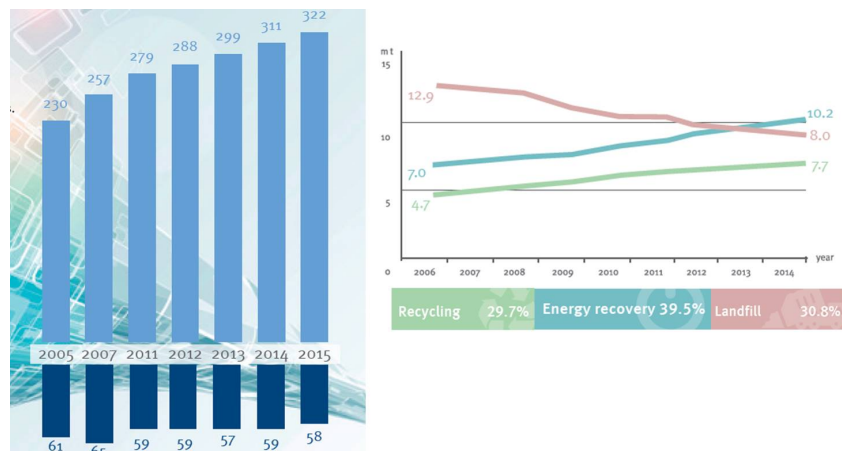


Figure 1.1. Word and Europe plastics production

Following the policy toward zero waste plastic and polymer to landfill by 2025 scenario, the inclusion of compounds such as polymer foam wastes as a recycled and reusable material in substitution of varying amounts of aggregates or fine compounds is therefore of great interest in the production of new materials, because of their physical and chemical characteristics, the reduction of other raw materials, and the energy and water savings. The subsequent study of their properties and the analysis of their stability are fundamental to test the behaviour that these compounds will have over time.

In general, countries with landfill ban (Switzerland, Austria, Netherlands, Germany, Sweden, Luxembourg, Denmark, Belgium and Norway) achieve higher recycling rates recovering more than 90% of plastic waste. An exchange of best practices and the implementation of new manufacturing processes for new materials would help the countries who are further back in this respect to improve their performance. A part of the solution with regard to polymer waste management resides in the fact that society understands that resources should be used efficiently and that the waste generated is a valuable commodity that shouldn't be wasted in landfills. When recycling is not the most viable option, energy recovery is the alternative. (Figure 1.2) Incineration in the recycling of polyurethane wastes is an important way especially for



those who can't use other methods of recycling wastes, but if the combustion process is incomplete, it will produce poisonous gas which seriously polluted the atmospheric.<sup>4</sup>

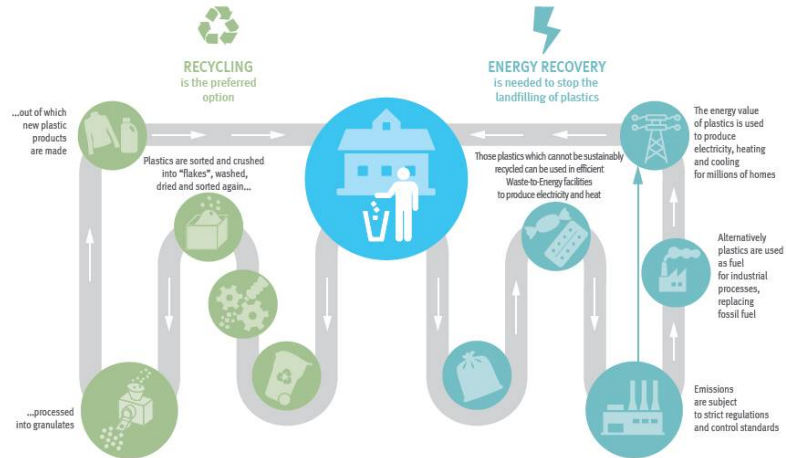


Figure 1.2. Schedule of recycling or energy recovery options

Polyurethane is a lightweight material that is potentially much more flexible and hydrophobic than other traditional lightweight materials, which may be useful to control subsequent water absorption rates.<sup>5</sup> The limitless conformations and formulations of polyurethanes enabled their use in a wide variety of applications. Research studies and tests have resulted in a number of recycling and recovery methods, which are economically and environmentally viable for polymer foam waste.<sup>6,7</sup>

<sup>4</sup> He JJ, Jiang L, JH Suna, Lo S. (2016) Thermal degradation study of pure rigid polyurethane in oxidative and non-oxidative atmospheres. Journal of Analytical and Applied Pyrolysis, 120: 269-283.

<sup>5</sup> Kowalczyk K, Spycharz T, Krala G. (2015) High-build alkyd urethane coating materials with a partially solvolyzed waste polyurethane foam. Polymer Engineering Science, 55: 2174-2183.

<sup>6</sup> Saikia N, de Brito J. (2012) Use of plastic waste as aggregate in cement mortar and concrete preparation: A review. Construction and Building Materials 34: 385-401.

<sup>7</sup> Siddique R, Khati J, Kaur I. (2008) Use of recycled plastic in concrete: A review. Waste Management, 28: 1835-1852.



There are four major categories of recycling, namely, mechanical, chemical and thermomechanical recycling, energy recovery, and product recycling.<sup>8</sup> The research focused on polyurethane mechanical degradation or physical treatment highlights recent attempts to take into account for recycling as a lightweight recycled aggregate in masonry mortars for exterior or interior coating in facades, as interior floor soils, mortar for grouting, coating materials and composite additives. In addition to their fabrication, the viability of these materials has also been investigated in terms of the final properties or the durability. In broad terms, the results allow us to determine the behaviour of the final recycled materials in accordance with the amount of recycled polyurethane incorporated in the mix.

## 1.2 Polyurethane foam wastes

There are two significant ways for recycling polyurethane foam wastes: mechanical physical recycling and chemical recycling.<sup>9</sup> One of the most effective ways to recycle polyurethane foams is to grind foams and to incorporate them into a new material (Figure 1.3). This method is could be performed at the industrial scale, the process does not alter the quality of polyurethane foams and is suitable to treat waste resulting from the disposal of polyurethane products even with a diverse composition, through densities within the range of 20-80kg/m<sup>3</sup>.<sup>10</sup>

Mechanical recycling covers recycling processes to reuse polyurethane without chemically decomposition. The foam must be reduced in the form of powder or chips and then reused in production generally mixed with other binders. The first step in mechanical recycling consists to reduce and homogenize the size of the foam.

---

<sup>8</sup> Weygand E. (1996) "Properties and applications of recycled polyurethanes," in Recycling and Recovery of Plastics, J. Brandrup, M. Bittner, M. Menges, and W. Michaeli, Eds., Hanser, Munich, 683.

<sup>9</sup> Yanga W, Dongb Q, Liu S, Xie H, Liu L, Li J. (2012) Recycling and disposal methods for polyurethane foam wastes. Procedia Environmental Sciences 16:167-175.

<sup>10</sup> Cregut M, Bedas M, Durand MJ, Thouand G. (2013) New insights into polyurethane biodegradation and realistic prospects for the development of a sustainable waste recycling process. Biotechnology Advances, 31:1634-1647.



Figure 1.3. Different PU foam samples after mechanical grinding

Most of the mechanical systems require a shearing effect that breaks the structure of the foam. Mechanical recycling reduces the waste into particles of a few millimetres up to powders. Common systems used for the recycling of polyurethane foams are systems equipped with rotate cylinders at different speeds thus making it possible to break the polyurethane foam. The size of the powder is quite homogeneous because it is sorted in separators. The second stage of mechanical recycling is the reuse of the material in the form of powder. It is often used in the polyurethane industry as inert filler or as a diluent for polyols used to produce new polyurethane foams.

Chemical recycling includes glycolysis, hydrolysis, aminolysis and thermochemical and biodegradation processes. In this case, the objective is to recover the initial raw materials, especially to produce a high-quality recycled polyol usable in a new formulation of polyurethane of the same type. The case of recycling a polyol to obtain polyurethane of another type is scarce. On the other hand, probably the bigger novelty falls on the biodegradation processes.

Degradation in polyurethane after service remains an environmental challenge at the end-of-service life. Biodegradation is the action of microorganisms that causes decomposition of polymeric chains into smaller molecules. Polyurethane, even in the absence of additives, is quite resistant to stresses because of its heterogeneous structure and due



to the nature of its building blocks and their relative ratio. Therefore, this characteristic has conducted to focus on the assessment of its susceptibility to biodegradation.<sup>11</sup>

The ability to upgrade polyurethane wastes to chemical compounds with a higher added value is especially attractive. The results of few studies presented that susceptibility to degradation was nature-dependent and that each part of the morphological structure, possessed also a native divergent susceptibility to a chemical attack.<sup>12</sup>

The biodegradation of polymeric substances is a function of the chemical structure, molecular orientation, crystallinity and the density of cross-linking, and can be induced either by hydrolysis or oxidation reactions from chemical or biochemical origins and involving natural or from other sources.<sup>13,14</sup> Polyurethane degradation action is achieved by a number of glycolysis reagents and catalysts that are generally found to be expressed under various conditions.<sup>15</sup> Along with the fact that different enzymes devoted to biodegradation are found in a variety of microorganisms, the literature proposed that the product of degradation contains mainly the polyol type, and the hydrolysis-susceptible ester bonds.<sup>16</sup>

---

<sup>11</sup> Howard GT, Norton WN, Burks T. (2012) Growth of Acinetobacter generic P7 on polyurethane and the purification and characterization of a polyurethanase enzyme. Biodegradation, 23:561-73

<sup>12</sup> Chevali V, Kandare E. (2016) Rigid biofoam composites as eco-efficient construction materials. Biopolymers and Biotech Admixtures for Eco-Efficient Construction Materials, 275-304.

<sup>13</sup> Oprea S. (2010) Synthesis and properties of polyurethane elastomers with castor oil as crosslinker. Journal of the American Oil Chemists Society, 87, 313-320.

<sup>14</sup> Molero C, de Lucas A, Rodriguez JF. (2008) Influence of the use of recycled polyols obtained by glycolysis on the preparation and physical properties of flexible polyurethane. Journal of Applied Polymer Science, 109:617-626.

<sup>15</sup> Molero C, Mitova V, Troev K, Rodriguez JF. (2010) Kinetics and mechanism of the chemical degradation of flexible polyurethane foam wastes with dimethyl H-phosphonate with different catalysts. Journal of Macromolecular Science, Part A: Pure and Applied Chemistry, 47: 983-990.

<sup>16</sup> Zhu P, Cao ZB, Chen Y, Zhang XJ, GR Qian, Chu YL, Zhou M. (2014) Glycolysis recycling of rigid waste polyurethane foam from refrigerators, Environmental Technology, 35:21, 2676-2684.



## 1.3 Recycled lightweight polyurethane materials foam wastes

The expected advantages of recycled polyurethane compounds, in terms of effectiveness, performance and production costs could contribute to ensure the impact of the final materials. These recycled materials are technically possible, innovative and diverse. If they are used in combination with the correct binders, the final properties are enough regarding traditional products. One interesting property that improves with the addition of crushed polyurethane waste is the thermal conductivity, which increases with respect to the reference material. This property suggests its usefulness as thermal insulation in renderings or prefabricated construction boards. Other works focuses on the potential applications of these materials concerning the age test with the aim of determining their durability through other forms of testing, obtaining similar technical properties than competing non-recycled mortar like low density, enough mechanical strength and fire resistance.

The proposed materials also comply with the principle of obtaining environmentally-friendly materials which contribute to the sustainable development of our surroundings. The research about this topic will allow the knowledge of reusing possibilities of the polyurethane, and the product fine-tuning through the end-users experience will let the replication of the product uptake well beyond the study life-cycle.

### 1.3.1. Recycled lightweight polyurethane plaster materials

One option available to the materials scientist to achieve this objective is the utilization of rigid foams in developing lightweight structures. One of the mechanical recycling options is grinding PU foams into powders allowing them to be reused as fillers in a new plaster material. In recent years, interest has been growing in the use of gypsum as one of the most sustainable mineral binders but is scarce the research carried out taking into account the inclusion of recycled polyurethane in the matrix of plaster composites.<sup>17</sup>

---

<sup>17</sup> Lushnikova N, Dvorkin L. (2016) Sustainability of gypsum products as a construction material, in Sustainability of Construction Materials. Woodhead Publishing Series in Civil and Structural Engineering, 643-681.



Studies made are based on experimental analysis that demonstrates the compatibility of polyurethane with plaster by incorporating different proportions of the recycled polyurethane foam to obtain a new lightweight plaster material with thermal insulating properties.<sup>18</sup> Plaster mixtures are prepared using differing volumes of polyurethane foam waste from different sources and ground to different granulometric sizes.

The characteristics of the specimens in literature are defined and tested by fixing the quantity of water to obtain a good workability and then studying different properties.<sup>19</sup> In accordance with this parameter, the amount of water needed for a suitable consistency increases with the percentage of added foam. This increase in water contributes to the workability time of the samples, not only lengthening it but also improving the time that elapses before the onset of setting. All the results in reference show that the thermal behaviour is correlated with the apparent density values of the material<sup>20</sup> (Table 1.1). The polyurethane quantity decreases the density while increasing its thermal resistance proportionally, which falls by up to 66% relative to the reference material, without polyurethane foam wastes. This property suggests its effectiveness as thermal insulation in renderings and prefabricated plasterboards.

The mechanical strength significantly depends on the density of the material but not of the type of polyurethane waste in use. Therefore, although in principle it might be thought that the foams with finer granulometry could obtain better mechanical properties,<sup>21</sup> the result show that no significant differences between the results obtained. In both cases, a logical decrease in strength is observed as larger percentages of polyurethane foam are replaced.

---

<sup>18</sup> Gutiérrez-González S, Gadea J, Rodríguez A, Junco C, Calderón V. (2012) Lightweight plaster materials with enhanced thermal properties made with polyurethane foam wastes. Construction and Building Materials, 28:653-658.

<sup>19</sup> M del Río M, F. Hernández Olivares. (2004) Lightened blaster: alternative solutions to cellular solids addition. Materiales de Construcción, 54:65-76.

<sup>20</sup> Serhat BM, Kahraman E. (2011) Modifications in the properties of gypsum construction element via addition of expanded macroporous silica granulates. Construction and Building Materials, 25:3327-3333.

<sup>21</sup> Eve S, Gomina M, Hamel J, Orange G. (2006) Investigation of the setting of polyamide fibre/latex-filled plaster composites. Journal of European Ceramic Society, 26:41-46.



Sample	Ration PU/Plaster	Dry density (Kg/m <sup>3</sup> )	Thermal Conductivity (W/m · K)	Flexural strength (MPa)	Compressive strength (MPa)
Plasterwork with perlite	0/1	900	0.1800	---	---
Plasterwork	0/1	1400	0.3000	---	---
Concrete with lightweight fines	--	1800	0.3300	---	---
Y0 (reference)	0/1	1477	0.3057	6.2	15.5
Y0.5G	0.5/1	1323	0.2931	3.8	9.8
Y1G	1/1	1140	0.2626	2.4	6.0
Y2G	2/1	795	0.1828	1.2	2.8
Y3G	3/1	590	0.1105	0.8	1.2
Y4G	4/1	516	0.1014	0.6	0.9
Y0.5W	0.5/1	1258	0.3160	3.9	9.6
Y1W	1/1	1114	0.2701	2.5	6.3
Y2W	2/1	879	0.1861	1.0	2.3
Y3W	3/1	674	0.1285	0.5	1.4
Y4W	4/1	535	0.1039	0.2	1.0

Table 1.1. Density, thermal conductivity and mechanical properties of lightweight plaster materials recycled with different polyurethanes

However, and in accordance with standards, the minimum requirements that should be reached are 1 MPa flexural strength and 2 MPa compressive strength. In view of these results, it may be said that the dosages that satisfy both requirements are materials with ratio PU/plaster 2/1 or lower, despite the considerable volume of polyurethane foam added in all the cases.



Moreover, some studies confirm the reaction to fire of these composites measured with the non-combustibility test confirmed that, taking only into account the contribution of the materials to fire development, its composition tested correspond to Euroclasses A2 (non-combustible) according to European fire reaction classification of building materials for homogeneous products.<sup>22</sup>

### 1.3.2. Recycled lightweight polyurethane mortar materials

Getting the possibility of use polymer foams from industrial waste as a dry aggregate in the modified mortars with cement based materials there are no many basic investigations about this topic either. In all the cases, the manufacture and characterization of quality lightweight mortars has been performed in a simple way, beginning with the progressive elimination of aggregates which were substituted by ground rigid polyurethane foam waste materials or another polymer foam wastes, with a view to finding compound materials that comply with current legislation, attractive for use in industry.<sup>23,24</sup>

The proposed product partially or totally replaces the aggregate with polyurethane foam which has been previously shredded. The incorporation of this waste requires no substantial changes to manufacturing technology, a further advantage. From a similarly economic perspective, there will be important saving in raw materials and in the treatment and elimination of the waste generated in production (Figure 1.4).

---

<sup>22</sup> Alameda L, Calderón V, Junco C, Rodríguez A, Gadea J, Gutiérrez-González S. (2016) Characterization of gypsum plasterboard with polyurethane foam waste reinforced with polypropylene fibers. *Materiales de Construcción*, 66,100.

<sup>23</sup> Ferrández V, Bond T, García-Alcocel E, Cheeseman CR. (2014) Lightweight mortars containing expanded polystyrene and paper sludge ash. *Construction and Building Materials*, 61:285-292.

<sup>24</sup> Bignozzi MC, Saccani A, Sandrolini F. (2000) New polymer mortars containing polymeric wastes. Part 1. Microstructure and mechanical properties. *Composites Part A: Applied Science Manufacturing*, 31 (2): 97-106.

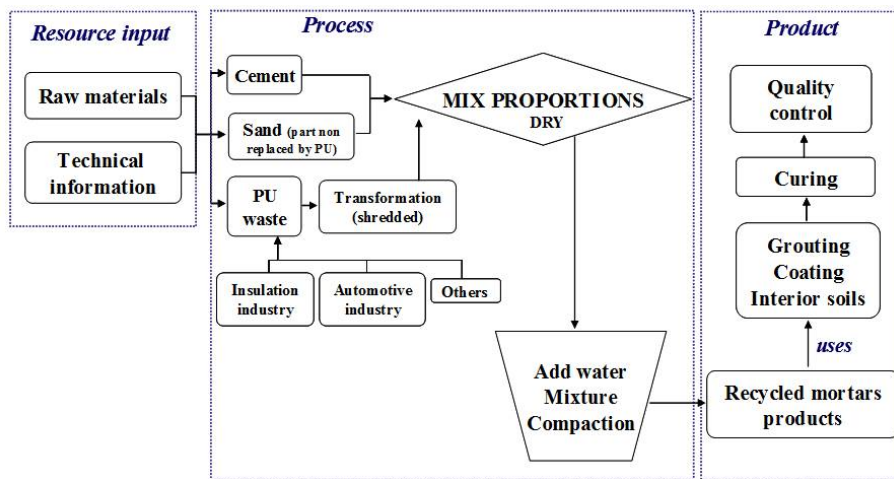


Figure 1.4. Flow charts with the process and fabrication of the recycled lightweight mortar with PU

Based on these premises, the same raw materials that other mortars are normally used (cement, additives and water) with recycled polyurethane with grain size of 0-6 mm used as an aggregate replacing traditional sand, perlite and vermiculite.<sup>25</sup> Like this, we use composites that are also dry aggregates which don't need to be extracted with the environmental impact and also without subsequent processing generally in the form of heating, in order to expand the components make the mortar lighter and with greater insulating characteristics.

Some studies have reported on the positive influence of these recycled aggregates on their manufacture and the determination of stability over time even with respect other traditional aggregates. Previous experiences conduce to think that this polymer is capable of reducing the amount of dry sand used by ranges containing shredded PU foam fractions of 13-33%,<sup>26</sup> or between 25 and 50%<sup>27</sup> and other

<sup>25</sup> Mounanga P, Gbongbon W, Poullain P, Turcry P. (2008) Proportioning and characterization of lightweight concrete mixtures made with rigid polyurethane foam wastes. Cement Concrete Composites, 30: 806-814.

<sup>26</sup> Fraj AB, Kismi M, Mounanga P. (2010) Valorization of coarse rigid polyurethane foam waste in lightweight aggregate concrete. Construction and Building Materials, 24:1069-1077.



authors reach large quantities between 25% and up to 100%,<sup>28</sup> all of them with replacement in volume. The batching depends on the properties of the final product required in each case, obtaining materials more flexible and hydrophobic than other traditional products.

The same works evaluate the durability of these mixtures through various accelerated tests in accordance with current norms. The ageing tests employed to assess the toughness of the recycled mortars are salt spray test, sulphur dioxide testing (Kesternich test), hot water to evaluate the hydrolysis of polymer, freeze cycles and hot dry atmospheres. In all cases, even in the most aggressive standardized tests for the determination of the durability of panels of polyurethane used in construction, it has been confirmed that the mechanical strengths remained practically unaffected with respect to the reference specimens not subjected to any climatic test<sup>29</sup> (Figure 1.5).

The specification of an appropriate plan for the use of these lightweight mortar, a key task for the location of the production; so that in order to test the mortar as a lining element we must define whether this will be indoor lining, intermediate lining, outdoor lining and insulate lining. It is not only technically possible and immediately applicable to introduce the lightweight mortar with polyurethane foam in the construction industry, but also feasible find the requests under currently applicable construction regulations.

---

<sup>27</sup> Kismi M, Mounanga P. (2012) Comparison of short and long-term performances of lightweight aggregate mortars made with polyurethane foam waste and expanded polystyrene beads. MATEC Web of Conferences, 2, article number 02019. Proceedings on 2nd International Seminar on Innovation and Valorization in Civil Engineering and Construction Materials.

<sup>28</sup> Gadea J, Rodríguez A, Campos PL, Garabito J, Calderón V. (2010) Lightweight mortar made with recycled polyurethane foam. Cement Concrete Composites, 32:672-677.

<sup>29</sup> Junco C, Gadea J, Rodríguez A, Gutiérrez-González S, Calderón V. (2012) Durability of lightweight masonry mortars made with white recycled polyurethane foam. Cement Concrete Composites, 34: 1174-1179.

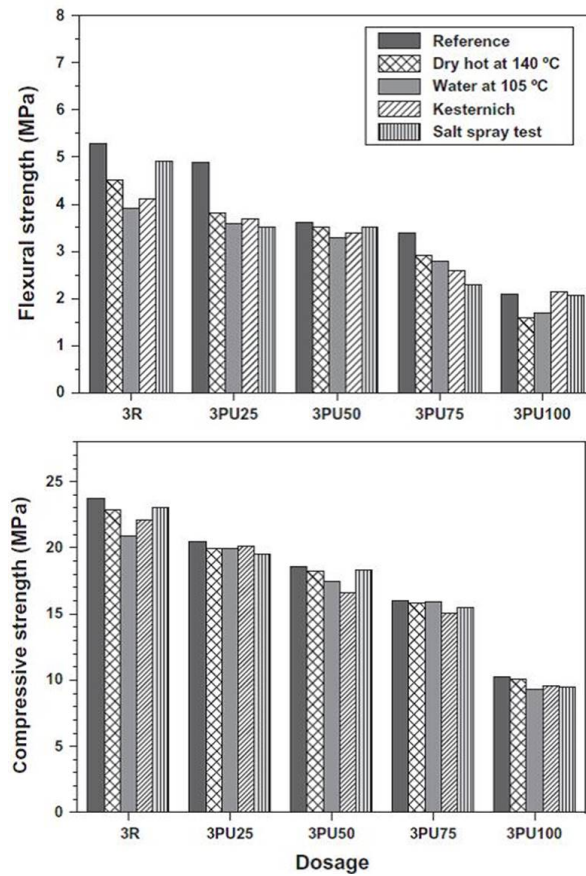


Figure 1.5. Mechanical strength after durability tests of mortars where sand has been replaced by foam from 25% to 100%.

### 1.3.3. Recycled lightweight polyurethane asphalt materials

Road transport is one of the most widely used means of mobility for people and goods. The construction and conservation of this type of infrastructure therefore involves very significant economic costs for various public administrations. Hot bituminous mixtures require large amounts of aggregates and asphalt binders for road surfacing and for other sorts of bituminous surface courses. Hence, investigation into the



use of recycled materials for the manufacture of bituminous surface courses is of great interest from an environmental point of view.<sup>30</sup>

The application of various types of waste materials for modification of asphalts has been successfully used in road pavements, obtaining asphalt-polymeric composites sometimes well-known and regulated.<sup>31,32</sup>

Among the wide variety of waste products that may be used in the preparation of sustainable bituminous mixtures, the use of polymers as recycled raw materials is of great interest for the improvement of these types of waste products and their environmental management.<sup>33</sup> Thermoplastics have dominated in these uses, but nowadays, the literature on the use of polyurethane foam reports good results and have been studied to understand the possibilities to use, but based on manufacture of the polymer in situ, rather than the use of the material as a pre-prepared waste product.

Bitumen source is a significant factor in the advance of new bituminous products, such as dimensionally stable bituminous polyurethane foams, for building applications. Although it is known that PU is not very compatible with bitumen as a consequence of the instability of the resulting system, articles on asphalt-polyurethane composites deal with the practical aspects of obtaining and applying them. The reactions involved in bitumen modification follow by using different techniques, such as thin layer chromatography or Fourier transform infrared spectroscopy. Conclusions involved that rheological properties of foamed bitumen are improved and the degree of enhancement is dependent on bitumen characteristics. Another cases also studied the effect of PU as reactive polymer with functional groups

---

<sup>30</sup> Casey D, McNally C, Gibney A, Gilchrist MD. (2008) Development of a recycled polymer modified binder for use in stone mastic asphalt. Resources Conservation and Recycling, 52:1167-1174.

<sup>31</sup> Poulikakos LD, Papadaskalopoulou C, Hofko B, Gschösser F, Cannone Falchetto A, Bueno M, Arraigada M, Sousa J, Ruiz R, Petit C, Loizidou M, Partl MN. (2017) Harvesting the unexplored potential of European waste materials for road construction. Resources, Conservation and Recycling, 116: 32-44.

<sup>32</sup> Huang Y, Bird RN, Heidrich O. (2007) A review of the use of recycled solid waste materials in asphalt pavements. Resources, Conservation and Recycling, 52: 58-73.

<sup>33</sup> Yildirim Y. (2007) Polymer modified asphalt binders. Construction and Building Materials, 21:66-72.



able to chemically interact with bitumen compounds for obtaining polyurethane modified bitumen<sup>34</sup> (Figure 1.6).



Figure 1.6. Modified bitumen with PU foam wastes

Thus, despite bitumen composition, dimensionally stable bituminous foams can be successfully obtained, even from the softest base<sup>35</sup>. More stable and less deformable bituminous mixtures were obtained with a lower quantity of cavities, which contributes to greater hardness. On the basis of these results, the quantity of foam present in the composition is the most important factor to explain the variation in the subsequent properties of these composites and its advantages against other conventional products.<sup>36</sup>

With the intention to increase the existing scope of knowledge about PU asphalts, further works seem to focus on the potential applications of these mixtures, with the aim of determining their kinetic relationships and durability through other forms of testing, in order to obtain materials with a practical application for road construction's use.

---

<sup>34</sup> Carrera V, Cuadri AA, García-Morales M, Partal P. (2014) Influence of the prepolymer weight and free isocyanate content on the rheology of polyurethane modified bitumens. European Polymer Journal, 57: 151-159.

<sup>35</sup> Izquierdo MA, Navarro FJ, Martínez-Boza FJ, Gallegos C. (2012) Bituminous polyurethane foams for building applications: Influence of bitumen hardness. Construction and Building Materials, 30: 706-713.

<sup>36</sup> Singh B, Gupta M, Kumar L. (2006) Bituminous polyurethane network: preparation, properties and end use. Journal of Applied Polymer Science, 101: 217-226.



## 1.4 New additives and fillers to improve the properties of lightweight polymer mortars

At present, different polymer aggregates are used in mortars with lower densities and better workability, although generally done without substituting sand or cement, which gives rise to higher water/conglomerate ratios than those needed in conventional mortars.<sup>37</sup>

Besides, polymer foam wastes are lightweight materials that are potentially much more flexible and hydrophobic than other traditional lightweight materials, such as perlite, expanded glass or hollow microspheres, which may be useful to control water absorption rates.<sup>38</sup> Other authors reported on the positive influence of aggregates on mortar durability, but the specific references relative to their manufacture and the stability over time of the mix between aggregate and recycled polymer are scarce<sup>6</sup>. In this way, previous studies demonstrated that a high porosity can be strongly related to a low density, worse mechanical properties (such as a low strength), and good thermal insulating properties (such as low thermal conductivity).<sup>39,40</sup> With the intention to enhance the mechanical strengths, many fibres and additives were also used to reinforce the materials.<sup>41</sup> These additions contribute somewhat to the improvement in terms of mechanical or thermal properties, but they show also some drawbacks that need to be studied in a deeper way.

---

<sup>37</sup> Czarnecki C. (2010) Polymer-cement concretes, Cement-Wapno-Beton, 15:63-85.

<sup>38</sup> Ruiz-Herrero JL, Velasco Nieto D, López-Gil A, Arranz A, Fernández A, Lorenzana A, Merino S, De Saja JA, Rodríguez-Pérez MA. (2016) Mechanical and thermal performance of concrete and mortar cellular materials containing plastic waste. Construction Building Materials, 104: 298-310.

<sup>39</sup> Courard L. (2002) Evaluation of thermodynamic properties of concrete substrates and cement slurries modified with admixtures, Materials Structures, 35:149-155.

<sup>40</sup> Hognies M, Gutiérrez-González S, Rodríguez A, Calderón V. (2014) Effects of the use of polyamide powder wastes on the microstructure and macroscopic properties of masonry mortars. Cement Concrete Composites, 52:64-72.

<sup>41</sup> Reis JML, Motta EP. (2014) Mechanical behavior of piassava fiber reinforced castor oil polymer mortars. Composite Structures, 111:468-472.



With the intention of eliminating the limitation of mechanical strength arising from the use of polymers, and in an effort to study this field of investigation in greater depth, the chemical properties, the cement pastes of recycled polyurethane mortars are modified with non-ionic surfactants, due to probably they increased the effect on the hydration of the clinker.

The use of non-ionic surfactants, which are known to modify the microstructure after hydration<sup>42,43</sup> and to promote the adhesion of pigments at the surface of mortar are very interesting to apply in these kind of recycled materials. By coupling several substitution rates of sand by the polymer wastes and the use of several non-ionic surfactants (with different hydrophilic-lipophilic balance (HLB)), this work leads to give an overview of the compressive and flexural strengths, the bulk density, the porosity and microstructure that can be achieved for these new lightweight structural mortars.

This alteration produced an important change in mechanical strength to achieve recycled structural materials of low density with regard to lightweight conventional mortars. In addition, these additives improved other properties including workability, compaction of the matrix, and avoided polyurethane particle disaggregation, helping to improve the mechanical strength of the matrix under flexion, compression, ductility, thermal strength and durability, reinforcing the materials against such agents as fire.

On the other hand, mortars are susceptible to cracking due in great part to the fragility of the cement paste. This fragility is due to shrinkage that occurs within the cement paste, because water is lost by evaporation, and especially so in these recycled mortars, especially if the requirement of water is higher than usual. (Figure 1.7) Although simply an esthetical effect, it can affect the structural durability of the material.

---

<sup>42</sup> Kong X, Emmerling S, Pakusch J, Rueckel M, Nieberle, J. (2015) Retardation effect of styrene-acrylate copolymer latexes on cement hydration. Cement Concrete Research, 75:23-41.

<sup>43</sup> Gueit E, Darque-Ceretti E, Tintillier P, Hognies M. (2012) Surfactant-induced growth of a calcium hydroxide coating at the concrete surface. Journal of Coating Technology Research, 9:337-346.

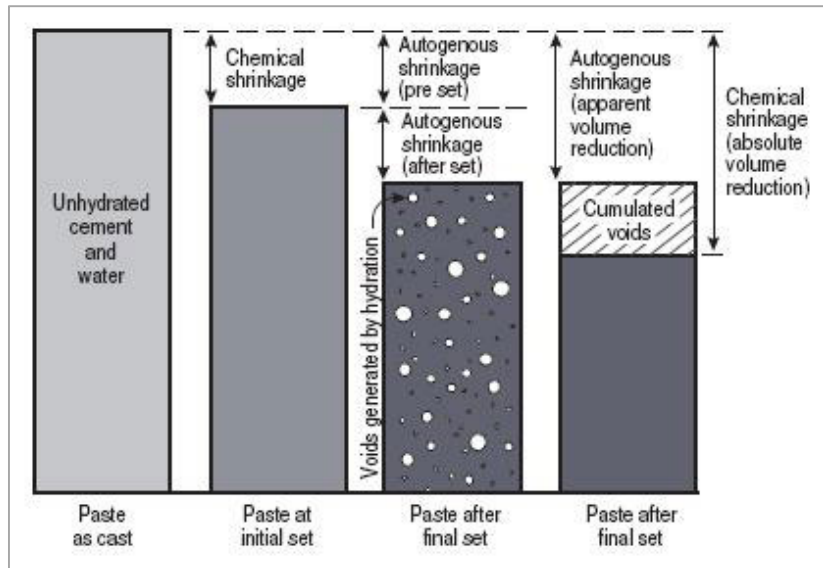


Figure 1.7. Shrinkage of the cement paste.

Drying shrinkage can be reduced in at least two different ways, either by adding additives that reduce the surface tension of the water, or by reducing the volume of small pores. The work presented in this thesis centers on the second approach, which implies the modification, through the smallest pores sizes, of the hydration process of the cement.

The physical bonds in the principal binding phase of practically all mortars and concretes, known as C-S-H gels, are highly nanoporous amorphous calcium silicates, of variable compositions. The smallest porosity is always given by the nanopores of this gel, which produces a relatively high drying shrinkage. Thus, one way of approaching this problem consists in forming different hydrates with a porosity that is inherently far less ultrafine. This objective is achieved in this study by using crystalline phases of afwillite ( $\text{Ca}_3(\text{SiO}_3\text{OH})_2 \cdot 2\text{H}_2\text{O}$ ; or in its oxidized form ( $\text{C}_3\text{S}_2\text{H}_3$ ), the production of which was optimized in a seeding process and subsequent addition of the seeds. The formation of afwillite in



tricalcium silicate pastes initiated by setting with crystals determines the effects on development of tensile strength.



## **Capítulo 2**

---

## **Objetivos**





## 2.1 Objetivos generales

Los objetivos principales a desarrollar en esta Tesis Doctoral se pueden dividir en dos bloques diferenciados que conducen al mismo propósito, mejorar las mezclas de morteros reciclados con poliuretano tanto en estado fresco como endurecido, consiguiendo propiedades comparables con materiales estructurales.

Por una parte, se pretende sintetizar gérmenes de afwillita a partir de silicato tricálcico y sembrarlo en pastas de C<sub>3</sub>S y en lechadas y pastas endurecidas de cemento, con el fin de disminuir el requerimiento de agua y la retracción de secado.

Por otro lado, se busca la mejora mecánica sustancial en morteros aligerados con residuos triturados de poliuretano, a través de la incorporación de una serie de aditivos iónicos surfactantes, que modifican y compactan la estructura interna del material para conseguir propiedades estructurales.

## 2.2 Objetivos específicos

La primera parte de la investigación tiene la finalidad de sintetizar gérmenes de afwillita por hidratación y analizar su comportamiento al introducirlo en pastas de C<sub>3</sub>S y posteriormente en lechadas y en pastas endurecidas de cemento. Los objetivos de esta parte de la investigación consisten en:

- Realizar mediciones por análisis termogravimétrico (TGA) y difracción de rayos X (XRD) para cuantificar la influencia de ciertos parámetros (relación en peso de agua, granulometría Blaine del C<sub>3</sub>S, tiempo de hidratación, empleo de aditivos superplastificantes y pre-siembra con gérmenes).
- Determinar la estabilidad de la afwillita a lo largo del tiempo.



- Introducir los gérmenes de afwillita sintetizados y purificados en pastas de C<sub>3</sub>S para cuantificar el crecimiento de afwillita en función del tiempo por análisis termogravimétrico (TGA).
- Investigar la tasa de hidratación en este proceso de siembra mediante el método del picnómetro.
- Estudiar las propiedades de las pastas endurecidas de C<sub>3</sub>S sembradas con afwillita y su influencia en la microestructura final mediante porosimetría de intrusión de mercurio (MIP) y microscopía electrónica de barrido (SEM), resistencia mecánica a compresión y propiedades de retracción por secado.
- Analizar el crecimiento y el contenido de afwillita en lechada de cemento y en pastas endurecidas de diferentes cementos.
- Comprobar la influencia de las relaciones agua/cemento, la adición de aditivos superplastificantes y la temperatura de curado.
- Ensayar la siembra de afwillita en pastas con alita sintética o con diferentes relaciones C<sub>3</sub>S/C<sub>3</sub>A en presencia de impurezas y de aluminatos de calcio.
- Medir las propiedades de retracción por secado de las pastas sembradas con afwillita y la influencia del crecimiento de la afwillita en la microestructura.

La segunda parte consiste en realizar un estudio del comportamiento de morteros realizados con cementos tipo Portland y cementos con adiciones, arena, agua y residuos de espuma de poliuretano, reemplazando diferentes porcentajes de arena por poliuretano, con el objetivo de analizar su comportamiento y averiguar si es posible mejorar las propiedades de estos materiales. En esta segunda fase, se pretenden alcanzar los siguientes objetivos:



- Determinar las dosificaciones adecuadas para elaborar un estudio completo de las sustituciones de árido por residuo de poliuretano, en porcentajes del 25% al 100%.
- Aditivar las mezclas obtenidas con productos iónicos poliméricos surfactantes con distinto grado de hidrofobicidad, y comprobar los resultados que se obtienen a través de diferentes técnicas de caracterización.
- Caracterizar cada mezcla mediante sus propiedades en estado fresco y en estado endurecido, su comportamiento físico y mecánico.
- Profundizar en la capacidad estructural de estos materiales, determinando las posibilidades de aplicación.
- Analizar la microestructura mediante un microscopio electrónico de barrido, correlacionando los resultados con la microporosidad mediante porosimetría de intrusión de mercurio (MIP) y la macroporosidad a través de la tomografía axial computarizada (TAC).
- Estudiar la degradación térmica en función de la temperatura mediante termogravimetría (TGA) y el comportamiento frente a combustión para estudiar su contribución al fuego.
- Determinar la viabilidad final del uso de estos morteros en construcción.



# **Chapter 3**

---

## **Use of C<sub>3</sub>S paste as a model to add a flyash-based filler (or seeds)**





### 3.1. Introduction

The shrinkage of cement paste results not only from the volume change due to hydration reaction of the compounds with water but also from the interaction between the paste and the environment.<sup>44</sup> A part of the volume change particularly associated with free water evaporation from capillary pores of cement paste is known as drying shrinkage. This drying shrinkage occurs mainly after paste setting and may lead to subsequent cracking, which is widely present in concrete and becomes severely harmful in certain insulating and lightweight concrete with high porosity. Indeed, the drying shrinkage is closely related to capillary tension in the pores of cement paste, which can be expressed as twice the surface tension divided by the pore radius. Thus, it is possible to reduce shrinkage by reducing capillary pore tension in two ways: either by adding surface tension reducing admixtures or by increasing pore size. This work is focused on this second way and the possibility of reducing drying shrinkage by replacing amorphous C-S-H gel network in C<sub>3</sub>S paste with crystalline afwillite ( $\text{Ca}_3\text{Si}_2\text{O}_7 \cdot 3\text{H}_2\text{O}$ ) network with larger pores.

The balance between the different phases in the CaO-SiO<sub>2</sub>-H<sub>2</sub>O system is highly dependent on thermodynamic conditions. Under ambient conditions, C-S-H amorphous form is a stable phase but it was shown in literature that the synthesis of afwillite could be performed under hydrothermal conditions, the afwillite probably being a crystalline phase stable (or metastable at a relatively high temperature).<sup>45</sup>

Although there are still controversies about the stability of phases according to the temperature, some authors were able to create afwillite in a paste containing lime and silica after 60 days of reaction at a temperature of 85°C (but not possible at 55°C).<sup>46</sup> However, some authors observed the creation of afwillite during hydrothermal treatment of C-S-H at 55°C for 730 days, deducing that afwillite was probably a phase thermodynamically stable at 55°C. They also presented

<sup>44</sup> Acker P, Ulm FJ. (2001) Creep and shrinkage of concrete: physical origins and practical measurements, Nuclear Engineering and Design 203, 143-158.

<sup>45</sup> Richardson IG. (2008) The calcium silicate hydrates. Cement and Concrete Research, 38:137-158.

<sup>46</sup> Lachowski EE, Hong SY, Glasser FP. (1997) Crystallinity in C-S-H gels: Influence of preparation and cure conditions, 2nd International RILEM Workshop on Hydration and Setting, 11-13.



experimental results showing that afwillite is stable at 85, 130 and 150°C for 5 months and that a coexistence between jennite and afwillite is stable from 55 to 150°C for 5 months, confirming previous studies.

Then, the synthesis of afwillite under a variety of conditions has been studied in different works. Afwillite can be fabricated from ball-mill hydration of C<sub>3</sub>S slurry at room temperature.<sup>47</sup> Afwillite formed from eventual conversion of C-S-H gel under long grinding in the ball-mill. The same grinding process has been used to produce successfully afwillite from lime and silica. It was also cited that hydration of C<sub>3</sub>S would produce afwillite, instead of C-S-H gel, as the major product under hydrothermal conditions. Afwillite formation and growth in C<sub>3</sub>S paste during hydration at ambient conditions was first reported previously by seeding C<sub>3</sub>S paste with afwillite crystals which had been fabricated previously by ball-mill hydration of C<sub>3</sub>S.<sup>48</sup> It has been also proved that seeding C<sub>3</sub>S paste with afwillite helps to increase total porosity by 15-25%.<sup>49</sup>

### 3.2. Synthesis of afwillite germs using C<sub>3</sub>S-based slurries

#### 3.2.1. Preparation of the germs specimens

The synthesis of afwillite was realized within the hydration of C<sub>3</sub>S under different ball-mill conditions (as shown by Table 3.1).

W/C	B/C	Superplasti-cizers (weight ratio/C <sub>3</sub> S)	Pre-seeding with afwillite germs (weight ratio/C <sub>3</sub> S)	Ball-mill hydra-tion time (h)	Blaine of C <sub>3</sub> S (cm <sup>2</sup> /g)	D <sub>10</sub>	D <sub>50</sub>	D <sub>90</sub>
4 9	From 0.4 to 23.4	0 Optima 203 (0.035) Premia 190 (0.035)	0 0.02	24, 48, 72, 96, until 264	3800 4600 6600	3.17 2.24	8.46 7.22	23.89 19.05

Table 3.1. Summary of all the experimental conditions tested to synthesize afwillite germs by ball-mill hydration of C<sub>3</sub>S slurry

<sup>47</sup> Kantro DL, Brunauer S, Weise CH. (1959) The ball-mill hydration of tricalcium silicate at room temperature. Journal of Colloidal Science, 14:363-376.

<sup>48</sup> Chen JJ, Thomas JJ, Taylor H, Jennings HM. (2004) Solubility and structure of calcium silicate hydrate, Cement and Concrete Research, 34:1499-1519.

<sup>49</sup> Allen AJ, Thomas JJ, Jennings HM. (2007) Composition and density of nanoscale calcium-silicate-hydrate in cement. Nature Materials, 6:311-316.



A mixer Turbula® T2F (WAB, Muttenz, Switzerland) was used for the synthesis experiments (as shown in Figure 3.1). The machine got a motor power of 0.18 kW. Rotation speed of the mixer in all experiments was configured constant at 23 rounds per minute.

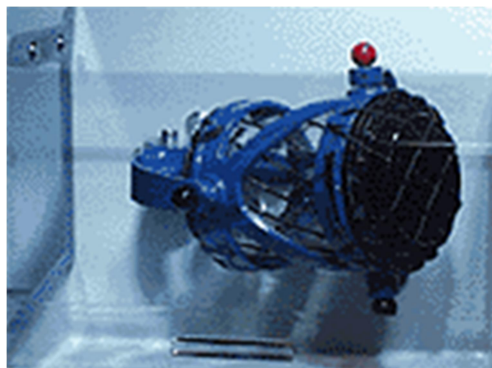
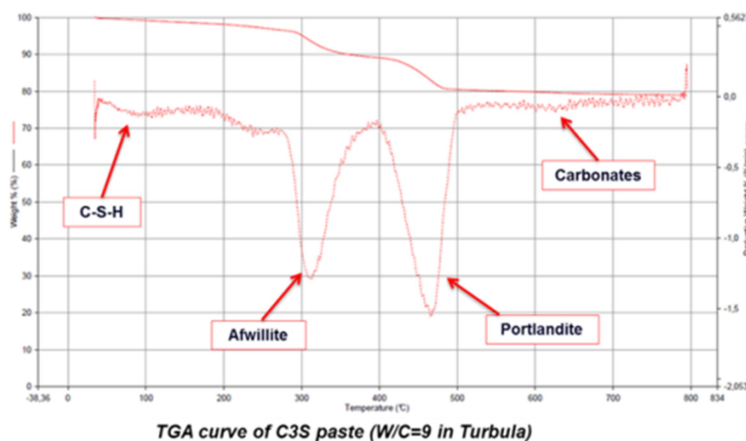


Figure 3.1. Turbula ®

C<sub>3</sub>S was mixed with large amount of demineralised water in order to obtain diluted slurry. The main water/C<sub>3</sub>S (W/C) weight ratio used was 9 to form highly diluted slurry. However, some tests were also done using denser slurry and using W/C=4. The milling process was produced by mixing C<sub>3</sub>S slurry with balls made of stainless steel (1 cm in diameter) in the Turbula®. Different balls/C<sub>3</sub>S (B/C) weight ratio were tested between 0.4 and 23.4. All batches were treated with a continuous milling. Each slurry was sampled after 24 h, 48 h and until 96h or 168h of ball-mill hydration, dried under vacuum to remove the excess of water, in order to track the growth of afwillite according to time (by TGA, as shown in Figure 3.2, and XRD).



a)



b)

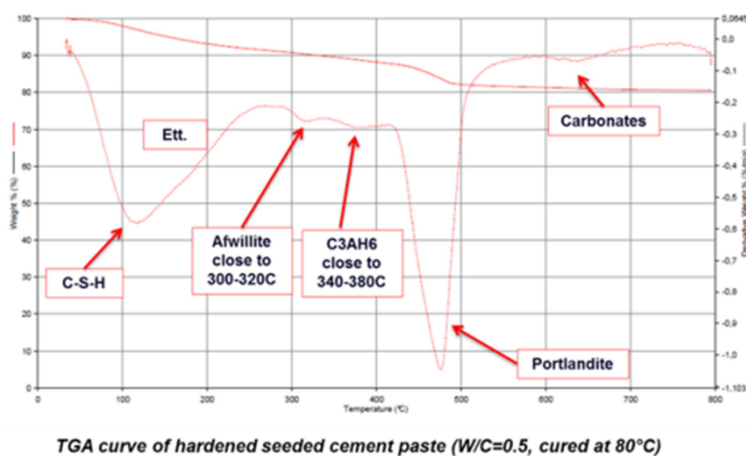


Figure 3.2 TGA curves: (a) seeded slurries; (b) seeded pastes

### 3.2.2. Granulometry Blaine of C<sub>3</sub>S

In the first series, three batches of slurry of C<sub>3</sub>S were launched with different granulometry: 3800, 4600 and 6600 cm<sup>2</sup>/g Blaine (as shown in Figure 3.3). The grinding of C<sub>3</sub>S was performed using a planetary Ball Mill agate (PM 400 from Retsch Technology GmbH).



### 3.2.3. Superplasticizer-based admixtures

C<sub>3</sub>S was mixed with two distinct superplasticizer-based admixtures (Chryso® Fluid Optima 203 and Premia 190, with respective dried extract of 21.8% and 20.0%), which are supposed to influence the hydration rate and may delay the formation of C-S-H in certain conditions.<sup>50</sup> A weight ratio of superplasticizers (dried extract) compared to C<sub>3</sub>S=0.035 was used into certain C<sub>3</sub>S slurries (W/C=9) milled into the Turbula®; while a weight ratio (dried extract of superplasticizer/C<sub>3</sub>S) of 0.004 was used into some C<sub>3</sub>S pastes (W/C=0.35) manufactured to studies the properties at hardened state.

### 3.2.4. “Pre-seeding” of C<sub>3</sub>S slurry with afwillite germs

The afwillite successfully produced were used as germs to seed the slurries of C<sub>3</sub>S before being hydrated under ball-mill. Before use, the afwillite germs were then purified by leaching the co-product (calcium hydroxide) with demineralized and de-carbonated water (by boiling process) until the pH of the slurry went below the pH of saturated solution of calcium hydroxide, which is 12.7. The dosage of this “pre-seeding” was determined to add afwillite germs (weight ratio compared to C<sub>3</sub>S=0.02) in the slurry. Most of the tests were done using the 4600 cm<sup>2</sup>/g Blaine plus some tests using the 3800 and 6600 cm<sup>2</sup>/g Blaine.

### 3.2.5. Combine afwillite-based germ pre-seeding and superplasticizer

In the final tests, C<sub>3</sub>S was mixed in Turbula® using the two different admixtures and a pre-seeding with afwillite germs (respective weight ratios of 0.035 and 0.02 compared to C<sub>3</sub>S).

---

<sup>50</sup> Seligmann P, Greening NR. (1964) Studies of the early hydration reactions of Portland cement by X-ray diffraction. Highway Research Record, 62:80-105.



### 3.2.6. Influences of granulometry, balls/C<sub>3</sub>S weight ratio and ball-mill hydration time

To study the influence of the Blaine, all the slurries consisted in mixing only C<sub>3</sub>S, water and balls (using W/C=9 and B/C=23.5). The results of TGA are reported in Figure 3.3.

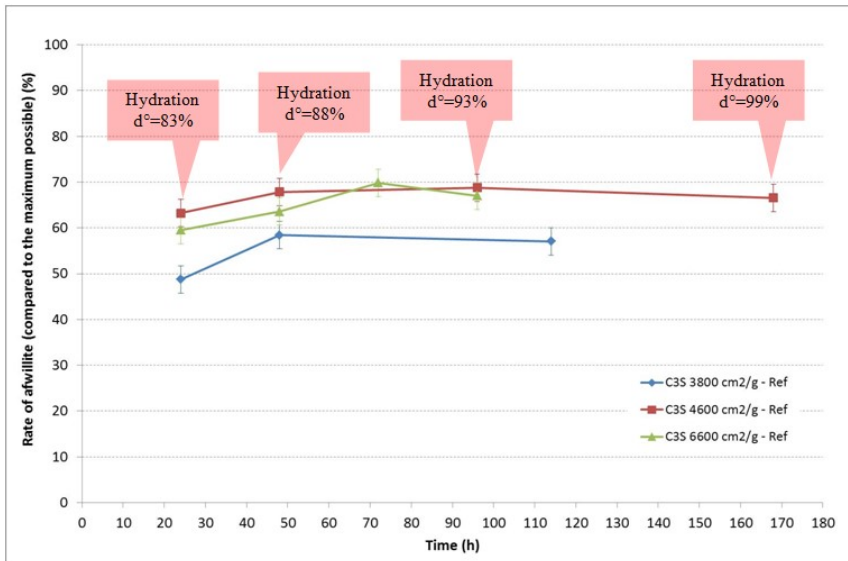


Figure 3.3. Influence of the Blaine of C<sub>3</sub>S on the synthesis of afwillite germs by ball-mill hydration into the Turbula ®

Among the different tests done, using a low Blaine (3800 cm<sup>2</sup>/g Blaine) seems to reduce the final content of afwillite compared to higher Blaine (4600 or 6600 cm<sup>2</sup>/g). The best results were obtained respectively after 48h and 72h for 4600 cm<sup>2</sup>/g and 6600 cm<sup>2</sup>/g Blaine, respectively, allowing the formation of 68-70% of the maximum afwillite theoretically possible (see Eq. 3.1).



**Ca<sub>3</sub>SiO<sub>5</sub>** : alite

**Ca<sub>3</sub>Si<sub>2</sub>O<sub>7</sub>** : rankinite

**Ca(OH)<sub>2</sub>** : calcium hydroxide



In order to study the influence of the mechanical shocks necessary to generate nucleation of afwillite, the influence of the B/C ratio was established using slurries made of C<sub>3</sub>S (4600 cm<sup>2</sup>/g Blaine). In this case, two distinct W/C ratios were used (4 and 9) in order to test dense and diluted slurries (as shown in Figure 3.4). To reduce the amount of TGA analyses, the choice was made to determine the content in afwillite after 48h of ball-mill hydration in Turbula® (an enough long grinding time according to previous experiments).

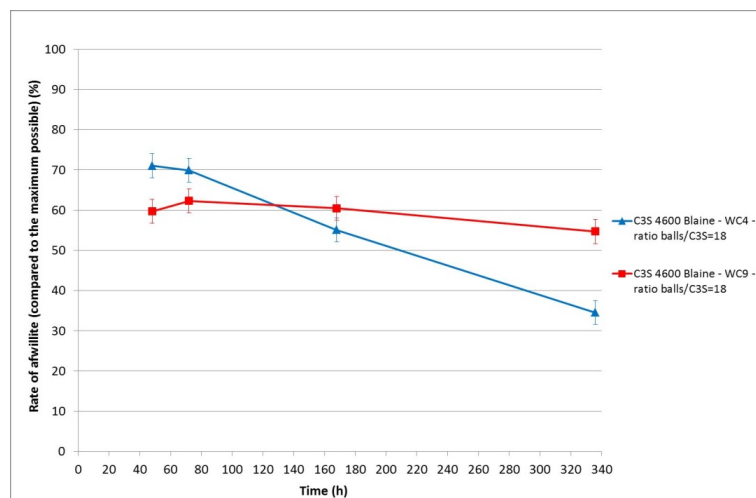


Figure 3.4. Variation of the content of afwillite synthesized according to the time of ball-mill hydration into the Turbula®

As shown by Figure 3.5, the amount of afwillite detected by TGA increases with the mass of balls used until an asymptote, the minimum value of B/C ratio to obtain the maximum of afwillite depending on the W/C ratio (and then depending on the dilution of the slurry).

Moreover, the influence of a long ball-milling time was studied. In this case, C<sub>3</sub>S Blaine of 3800 cm<sup>2</sup>/g, W/C=4, B/C<sub>3</sub>S=0.34 were used. As shown by Figure 3.3, the evolution of the content of afwillite detected by TGA reached approximate stabilisation after 24-48h, where afwillite constitutes about 50% of the maximum theoretical possible. No specific decrease of the afwillite content was detected until 264 h (11 days) of



ball milling in Turbula®. The result is conformed to that of Kantro et al.<sup>47</sup> who suggested afwillite grew gradually during almost one month and reached the theoretical maximum in the end.

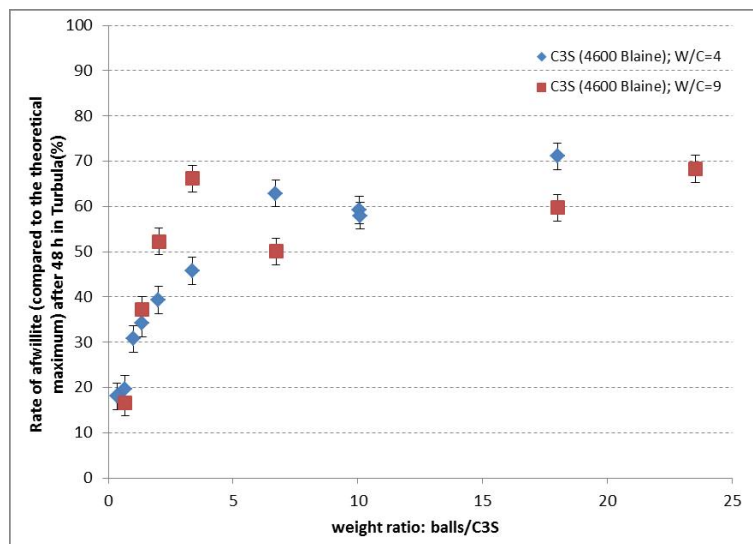


Figure 3.5. Contents of afwillite synthesized by ball-mill hydration after 48h into the Turbula® according to the W/C and Balls/C<sub>3</sub>S weight ratios

### 3.2.7. Influence of the superplasticizer-based admixtures

C<sub>3</sub>S (4600 cm<sup>2</sup>/g Blaine) was mixed in Turbula® with W/C=9 and B/C=23.5 with two different superplasticizers-based admixtures. As showed in Figure 3.6, the use of Optima 203 tends to delay significantly the formation of afwillite.

This result is consistent with literature, showing that this kind of superplasticizer tends to delay the hydration rate and the formation of C-S-H. The difference in terms of creation of afwillite is very high after 24h and is always non-negligible after 4 days of ball-mill into Turbula®. On the other hand, the use of Premia 190 did not affect the formation of afwillite after 24h and seems to show positive effect after 48h (75% of the maximum theoretical afwillite was formed), compared to a reference



C<sub>3</sub>S slurry without admixture. Some tests performed using other Blaine of C<sub>3</sub>S (3800/6600 cm<sup>2</sup>/g) confirmed the tendency concerning the influences of the both admixtures tested, as shown in Figure 3.6).

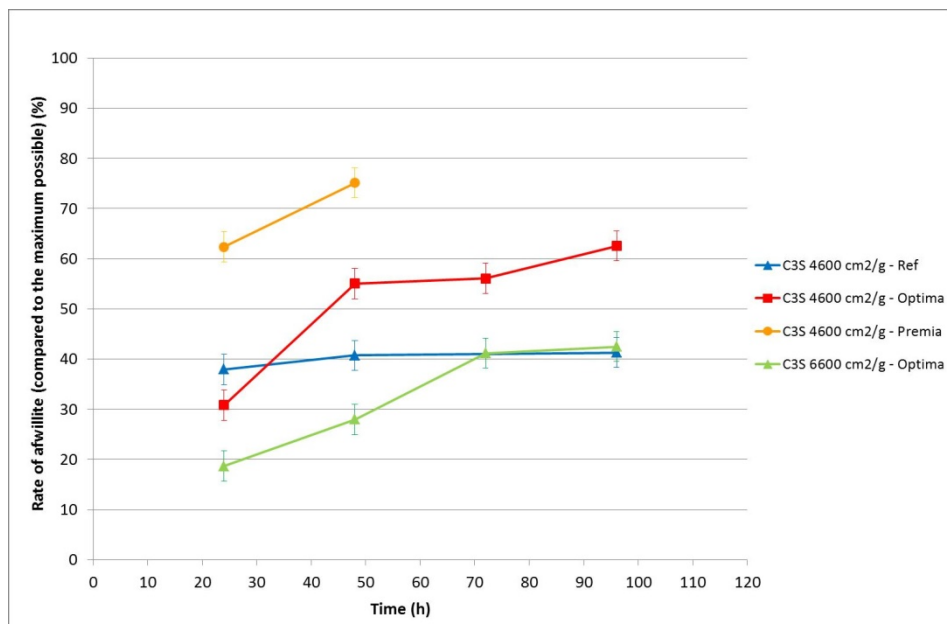


Figure 3.6. Influence of the superplasticizers on the synthesis of afwillite by ball-mill hydration into the Turbula ®

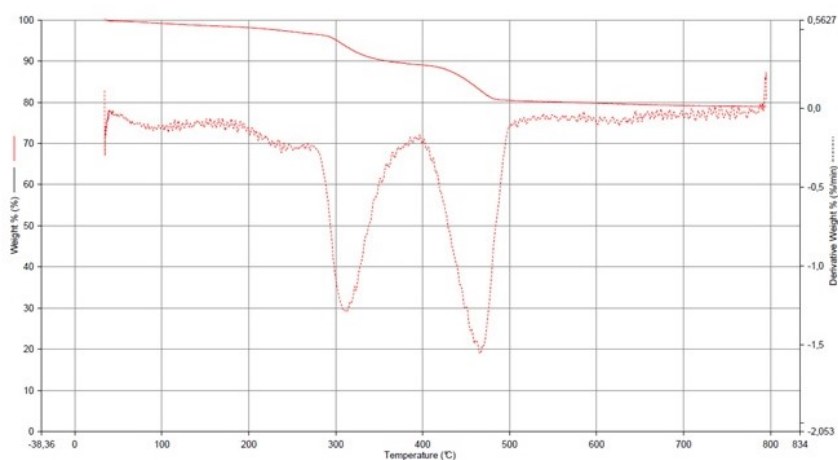
### 3.2.8. Seeding of C<sub>3</sub>S slurry with afwillite germs

First germs of afwillite successfully produced using a C<sub>3</sub>S slurry (4600 cm<sup>2</sup>/g Blaine, W/C=9, B/C=23.5) after 48h of ball-mill hydration in Turbula® were used in order to seed new C<sub>3</sub>S-based slurry hydrated with the same ball-mill process. Thermogravimetric analyses (TGA) was used to measure the variations in the mass of the two main phases (afwillite and portlandite) resulting from the hydration of C<sub>3</sub>S and of the eventual intermediate compounds that could form in the reaction between both. TGA data were recorded in a nitrogen atmosphere on a Setaram TGA/SBTA851 analyser from 20 mg of sample from room temperature to 800°C at a scan rate of 10°C/min. The specific peak at 320°C was assigned to afwillite, which is relevant considering previous values found



in literature (250-450°C<sup>51</sup> and 340°C<sup>52</sup>, respectively). The peaks at 450°C and 680°C, such as used commonly in literature<sup>53</sup>, were used to quantify the amount of portlandite and, eventuality, carbonates. C-S-H can be characterized by the peak about 90-120°C but their quantification is not relevant by this technic, considering the removal of residual water molecules coming from the sample.

(a)



<sup>51</sup> Moody KM. (1952) Thermal decomposition of afwillite. Mineralogical Magazine, 29:838-840.

<sup>52</sup> Maycock JN, Skalny J, Kalyoncu RS. (1974) Thermal decomposition of cementitious hydrates, R.S. Porter and J.F. Johnson Eds., Analytical Calorimetry, New York & London 697-711.

<sup>53</sup> Taylor HFW. (1997) Cement Chemistry, 2nd Ed. Thomas Telford Edition Publishing, London.

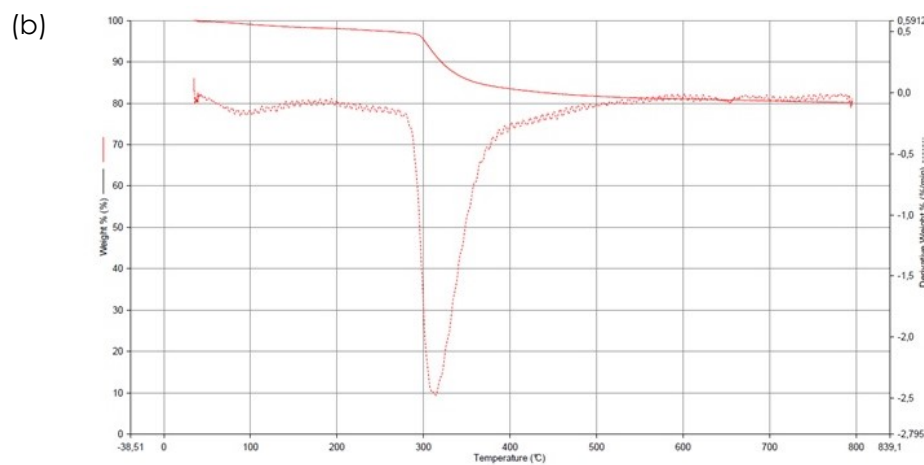


Figure 3.7. TGA curves of the germs of afwillite prepared by ball-mill hydration  
(a) before and (b) after leaching of the portlandite

As showed by TGA curve of Figure 3.7a, the first germs of afwillite produced were not pure and contained a co-product made of portlandite (30-40% of the content after sampling the C<sub>3</sub>S slurry at 48 h) and remaining C-S-H (about 10% by deduction of the contents of afwillite and portlandite). After leaching with demineralised and de-carbonated water, practically all the portlandite and a significant part of the remaining C-S-H were removed from the germs, which reached to a purity closed to 70% (see Figure 3.7b the TGA curve after leaching).

Then, the dosage in afwillite germs was determined to 0.02 compared to the weight of C<sub>3</sub>S (4600 cm<sup>2</sup>/g Blaine). As shown by Figure 3.8, more afwillite was detected by TGA after 24-48h of ball-mill process (78-79% of the maximum theoretically possible after 24h, compared to 65-70% without pre-seeding).

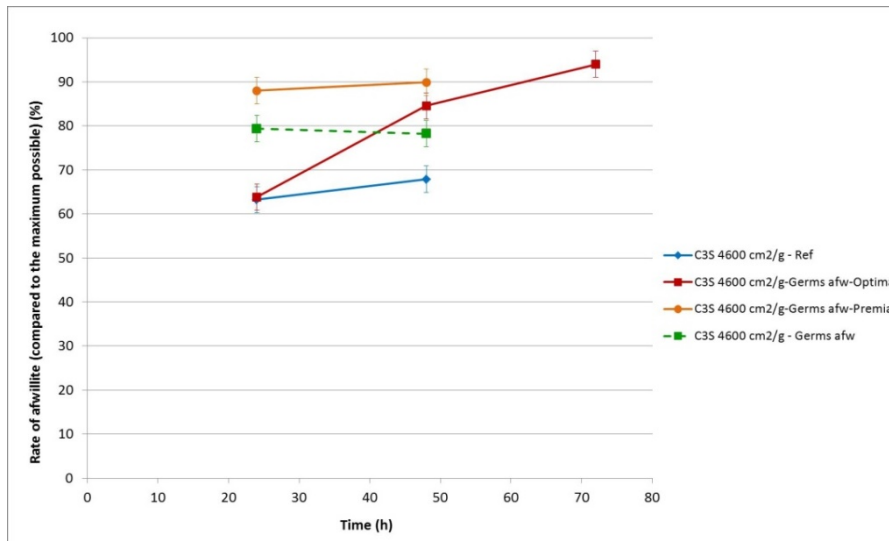


Figure 3.8. Influences of the addition of superplasticizers and afwillite pre-seeds into the slurry of C<sub>3</sub>S on the synthesis of afwillite germs by ball-mill hydration

### 3.2.9. Seeding of C<sub>3</sub>S slurry with afwillite germs and superplasticizer

For the last series of batches done into Turbula®, the effect of combining the addition of afwillite germs with the use of admixtures was tested. Indeed, afwillite germs and superplasticizer-based admixtures (with dosages of 0.02 and 0.035 compared to C<sub>3</sub>S weight, respectively) were added to the C<sub>3</sub>S slurry (4600 cm<sup>2</sup>/g Blaine, W/C=9, B/C=23.5) before starting the ball-mill hydration for 96h. As showed in Figure 3.6, more than 90% of the maximum theoretically possible for afwillite (according to Eq. 3.1) was obtained after 48h (with Premia 190) or 72h (with Optima 203).

After leaching the portlandite generated during the hydration of C<sub>3</sub>S (using demineralised and de-carbonated water), germs of afwillite with purity close to 100% were obtained (as deduced from TGA and XRD analyses, see Figure 3.9). XRD (X-ray diffraction) analyses were conducted on the specimens grounded to a powder-size < 63 µm. The XRD equipment (Philips PANalytical X'Pert Pro) is equipped with a



monochromatic cathode ( $\lambda=0.154$  nm). The acquisition of scans was done using the software X'Pert data collector.

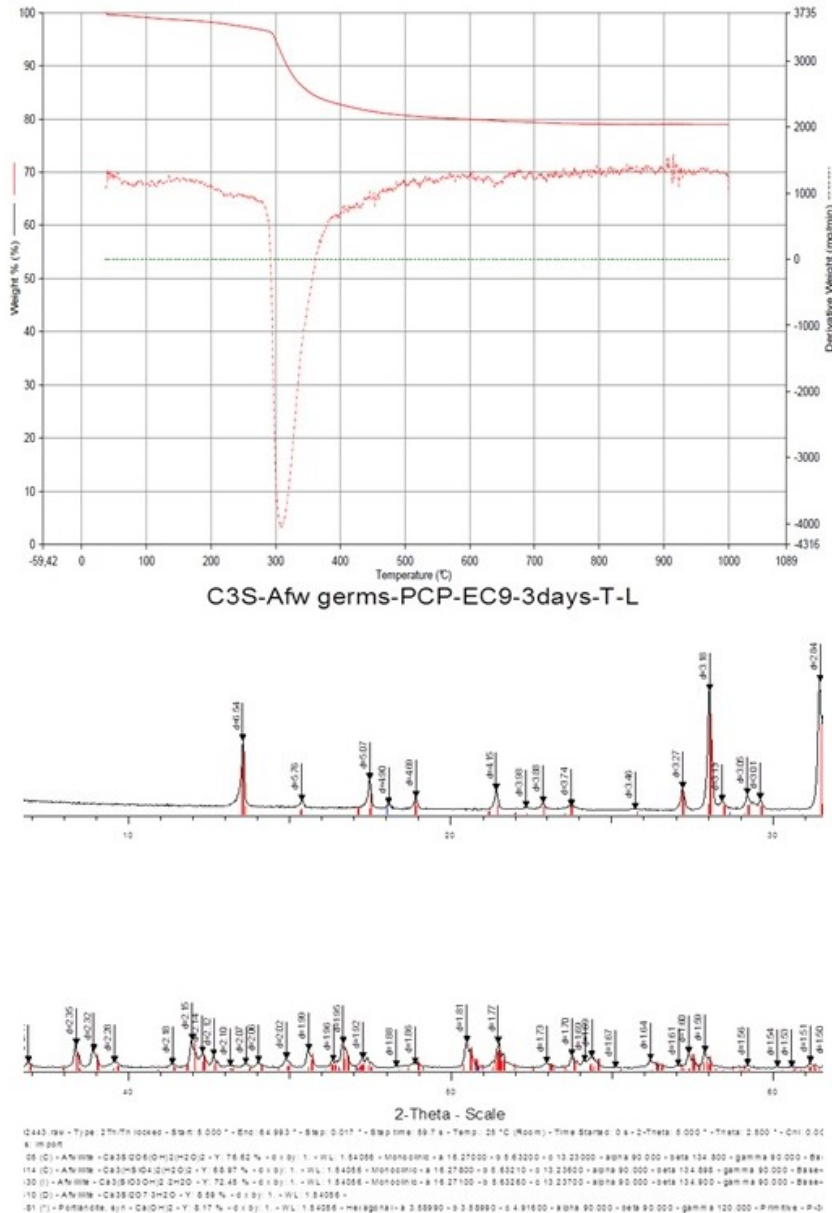


Figure 3.9. TGA curve and XRD spectrum of the purest germs of afwllite obtained after ball-mill hydration and leaching of the portlandite



Note also that the nitrogen BET specific surface area of these germs of afwillite was 4 m<sup>2</sup>/g<sup>-1</sup>, a value dramatically lower than the one (about 100-150 m<sup>2</sup>/g<sup>-1</sup>) commonly found for C-S-H in literature.<sup>54,55</sup>

### 3.3. Microstructure of C<sub>3</sub>S pastes seeded with afwillite germs

#### 3.3.1. Preparation of the specimens to investigate microstructural properties

Many reference and seeded C<sub>3</sub>S pastes were manufactured (as detailed in Table 3.2) to detect the growth of afwillite according to time (by TGA and XRD) and to study the influence of afwillite seeding on hydration rate and on different microstructural properties (porosity, drying shrinkage and compressive resistance).

The afwillite germs were manufactured by 48h of ball-milling in Turbula® of slurry containing C<sub>3</sub>S, superplasticizer and afwillite pre-seeds. They were then freshly grounded by hand in order to be carefully mixed with C<sub>3</sub>S before adding water. The main weight ratio between afwillite germs and C<sub>3</sub>S tested into the pastes was 0.02 but some tests were performed by seeding with a ratio of 0.01 and 0.04 in order to study the influence of this parameter. Most of the C<sub>3</sub>S pastes were casted in 5 mL polyethylene-based sealed tubes, except the ones dedicated to the drying shrinkage experiments, which were casted into cylindrical Teflon-based mould (160 · 20 mm). All the samples were cured at 100% relative humidity and 20°C during 7 or 28 days before being characterised. A water to cement ratio of 0.5 was mainly used to perform the hardened C<sub>3</sub>S pastes but a W/C of 0.35 (using addition of superplasticizer-based admixture, with a weight ratio/C<sub>3</sub>S=0.004 (dried extract)) were tested.

For TGA and XRD, the hardened pastes needed to be grounded to powder finer than 63 µm before analysis. When analyses using MIP or SEM were needed, the 5 mL hardened pastes were broken after the cure into

<sup>54</sup> Odler I. (2003) The BET-specific surface area of hydrated Portland cement and related materials, Cement and Concrete Research, 33:1049-2056.

<sup>55</sup> Thomas JJ, Chen JJ, Allen AJ, Jennings HM. (2004) Effects of decalcification on the microstructure and surface area of cement and tricalcium silicate pastes. Cement Concrete Research, 34: 2297-2307.



small pieces of around 1 cm<sup>3</sup> in volume, immersed in isopropanol for 2+7 days (solution renewed after 2 days) in order to stop the hydration, and finally dried in high vacuum. For the measurements of the compressive resistance, the tubes of 5 mL C<sub>3</sub>S pastes were directly used after 7 and 28 days of cure. Finally, the degree of hydration was studied on 5 g of pastes hydrated in pycnometer under water by measuring its chemical shrinkage.

Blaine of C <sub>3</sub> S (cm <sup>2</sup> /g)	W/C	Superplasticizers (weight ratio/C <sub>3</sub> S)	Pre-seeding with afwillite germs (weight ratio/C <sub>3</sub> S)	Methods of characterisation
3800	0.5	/	0 0.02	- TGA - Pycnometry - Compressive strength
3800	0.35	Optima 203 (0.004)	0 0.02	- TGA - Pycnometry - Compressive strength
4600	0.7	/	0.02	- TGA
4600	0.5	Premia 190 (0.004)	0.02	- TGA
4600	0.5	Optima 203 (0.004)	0.02	- TGA
4600	0.5	/	0.02 0 0.01 0.02 0.04	- TGA/XRD - Pycnometry - SEM - MIP - Drying shrinkage - Compressive strength
4600	0.35	Premia 190 (0.004)	0 0.02	- TGA - MIP - Compressive strength
4600	0.35	Optima 203 (0.004)	0 0.02	- TGA - MIP - Compressive strength
4600	0.35	/	0.02	- TGA

Table 3.2. Summary of the experimental conditions tested and methods of characterization used to study the growth of afwillite in C<sub>3</sub>S paste and its consequence on the hydration/microstructural properties.

### 3.3.2 Growth of afwillite into C<sub>3</sub>S pastes seeded with germs

Table 3.3 details the conditions of seeding afwillite germs into the pastes of C<sub>3</sub>S (4600 cm<sup>2</sup>/g Blaine) compared to weight ratio. Two different W/C ratios were tested: 0.5 (without any admixture) and 0.35



(using optima 203 or Premia 190). Table 3.3 allows also comparing the content in afwillite detected after 7 and 28 days (hydration stopped by immersing into ethanol followed by a drying under primary vacuum).

Blaine of C <sub>3</sub> S (cm <sup>2</sup> /g)	W/C	Superplas- ticizers (weight ratio/C <sub>3</sub> S =0.004)	Seeding with afwillite germs (weight ratio/C <sub>3</sub> S =0.02)	Rate of afwillite (/theoretical maximum)		Total porosity measured by MIP after <b>28 days (%)</b>
				7 days	28 days	
3800	0.50	No	No	0	0	23.6
	0.50	No	Yes	45	41	25.7
	0.35	Optima 203	No	0	0	11.1
	0.35	Optima 203	Yes	24	25	11.2
4600	0.70	No	Yes	36 (+/-2)	Not measured	Not measured
	0.50	Optima 203	Yes	20 (+/-2)	Not measured	Not measured
	0.50	Premia 190	Yes	22 (+/-2)	Not measured	Not measured
	0.50	No	No	0	0	27.1
	0.50	No	Yes	42 (+/-3)	41 (+/-2)	32.5
	0.35	Optima 203	No	0	0	Not measured
	0.35	Optima 203	Yes	27 (+/-3)	30 (+/-5)	Not measured
	0.35	Premia 190	No	0	0	6.0
	0.35	Premia 190	Yes	29 (+/-5)	29 (+/-5)	8.8
	0.35	No	Yes	24 (+/-3)	Not measured	Not measured

Table 3.3. Comparison between the rate of afwillite detected by TGA in C<sub>3</sub>S pastes (with/without seeding, according to the W/C ratio) and the total porosity measured by MIP.

The results highlighted that afwillite is growing rapidly in order to reach practically its maximum rate after 7 days of cure at 20°C/100% RH. In this case, the W/C ratio of 0.5 gave the best growth of afwillite with approximately 41-42% of the maximum theoretically possible. However, the tests of seeding performed using admixtures and a lower W/C ratio did not show a so high content in afwillite after 7 or 28 days, the content of afwillite establishing by TGA reaching only to a 27-30% of the maximum theoretically possible. Maybe this result could be explained by



the methodology used to cure the sample (the samples of pastes were sealed into a capsule) or a too low initial rate in afwillite considering all the C<sub>3</sub>S to hydrate.

The use of 3800 cm<sup>2</sup>/g C<sub>3</sub>S Blaine gave the same tendency about the influences of the W/C ratio and superplasticizers (note that only the Optima 203 was tested with C<sub>3</sub>S of 3800 cm<sup>2</sup>/g Blaine). Moreover, no significant difference in terms of final content of afwillite (detected by TGA after 7 and 28 days of hydration) was highlighted using a seeding with dosage of 0.01 and 0.04 of afwillite (compared to C<sub>3</sub>S weight).

### 3.3.3 Rate of hydration

Adding afwillite in C<sub>3</sub>S paste might modify its rate of hydration according to Davis and Young<sup>56</sup>. In this work, the rate of hydration of C<sub>3</sub>S pastes was evaluated by measuring the chemical shrinkage when hydrated in pycnometer under water at 20°C. This chemical shrinkage was measured using the Le Chatelier equation<sup>57</sup> by weighing C<sub>3</sub>S pastes, immersed in demineralized and boiled water, during the hydration time (from 1 to 91 days). The C<sub>3</sub>S pastes of 5 g were either mixed by hand for 1 minute before introducing into 20 mL glass pycnometers.

Figure 3.10 allows comparing the difference of chemical shrinkage between two samples made of reference C<sub>3</sub>S paste and two samples of C<sub>3</sub>S pastes seeded with afwillite (4600 cm<sup>2</sup>/g Blaine, W/C=0.5). If the final value of chemical shrinkage did not change a lot from one case to the other, the pastes seeded with afwillite had evidently a much higher rate of hydration.

<sup>56</sup> Davis RW, Young JF. (1975) Hydration and strength development in tricalcium silicate pastes seeded with afwillite. Journal American Ceramic Society, 58:67-70.

<sup>57</sup> Le Chatelier H. (1900) Sur les changements de volume qui accompagnent le durcissement des bétons. Bull. Soc. Encourag. Ind. Natl, 5: 54-57.

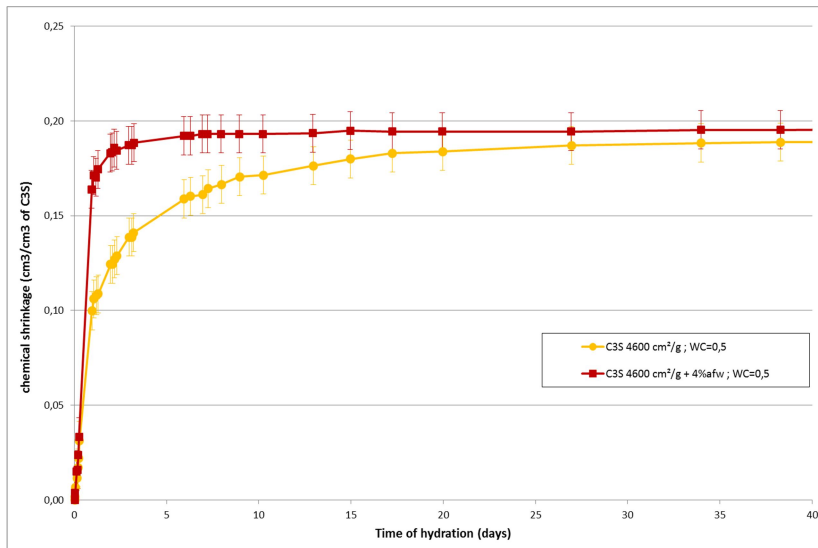
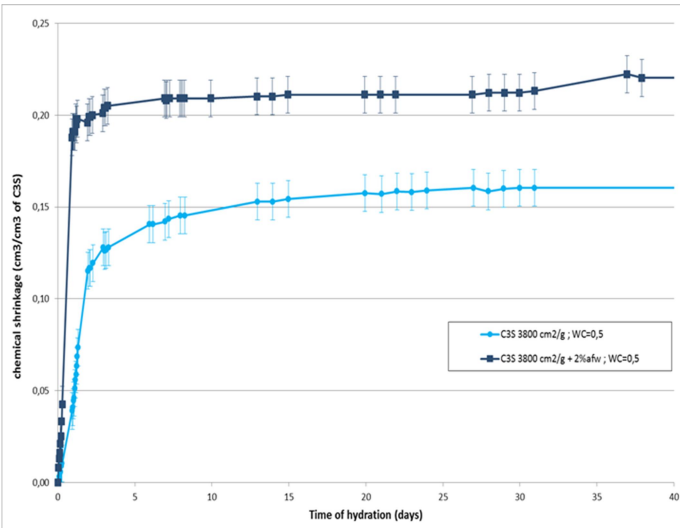


Fig 3.10 Rate of hydration (chemical shrinkage) of C<sub>3</sub>S pastes (4600 cm<sup>2</sup>/g)

Its chemical shrinkage became stable after 7 days whereas reference C<sub>3</sub>S pastes needed up to more than 3 weeks to reach this stabilization. This higher rate of hydration after 7 days in case of seeding with afwillite can explain why the total content of afwillite in C<sub>3</sub>S pastes (see TGA measurements in Table 3.3) did not significantly evolve between 7 and 28 days of hydration. These results are confirmed using a Blaine of 3800 cm<sup>2</sup>/g and a W/C=0.35 (with Optima 203), as shown by Figure 3.11. In this case, as in the other one, the C<sub>3</sub>S paste seeded with afwillite had a higher and faster rate of hydration compared with the reference one.



(a)



(b)

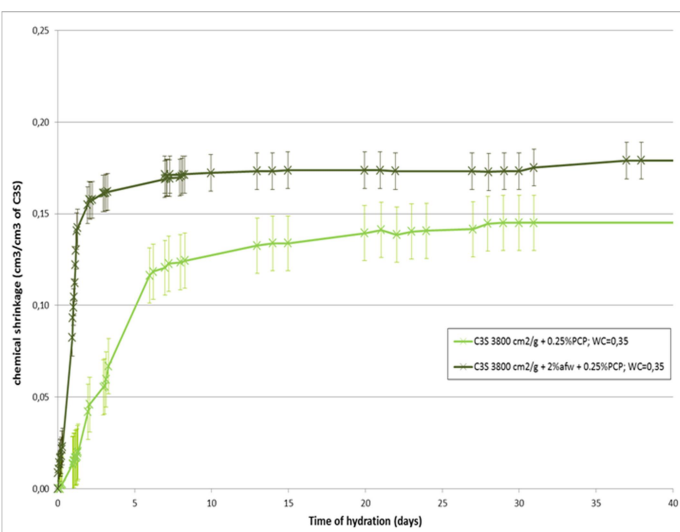


Fig 3.11 Rate of hydration (chemical shrinkage) of C<sub>3</sub>S pastes (3600 cm<sup>2</sup>/g)  
(a) C<sub>3</sub>S 3800 cm<sup>2</sup>/g; WC=0.50; (b) C<sub>3</sub>S 3800 cm<sup>2</sup>/g + PCP; WC=0.35

### 3.3.4 Microstructure observed by SEM

The microstructures of C<sub>3</sub>S pastes (4600 cm<sup>2</sup>/g Blaine, W/C=0.5) of reference or seeded with afwillite were compared using a high-resolution field effect gun digital scanning electron microscope (SEM FEG Quanta 400 from FEI Company, USA; with an accelerating voltage of 15 keV and a current intensity of 1 nA). Images of the cross-sections were recorded in



Back Scattering Electron mode (BSE) after being impregnated and polished. SEM/EDS helped to identify phases on a polished section of the paste, by measuring molar ratio Ca/Si.

Figure 3.12 depicts polished sections chosen from four specimens: two pastes of reference and two seeded pastes respectively hydrated during 7 days and 28 days old.

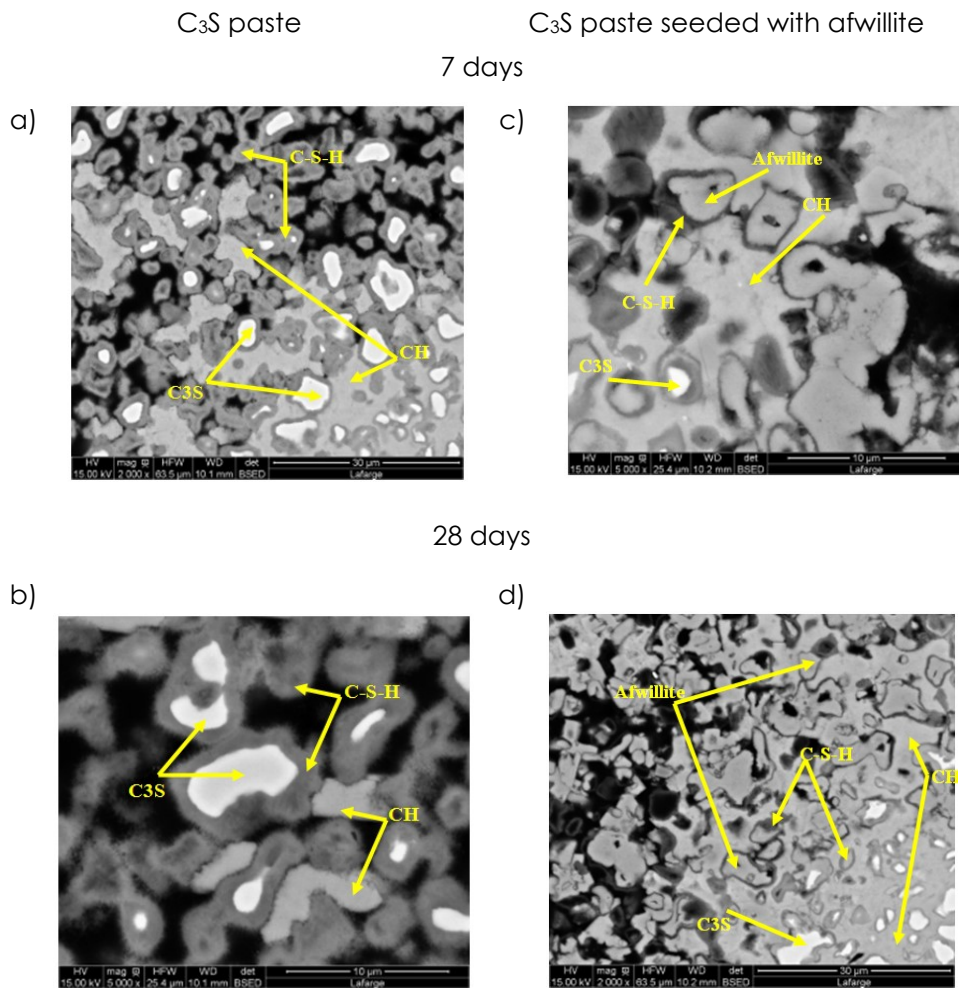


Figure 3.12. SEM images (in BSED mode) of polished cross-sections of C<sub>3</sub>S pastes after 7 and 28 days of hydration: (a,b) reference pastes; (c,d) seeded pastes (wt ratio afwillite/C<sub>3</sub>S=0.02).



In the SEM image in backscattering electron mode, the anhydrous C<sub>3</sub>S grains are coloured in white and hydrated phases with higher or lower porosity are in deeper or lighter grey. Because the seeded paste contains only a few remaining content of anhydrous grains at 7 days while the reference paste shows much more anhydrous area, the observations confirm that the seeded pastes were hydrated much faster than reference paste, as already demonstrated by the study of the hydration rate.

Moreover, X-rays microanalysis (and more precisely the analyse of the calcium/silicon ratio) help in identifying the different phases of the cross-sections. In the reference C<sub>3</sub>S paste, the product coating the anhydrous C<sub>3</sub>S is identified as C-S-H gel (with a high variability of the Ca/Si ratio). In this reference C<sub>3</sub>S paste, C-S-H gel begins (as well known in literature) to form on the surfaces of C<sub>3</sub>S in contact with water and gradually grows in two directions: internally into the C<sub>3</sub>S as water passes through capillary pores of C-S-H gel to reach inside C<sub>3</sub>S, and externally to finally create the cementitious matrix.<sup>58</sup> Large masses in the background in light grey colour are assigned to portlandite. Portlandite nucleates in a few sites and grows to external space in some regular directions. Finally plates or sheets of crystals are formed, as observed in this case. Portlandite crystals show more condensed microstructure than C-S-H gel so that it has lighter colour. In seeded C<sub>3</sub>S paste, small crystals of afwillite are scattered on the background of large masses of portlandite. They do show in similar colour, which may imply that afwillite has higher density than C-S-H gel. Afwillite should be formed and grown in the same way as C-S-H in unseeded C<sub>3</sub>S paste. Voids are observed inside some afwillite crystals. When afwillite grows inside a C<sub>3</sub>S grain and water passes inside, the core of the grain keeps dissolving and may leave a void space if afwillite formed cannot occupy it. Formation of those hollow shells or Hadley grains is as described in early works<sup>59</sup>.

Figure 3.13 compares the microstructure of two pastes (reference and seeded with afwillite) after 7 days of hydration.

<sup>58</sup> Dunstetter F, de Noirlfontaine MN, Courtial M. (2006) Polymorphism of tricalcium silicate, the major compound of Portland cement clinker I. Structural data: review and unified analysis. Cement and Concrete Research, 36:39-53.

<sup>59</sup> Kjellsen KO, Justnes H. (2004) Revisiting the microstructure of hydrated tricalcium silicate—a comparison to Portland cement. Cement Concrete Composites, 26:947-956.

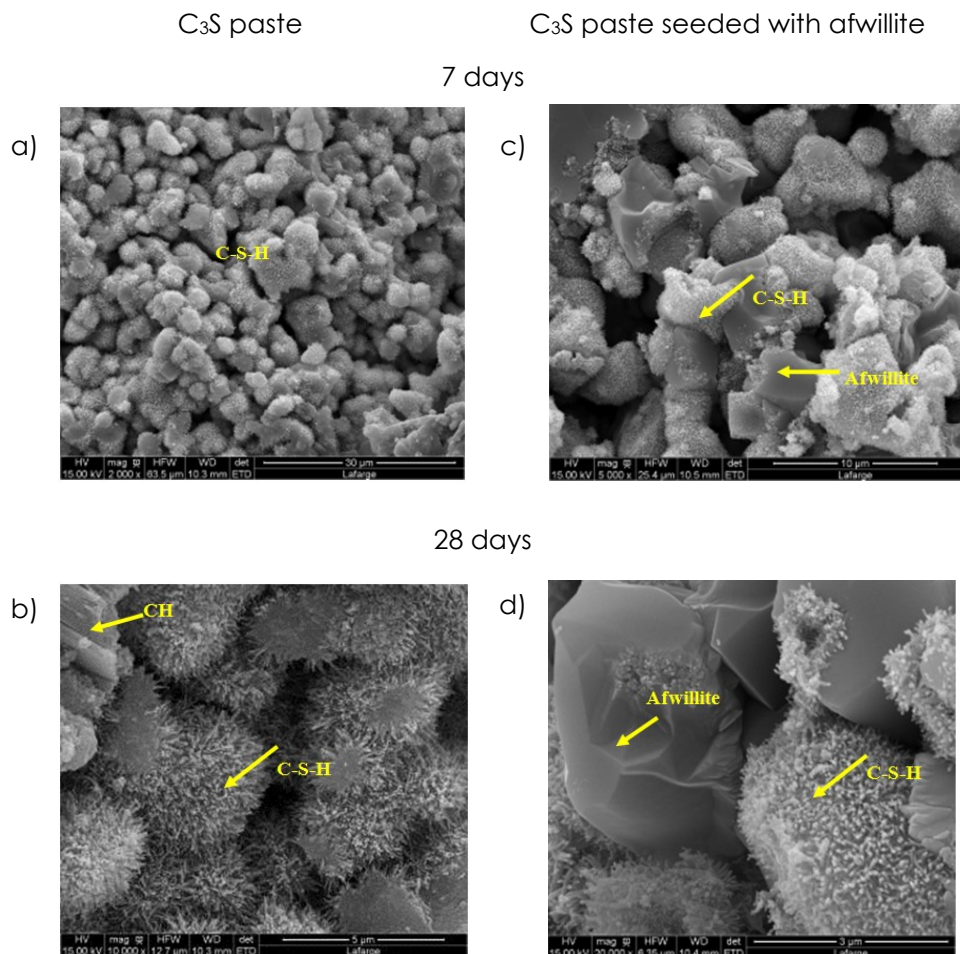


Figure 3.13. SEM images (in SE mode) of fractures of C<sub>3</sub>S pastes after 7 days of hydration: (a,b) reference pastes; (c,d) seeded pastes (wt ratio afwillite/C<sub>3</sub>S=0.02).

As shown by the SEM images done in secondary electron mode, C-S-H exists in form small fibrils, which are assembled in clusters in the pastes. Only observed in the seeded paste, crystals of afwillite of 3-5 µm in size constitute the network in the place of C-S-H gel. Their prismatic-like shape seems to be one of their characteristic.<sup>60</sup> Figure 3.14 shows these

<sup>60</sup> Kusachi I, Henmi C, Henmi K. (1989) Afwillite and jennite from Fuka, Okayama Prefecture, Japan. Mineralogical Journal, 14: 279-292.



pure afwillite germs. In such a way, microstructure of the seeded paste was coarsened. C-S-H gel does not disappear though because it covers crystals of afwillite. At low magnification, this afwillite network seems to be more porous than C-S-H gel network. Combined with Figure 3.12 showing that reference C<sub>3</sub>S paste have basically pores smaller than 0.1 μm in size while seeded paste have as many pores bigger than 0.1 μm as well, probably pore size of scale under 0.1 μm is mainly associated with micro porosity within C-S-H gel.

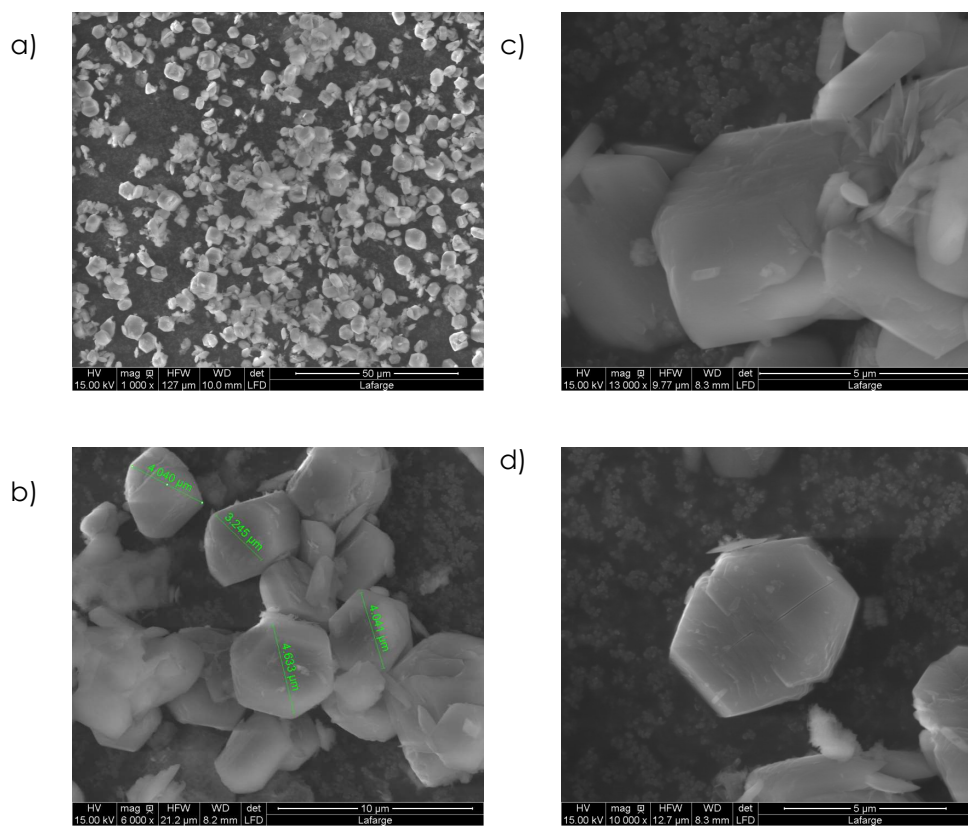


Figure 3.14 SEM images of pure afwillite germs: (a) distribution of afwillite germs; (b) size of crystals of afwillite of 3-5 μm; (c,d) prismatic-like shape.



### 3.3.5 Porosity deduced from MIP measurements

An essential hypothesis to prove in this work is that seeding C<sub>3</sub>S paste with afwillite can increase capillary pore size, which then may help to reduce drying shrinkage. On this purpose, the microstructure of a C<sub>3</sub>S (3800 cm<sup>2</sup>/g Blaine and 4600 cm<sup>2</sup>/g Blaine) paste seeded with afwillite was investigated by Mercury Intrusion Porosimetry technique (Autopore IV from Micromeritics, USA) and compared to the one of reference C<sub>3</sub>S paste. The pressure range of the porosimeter was from sub ambient up to 400 MPa, covering the pore diameter range from about 360 µm to 3 nm. Tests were carried out on (5x5x5) mm<sup>3</sup> samples cut from the core of the SP samples. The samples were dried in an oven at 45°C overnight before being tested. The advancing/receding contact angle was assumed to be 130°C, as recommended by Taylor<sup>53</sup> for ordinary cement pastes.

As demonstrated in Table 3.3, seeded C<sub>3</sub>S 4600 cm<sup>2</sup>/g Blaine paste at W/C=0.5 cured for 28 days contains about 40% of afwillite and the total porosity accessible to mercury was 32.5%, almost 20% higher in absolute value than that of the reference C<sub>3</sub>S paste, which was merely 27.1%. Concerning the C<sub>3</sub>S 4600 cm<sup>2</sup>/g Blaine paste mixed using W/C=0.35 and superplasticizers, an increase of the total porosity can also be highlighted, even if the very low range of values of porosity (due to the low W/C ratio) should be considered cautiously.

In case of seeded C<sub>3</sub>S 3800 cm<sup>2</sup>/g Blaine paste at W/C=0.5 cured for 28 days contains about 45% of afwillite and the total porosity accessible to mercury was 25.7%, a little higher than that of the reference paste, which was 23.6%. Concerning the C<sub>3</sub>S 4600 cm<sup>2</sup>/g Blaine paste mixed using W/C=0.35 and superplasticizers, the porosity is similar (close to 11%) due to the low W/C ratio.

Figure 3.15 allows the comparison done on C<sub>3</sub>S pastes (4600 cm<sup>2</sup>/g Blaine, W/C=0.5) hydrated for 28 days (cure at ambient temperature and 100% HR).

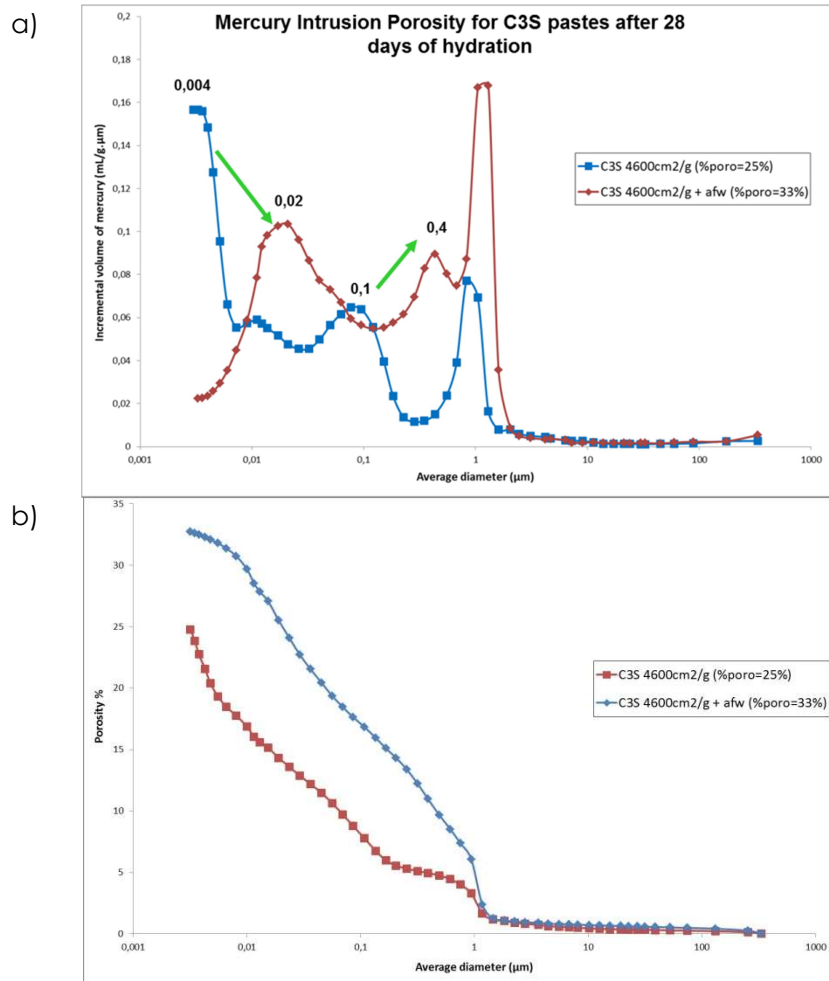


Figure 3.15 Distribution of the porosity of C<sub>3</sub>S pastes measured by MIP after 28 days of hydration: reference and seeded with germs of afwillite (wt ratio afwillite/C<sub>3</sub>S=0.02).

As for the distribution of pore sizes (Figure 3.15a), the average pore size increases in the presence of afwillite. Indeed, the seeded paste contained as many porosities of diameter > 0.05 μm while the reference C<sub>3</sub>S paste contained more porosities smaller than 0.01 μm (Figure 3.15b). If volume of pores with diameter < 0.1 μm does not change a lot, the increase of total porosity in the case of seeded paste is completely due to the porosities with diameter > 0.1 μm.



As for the distribution of pore sizes (Figure 3.15a), the average pore size increases in the presence of afwillite. Indeed, the seeded paste contained as many porosities of diameter > 0.05 µm while the reference C<sub>3</sub>S paste contained more porosities smaller than 0.01 µm (Figure 3.15b). If volume of pores with diameter < 0.1 µm does not change a lot, the increase of total porosity in the case of seeded C<sub>3</sub>S paste is completely due to the porosities with diameter > 0.1 µm.

### 3.4 Properties of hardened C<sub>3</sub>S paste seeded with afwillite germs

#### 3.4.1 Drying shrinkage of C<sub>3</sub>S paste seeded with afwillite

A C<sub>3</sub>S paste seeded with 2% afwillite and a reference C<sub>3</sub>S paste were compared in drying shrinkage study (4600 cm<sup>2</sup>/g Blaine, W/C=0.5).

For determining the water desorption isotherm and the drying shrinkage at 50% of relative ambient humidity (RH), three cylinder pastes were submitted to drying at constant temperature of (20±2)°C. The C<sub>3</sub>S pastes were casted in specific mould made of Teflon® and cured for 28 days at air (100% RH and temperature of 20°C (+/-2)).

Starting at 100% RH, the RH was reduced to 50% and the corresponding equilibrium mass water contents, as well as the variations of dimensions (considered as drying shrinkage) were measured according to time (from 1 to 28 days after the cure). The mass water content, representing the ratio between the mass of water in the specimen and the mass of the dry specimen, was determined by weighing. The constant mass of the sample was assumed when the mass changes are smaller than 0.1% of the total mass in three subsequently conducted measurements. Each cylinder was equipped of two pads allowing the measurement of the variation of dimensions of the specimen according to time. Drying shrinkage is calculated as length variation normalized by initial length (as shown in Figure 3.16a).

During the first 3 or 4 days, due to abrupt change of humidity from 100% RH to 50% RH, water evaporated from specimens rapidly generating significant drying shrinkage. Consequently, there is no clear difference between the two C<sub>3</sub>S pastes in size change. Afterwards, dimension variation of seeded paste started to be limited at a very low



speed soon within 10 days, whereas its counterpart continues to shrink at the initial logarithmic speed. Based on five months' investigation, drying shrinkage of C<sub>3</sub>S paste was significantly reduced, by a factor close to 2.5, if seeded with afwillite.

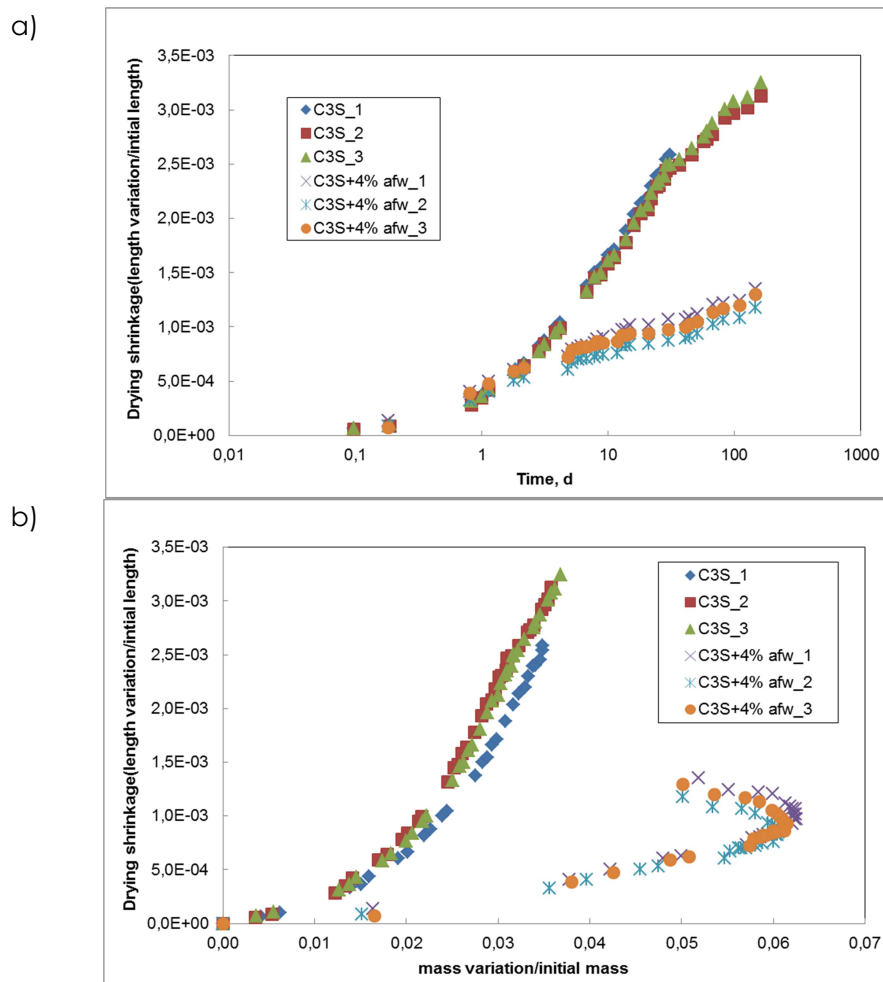


Figure 3.16. Drying shrinkage of reference C<sub>3</sub>S pastes and C<sub>3</sub>S pastes seeded with afwillite (wt ratio afwillite/C<sub>3</sub>S=0.02): (a) variation of length according to time; (b) variation of length according to the variation of mass

This finding is particularly important by proving experimentally the effect of afwillite on reducing the drying shrinkage, without letting alone the fact that seeded paste with higher porosity should be more sensible



to humidity fluctuation (on the contrary of the reference paste). Indeed, seeded paste did lose much more capillary water while being dried, as shown in Figure 3.16b. It resisted much better to water evaporation than reference paste since its drying shrinkage is several times lower at any level of water loss. Interesting side effect is that seeded paste was more easily carbonated. After about one month, seeded paste regained in mass and specimens in the end of five month contained large amount of calcium carbonate according to TGA, letting a future range of investigation about the effect of carbonation in presence of afwillite.

### 3.4.2 Compressive strength of C<sub>3</sub>S paste seeded with afwillite

Compressive strength was measured according to the EN 1015-11 standard<sup>61</sup>, after 7 and 28 days of curing at 20°C and 100% RH. Three different samples for each type of C<sub>3</sub>S pastes were tested under compression. The cylindrical pastes used as samples measured 25.0mm x 11.5mm. The compressive strength of pastes (3800 and 4600 cm<sup>2</sup>/g Blaine) seeded with afwillite (2% according to C<sub>3</sub>S weight) were compared to the ones of reference pastes. Different samples were done in order to check the influence of the W/C ratio (and the use of two distinct superplasticizers) by testing W/C of 0.5 and 0.35. As shown in Table 3.4 and Figure 3.17, and considering all the measurements done after 7 and 28 days of hydration, the compressive strength obtained in presence of afwillite are close to the ones the references pastes and may be considered as slightly higher (considering the incertitude of these experiments). The relative good performances of the seeded C<sub>3</sub>S pastes after 7 days could be explained by the higher rate of hydration than for the reference pastes, as established by the experiments of pycnometry (see Figure 3.9).

---

<sup>61</sup> EN 1015-11. (2000) Methods of test for mortar for masonry. Part 11. Determination of flexural and compressive strength of hardened mortar.



Blaine of C <sub>3</sub> S (cm <sup>2</sup> /g)	W/C	Super plasticizer- based admixtures (weight ratio/C <sub>3</sub> S=0. 004)	Afwillite seeding (weight ratio/C <sub>3</sub> S=0. 02)	Compressive strength (MPa)		
				1day	7days	28 days
3800	0.50	No	No	6	15	27
	0.50	No	Yes	6	17	19
	0.35	Optima 203	No	No hardening	54	91
	0.35	Optima 203	Yes	No hardening	45	79
4600	0.50	No	No	5	15	23
	0.50	No	Yes	6	14	17
	0.35	Optima 203	No	No hardening	90	99
	0.35	Optima 203	Yes	No hardening	91	111
	0.35	Premia 190	No	42	77	110
	0.35	Premia 190	Yes	57	85	135

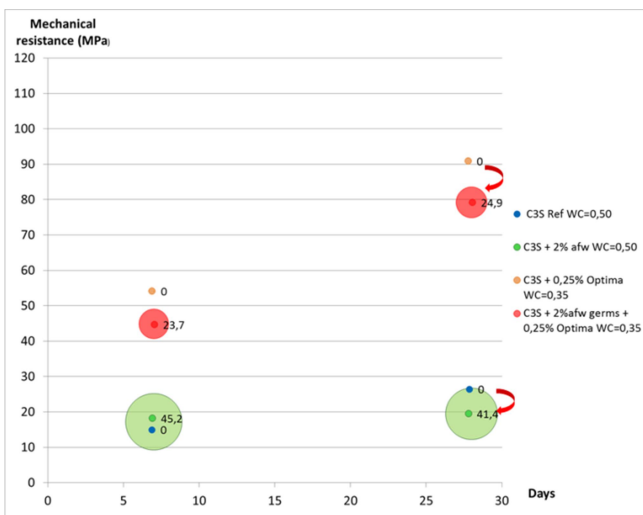
Table 3.4. Compressive strength measured on reference C<sub>3</sub>S pastes and seeded C<sub>3</sub>S pastes, according to the experimental conditions (W/C, use of superplasticizer).

Figure 3.17 allows the comparison done on C<sub>3</sub>S pastes (3800 Blaine and 4600 cm<sup>2</sup>/g Blaine, W/C=0.5 and W/C=0.35) hydrated for 28 days with the results of mechanical resistance. As demonstrated in Table 3.3, for C<sub>3</sub>S 3800 Blaine, the total porosity using afwillite germs increases and the mechanical resistance decreases in both W/C ratios. This reduction is smaller in case of W/C=0.35 (13%) than in case of W/C=0.50 (27%), maybe due to the lower porosity (11% in case of W/C=0.35 compared with 24-26% for W/C=0.50). When using C<sub>3</sub>S paste 4600 Blaine, after 28 days the total porosity using afw germs increases. The mechanical resistance for W/C=0.50 decreases a 26% when seeding with afwillite germs but in case of W/C=0.35 it increases with afwillite germs a 23% although porosity is bigger (from 6% without afwillite germs to 8.8% using them).

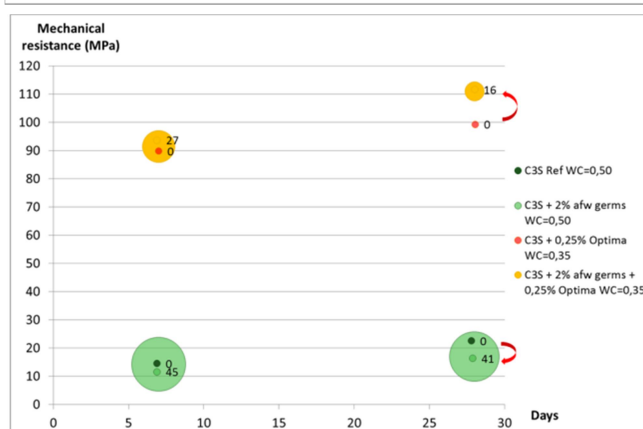


Chapter 3  
Use of C<sub>3</sub>S paste as a model to add afwillite-based filler (or seeds)

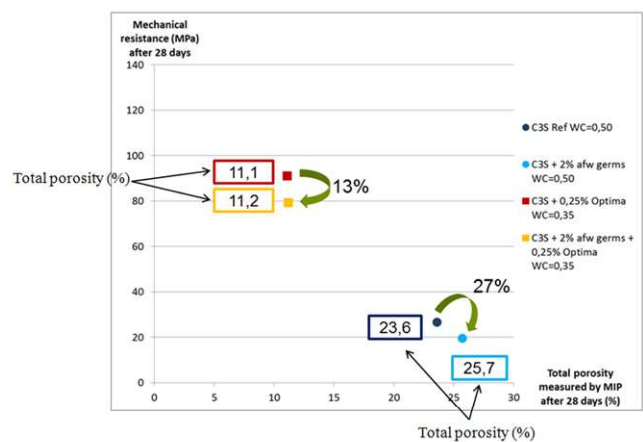
a)



b)



c)



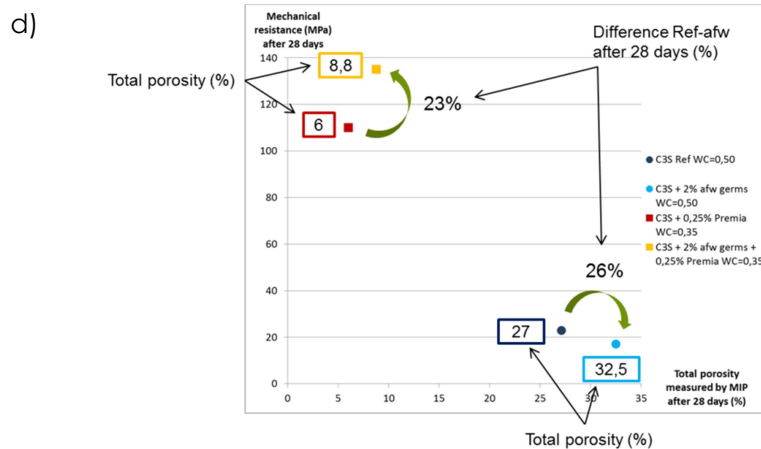


Figure 3.17 Compressive strength measured on reference C<sub>3</sub>S pastes and seeded C<sub>3</sub>S pastes: (a) compressive strength according to time for C<sub>3</sub>S 3800 cm<sup>2</sup>/g; (b) compressive strength according to time for C<sub>3</sub>S 4600 cm<sup>2</sup>/g; (c) compressive strength according to total porosity for C<sub>3</sub>S 3800 cm<sup>2</sup>/g after 28 days (%); (d) compressive strength according to total porosity for C<sub>3</sub>S 4600 cm<sup>2</sup>/g after 28 days (%)

However, the measurements performed after 28 days considering the pastes at W/C=0.5 (and whatever the Blaine) suggest that coarse microstructure of the seeded pastes seems to weaken the samples under compression stress. The difference of mechanical resistance in favor of the reference paste is the most significant after 28 days with the pastes done at W/C=0.5 (this conditions giving the highest rate of afwillite, as indicated by Table 3.3). The difference of mechanical resistance between reference and seeded pastes is lower using W/C ratio of 0.35 (and using superplasticizers) but this result could be explained by the lower rate of afwillite of this kind of samples.



## **Chapter 4**

---

### **Influence of the addition of afwillite on cement paste**





#### 4.1. Introduction

The shrinkage of cement paste results not only from the volume change due to hydration reaction of the compounds with water but also from the interaction between the paste and the environment.<sup>57,62</sup> This drying shrinkage occurs mainly after paste setting and may lead to subsequent cracking, which is widely present in concrete and becomes severely harmful in certain insulating and lightweight concrete with high porosity. Indeed, the drying shrinkage is closely related to capillary tension in the pores of cement paste, which can be expressed as twice the surface tension divided by the pore radius.<sup>53</sup> Thus, it is possible to reduce shrinkage by reducing capillary pore tension by increasing pore size. This work was focused on this second way and the possibility of reducing drying shrinkage by replacing amorphous C-S-H gel network in cement paste with crystalline afwillite ( $\text{Ca}_3\text{Si}_2\text{O}_7 \cdot 3\text{H}_2\text{O}$ ) network with larger pores.<sup>63,60</sup>

The balance between the different phases in the  $\text{CaO}-\text{SiO}_2-\text{H}_2\text{O}$  system is highly dependent on thermodynamic conditions. Under ambient conditions, C-S-H amorphous form is a stable phase but the synthesis of afwillite could be performed under hydrothermal conditions,<sup>64,65</sup> the afwillite probably being a crystalline phase stable. Then, the synthesis of this compound under a variety of conditions was studied in different works. Afwillite can be synthesized from ball-mill hydration of  $\text{C}_3\text{S}$  slurry at room temperature.<sup>45</sup> Saito and co-workers used the same grinding process to produce successfully afwillite from lime and silica.<sup>66</sup> Moreover, other studies confirmed that hydration of  $\text{C}_3\text{S}$  would produce afwillite, instead of C-S-H gel.<sup>53</sup> Indeed, Davis and Young proved then seeding  $\text{C}_3\text{S}$  paste with afwillite helps to increase total porosity by 15-25%.<sup>56</sup>

---

<sup>62</sup> Baroghel-Bouny V, Godin J. (2001) Experimental study on drying shrinkage of ordinary and high-performance cementitious materials, *Concrete Science Engineering*, 3: 13-22.

<sup>63</sup> Petch HE, Sheppard N, Megaw HD. (1956) The infra-red spectrum of afwillite,  $\text{Ca}_3(\text{SiO}_3\text{OH})_2 \cdot \text{H}_2\text{O}$ , in relation to the proposed hydrogen positions. *Acta Crystallographica*, 9:29-34.

<sup>64</sup> Hong SY, Glasser FP. (2004) Phase relations in the  $\text{CaO}-\text{SiO}_2-\text{H}_2\text{O}$  system to 200°C at saturated steam pressure, *Cement Concrete Research*, 34:1529-1534.

<sup>65</sup> Glasser FP, Hong SY. (2003) Thermal treatment of C-S-H gel at 1 bar  $\text{H}_2\text{O}$  pressure up to 200 °C. *Cement Concrete Research*, 33:271-279.

<sup>66</sup> Saito F, Mi G, Hanada M. (1997) Mechanochemical synthesis of hydrated calcium silicates by room temperature grinding. *Solid State Ionics*, 101-103: 37-43.



In the previous Chapter nº3, an effective synthesis of afwillite from ball-mill hydration of C<sub>3</sub>S-based slurry and an efficient growth of afwillite after seeding C<sub>3</sub>S pastes has been demonstrated, allowing the reduction by 2.5 times of the drying shrinkage. This present chapter is dedicated to the synthesis of afwillite from cement-based diluted slurries under ball-mill hydration and to the growth of afwillite in seeded cement-based pastes.

Different experiments have been undertaken according to the composition of Portland cement but also by testing specific cement: a oil-well cement (containing practically no tri-calcium aluminate but a high content of ferrite). For every samples obtained (slurry or hardened paste), the rate of afwillite was quantified by thermo-gravimetric analysis (TGA).<sup>52</sup> The influences of the W/C ratio, the addition of superplasticizer and some curing temperature were studied to find the best conditions that would favour the growth of afwillite. Moreover, some tests of seeding were also performed in slurries or pastes containing synthetic alite or various C<sub>3</sub>S/C<sub>3</sub>A ratios in order to model the growth of afwillite in presence of impurities and calcium aluminates. Finally, the drying shrinkage properties of seeded pastes<sup>67</sup> were studied to detect a possible influence of the coarse microstructure induced by the growth of afwillite.

## 4.2 Reactivity of different cement-based diluted slurries

### 4.2.1 Use of slurry to synthesize afwillite germs: preparation of the specimens

The synthesis of afwillite was realized within hydration of cement-based slurries under different ball-mill conditions. A mixer Turbula® T2F (WAB, Muttenz, Switzerland) was used for the synthesis experiments. All the conditions of ball-mill process were the same than in Chapter nº3. The cement was mixed with large amount of demineralised water in order to obtain diluted slurry (W/C=9).

The milling process was produced by mixing the slurry with balls made of stainless steel (1 cm of diameter) in the Turbula®. The balls/Cement (B/C) weight ratio of 23.4 was used. All batches were treated with a continuous milling. Each slurry (see Table 4.1) was sampled after 24h, 48h,

<sup>67</sup> Theiner Y, Hofstetter G. (2012) Evaluation of the effects of drying shrinkage on the behavior of concrete structures strengthened by overlays. Cement Concrete Research, 42: 1286-1297.



72h and until 7 or 14 days of hydration, then dried under vacuum to remove the excess of water, in order to track the growth of afwillite (using TGA and XRD) according to time. Measurements by TGA establish variations in the mass of the two main phases (afwillite and portlandite) resulting from hydration of alite contained into the cement. TGA data were recorded in a nitrogen atmosphere on a Setaram TGA/SBTA851 analyser from 20 mg of sample from room temperature to 800°C at a scan rate of 10°C/min. The specific peak at 320°C was assigned to afwillite, which is relevant considering previous values found in literature (250-450°C<sup>51</sup> and 340°C <sup>iError! Marcador no definido.<sup>63</sup> respectively). Moreover, the respective peaks at 450°C and 680°C, such as used commonly in literature<sup>53</sup>, were used to quantify the amount of portlandite and, eventually, carbonates. A peak at 90-120°C can characterize C-S-H but their quantification is not relevant by TGA, considering the removal of residual water molecules coming from the sample. Moreover, distinct peaks highlight respectively ettringite and calcium sulfoaluminate. The amount of ettringite depends on C<sub>3</sub>A (and C<sub>4</sub>AF) contained in each type of cement but its characteristic TGA peak (about 150°C) should not affect the quantification of afwillite.</sup>

Type of Cement (factory)	Blaine (cm <sup>2</sup> /g)	Alite (%w)	Belite (%w)	Tri-calcium aluminate (%w)	Ferrite (%w)	MgO (%)	K <sub>2</sub> O (%)	Na <sub>2</sub> O (%)	D10	D50	D90
White OPC n°1 (Le Teil)	4600	69	22	4	0.5	0.6	0.4	0.2	3.2	12.8	36.2
White OPC n°2 (Le Teil)	4600	65	27	3	0.1	0.5	0.5	0.3	2.3	13.3	36.8
	6890								1.9	11.8	36.2
Grey HTS OPC (Le Teil)	4600	63	23	1.4	8	0.9	0.2	0.1			
	6000								1.7	8.3	47
Grey OPC (SPLC)	4600	61	16	6.6	10.5	1	0.9	0.2	2.6	15.5	42.6
Oil-well (Joppa)	3120	68	10	0.7	14	0.8	0.6	0.2	3.3	18.1	69.1

Table 4.1. Composition and granulometry (Blaine, D10, D50, D90) of the different cements tested (the weight ratios from Rietveld X-Ray diffraction and X-ray Fluorescence measurements).



On the contrary, the peak assigned to the calcium sulfoaluminate (about 380°C) was detected after a cure at high temperature and was more disturbing to quantify the afwillite. Note that all the contents of afwillite discussed in this work were compared to the maximum content theoretically possible to form, which depends on the content of alite composing the cement (as previously explained but also confirmed by new experiments, belite, ferrite or tri-calcium aluminate were not supposed to form afwillite under the ball-mill conditions tested). XRD analyses were made as described in Chapter n°3.

#### 4.2.2 Granulometry (Blaine) of cements

As shown by Table 4.1, different Blaine have been used for some cements (white and grey HTS OPC) to establish the effect of the fineness. The grinding of cement was performed using a planetary Ball Mill agate (PM 400 from Retsch Technology GmbH).

#### 4.2.3 Superplasticizer-based admixtures

The cement is mixed with two distinct superplasticizer-based admixtures (Chryso® Fluid Optima 203 and Premia 196), which are supposed to influence the hydration rate in certain conditions. A weight ratio of (dried extract) superplasticizers compared to cement=0.035 was used into cement-based slurries ( $W/C=9$ ) milled into the Turbula®; while a weight ratio (dried extract of superplasticizer/cement) of 0.004 was used to mix cement-based pastes ( $W/C$  of 0.50 or 0.35) manufactured to study the properties at hardened state.

#### 4.2.4 “Pre-seeding” of slurry with afwillite germs

The afwillite successfully produced after ball-mill hydration of C<sub>3</sub>S-based slurry is used as germs to seed the slurries of cement before being hydrated under ball-mill. Before use, the germs were purified by leaching the co-product (calcium hydroxide) with demineralized and de-carbonated water (by boiling process) until the pH went below the one of saturated solution of calcium hydroxide, which is 12.7. The dosage of this “pre-seeding” was defined to mix the afwillite germs (final purity close to 90 %, weight ratio compared to cement=0.02) with cement powder before adding water to form a slurry.



Note also that a similar procedure was used to seed slurries composed of C<sub>3</sub>S and alite in order to study the influence of the composition of alite (and its content of impurities) on the growth of afwillite during ball-mill hydration.

#### 4.2.5 Combine afwillite-based pre-seeding and superplasticizer

For specific cases, the cement was mixed in Turbula® with one of the admixture and afwillite (pre-seeding) germs (respective weight ratios of 0.035 and 0.02 compared to cement).

#### 4.2.6 Effects of the type of cement and granulometry (Blaine)

Several reference slurries (W/C=9, B/C=23.4) were tested in Turbula® in order to establish the influence of the ball-mill hydration according to the composition of cement and their granulometry (Blaine). The highest contents of afwillite were detected after 48-72h of hydration for all the Portland and oil well cements. (Figure 4.1).

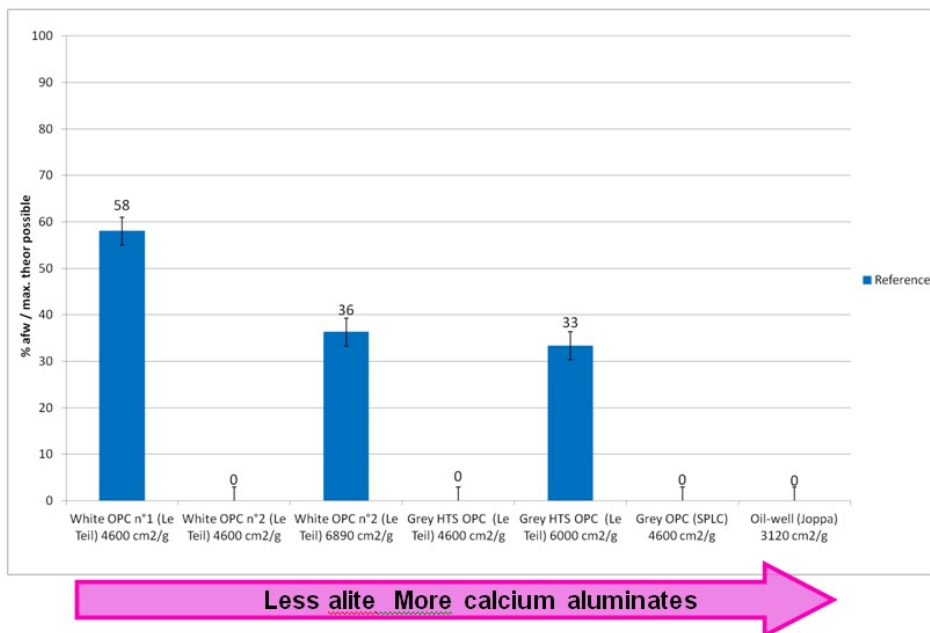


Figure 4.1. Contents of afwillite synthesized by ball-mill hydration according to the type of cement and granulometry (Blaine)



As shown by the TGA results detailed in Figure 4.1, the reference slurry containing white OPC n°1 ( $4600 \text{ cm}^2/\text{g}$  Blaine, containing 69% of alite) gave the best result in terms of growth of afwillite (58% of the maximum theoretically possible, deduced from the Eq. (4.1)).



**Ca<sub>3</sub>SiO<sub>5</sub>** : alite

**Ca<sub>3</sub>Si<sub>2</sub>O<sub>7</sub>** : rankinite

**Ca(OH)<sub>2</sub>** : calcium hydroxide

This white OPC n°1 was the only one able to grow afwillite using a common Blaine. However, the slurries based on white OPC n°2 or grey HTS OPC with high Blaine ( $6000$  and  $6890 \text{ cm}^2/\text{g}$  respectively) allowed also the growth of afwillite. Moreover, no afwillite was detected (until 7-14 days of ball-mill hydration) using the reference slurries containing grey OPC (SPLC) and oil well cements, which were characterized by a low ratio or an absence of alite and a high ratio in tri-calcium aluminate and/or ferrite.

In conclusion, these results about reference slurries indicated that the growth of afwillite under ball-mill hydration was first governed by the content of alite (which is necessary to generate afwillite) but also by the interstitial phases (made of tri-calcium aluminate and ferrite) that may poison the growth of afwillite from the surface of alite. The granulometry (Blaine) may be also considered such as a second order parameter that may boost the growth of afwillite using certain cements (containing a low content in tri-calcium aluminate such as white OPC n°2 and grey HTS OPC). The action of the grinding process could be more complex to understand because this process could affect heterogeneously the final size of different phases composing the cement.

#### 4.2.7 Influence of the superplasticizer-based admixtures

Different cements were hydrated in Turbula® using W/C=9 and B/C=23.4 and in presence of superplasticizers (which could disturb hydration at early age but also would improve the fluidity and mixing). As



showed in Figure 4.2, the effects of Premia 196 and Optima 203 were similar in terms of final content of afwillite. The main difference was that Optima 203 delayed the hydration rate for about one day and, then, delayed the time when the maximum rate of afwillite was detected.

The addition of superplasticizer seems to affect the growth of afwillite using white OPC n°1 (containing a highest content in alite and working the best as reference slurry to synthesize afwillite). On the other hand, the results highlighted that superplasticizers helped in creating afwillite in slurries containing belite and Portland cements (white n°2, grey HTS and grey SPLC with Blaine close to 4600 cm<sup>2</sup>/g). At this stage of the study, we did not understand the mechanism responsible for the positive action of superplasticizer in terms of growth of afwillite but we could hypothesize that the superplasticizers would interact with the dissolution of tri-calcium aluminate composing the interstitial phase.

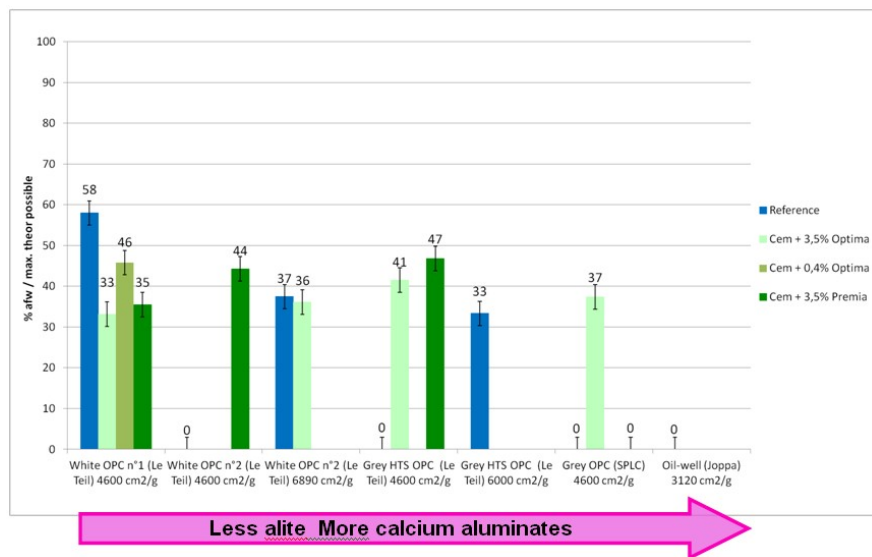


Figure 4.2. Influences of the addition of superplasticizers into the cement-based slurries on the synthesis of afwillite by ball-mill hydration.

#### 4.2.8 Seeding of cement-based slurries with afwillite germs

Germs of afwillite successfully produced using a C<sub>3</sub>S-based slurry (4600 cm<sup>2</sup>/g Blaine, W/C=9, B/C=23.4) after 48h in Turbula® were used to seed cement-based slurries hydrated by ball-milling (weight dosage of 0.02 afwillite compared to cement). As shown by Figure 4.3, a little more



afwillite was detected after 48h of ball-mill hydration using white OPC n°1 (64% of the maximum afwillite theoretically possible, compared to 58% without pre-seeding).

The comparison of the results according to the type of cement used seems to show that the positive influence of the "pre-seeding" with afwillite was generally less effective when the cement contained less alite.

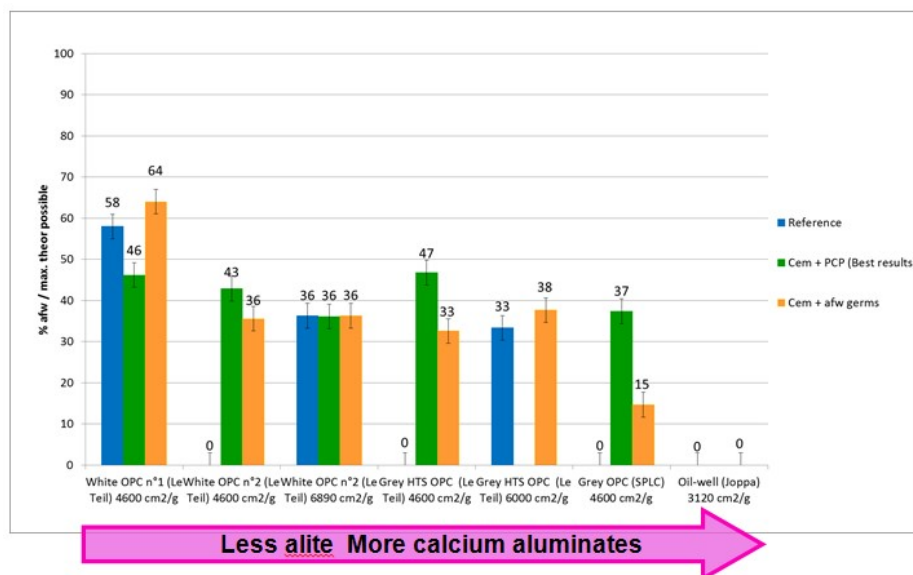


Figure 4.3. Influences of the addition of superplasticizers and afwillite pre-seeds into the cement-based slurries on the synthesis of afwillite by ball-mill hydration

#### 4.2.9 Seeding of slurries with afwillite germs and superplasticizer

The effect of combining the additions of afwillite and superplasticizers was tested (respective dosages of 0.02 and 0.035 (dried extract) compared to cement). As showed in Figure 4.4, synergy between additions of superplasticizers and afwillite germs was detected using all the type of cements tested. The maximum content of afwillite (reaching 74% of the maximum possible rate) was still always detected by using white OPC n°1 (Blaine of 4600 cm<sup>2</sup>/g, containing the highest rate of alite). This positive synergy was also efficient to enhance the growth of afwillite by using the other Portland and oil well cements (containing a more significant rate of tri-calcium aluminate/ferrite).

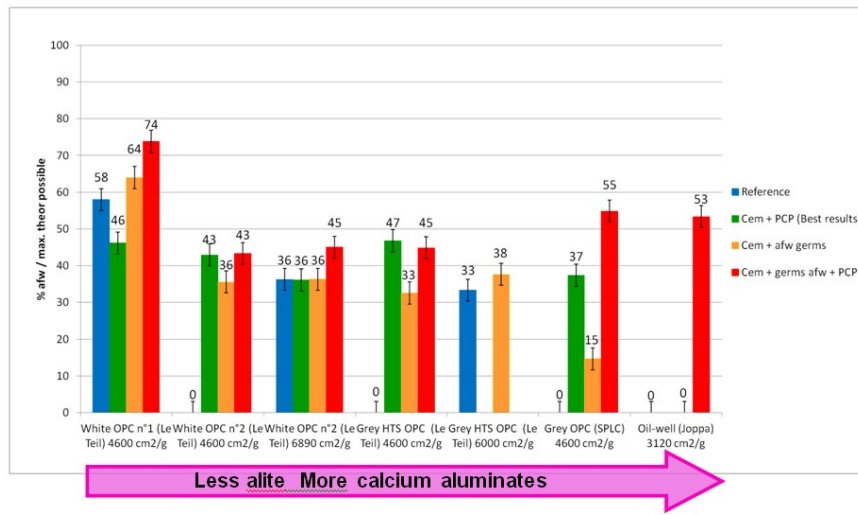


Figure 4.4. Influences of the addition of superplasticizers and afwillite pre-seeds into the cement-based slurries on the synthesis of afwillite by ball-mill hydration

### 4.3 Growth of afwillite in seeded cement-based pastes

#### 4.3.1 Seeding of cement-based pastes: Preparation of the specimens

Many reference and seeded cement pastes were manufactured (as detailed in Table 4.2) to detect the growth of afwillite according to time (mainly by TGA) and to study the influence of this seeding on drying shrinkage properties.

The afwillite germs were carefully mixed after grinding with cement powder (weight ratio compared to cement=0.02) before adding water. The same procedure of mixing was used for seeded pastes composed of  $\text{C}_3\text{S}+\text{C}_3\text{A}$  in order to model the influence of the calcium aluminates on the growth of afwillite. The different  $\text{C}_3\text{S}:\text{C}_3\text{A}$  ratios tested were: 95:5; 99:1; 100:0. The dosage of afwillite was also 0.02 compared to the weight content of  $\text{C}_3\text{S}$ .

Water to cement (or  $\text{C}_3\text{S}$ ) ratio of 0.5 was mainly used to manufacture these pastes. Other W/C ratios such as 0.70 and 0.35 were also used to perform a few tests with certain cements. In other cases (mainly by using W/C=0.35), superplasticizer-based admixtures (weight ratio/cement=0.004 (dried extract)) were also added to improve the mixing of the paste.



Type of cement (factory)	Blaine (cm <sup>2</sup> /g)	W/C	Superplasticizer (ratio /Cement)	Curing T <sup>a</sup> (°C)	Methods of characterization
White OPC n°1 (Le Teil)	4600	0.70	0	20°C	TGA
		0.50	Premia (0.004)	20°C	TGA
		0.50	Optima (0.004)	20°C	TGA
		0.50	0	20°C	TGA; XRD
		0.50	0	80°C	TGA; drying shrinkage
		0.35	0	20°C	TGA
		0.35	Premia (0.004)	20°C	TGA; drying shrinkage
		0.35	Premia (0.004)	80°C	TGA
		0.35	Optima (0.004)	20°C	TGA
		0.35	Optima (0.01)	20°C	TGA
White OPC (Le Teil) n°2	4600	0.50	0	20°C	TGA; XRD; drying shrinkage
		0.50	0	20°C	TGA; XRD; drying shrinkage
	6890	0.35	Premia (0.004)	20°C	TGA
		0.35	Premia (0.004)	80°C	TGA
		0.50	0	80°C	TGA
Grey HTS OPC (Le Teil)	6000	0.50	0	80°C	TGA
		0.35	Premia (0.004)	20°C	TGA
Grey OPC (SPLC)	4600	0.70	0	20°C	TGA
		0.50	Premia (0.004)	20°C	TGA
		0.50	Optima (0.004)	20°C	TGA
		0.50	0	20°C	TGA; XRD; drying shrinkage
		0.50	0	80°C	TGA; drying shrinkage
		0.35	No	20°C	TGA
		0.35	Optima (0.004)	20°C	TGA
		0.35	Premia (0.004)	20°C	TGA; drying shrinkage
		0.30	Optima (0.004)	20°C	TGA
Oil-well (Joppa)	3120	0.50	0	80°C	TGA; XRD; drying shrinkage
		0.35	Optima (0.004)		TGA
		0.35	Premia (0.004)		TGA
		0.30	Optima (0.004)		TGA

Table 4.2. Summary of the experimental conditions and characterization methods used to study the growth of afwillite in cement pastes and its consequence on the drying shrinkage properties. All the cement pastes were manufactured as reference or using the seed with afwillite germs (weight ratio/Cement=0.002).



Most of the cement pastes were casted in 5 mL polyethylene-based sealed tubes, except the ones dedicated to the drying shrinkage experiments, which were casted into cylindrical Teflon-based mould (160 mm×20 mm). As detailed in Table 4.2, most of the samples were cured at 100% relative humidity and 20°C during 7 or 28 days before being characterized. However, certain cement pastes were cured at 80°C until 28 days to establish if this higher temperature would favor the hydration in afwillite and because this temperature remains necessary to hydrate the oil-well cement tested (containing a very low content of C<sub>3</sub>A).

Before performing TGA quantification, hydration of the hardened pastes was first stopped by immersing in isopropanol for 2+7 days (solution renewed after 2 days), and then dried in high vacuum, before being grounded to powder finer than 63 µm.

#### 4.3.2 *Growth of afwillite in seeded cement-based pastes*

Table 4.3 details the contents of afwillite detected by TGA after 7 or 28 days of hydration of the cement-based pastes (cure at 20°C/100% RH). The influences of the type of cement, the W/C ratio and the curing temperature have been then investigated.

The results highlighted that content of afwillite reached practically its maximum rate after 7 days of hydration. No specific variation about the rate of afwillite was detected between 7 and 28 days, showing a rapid kinetics of hydration induced by seeding with afwillite germs and confirming previous results obtained with seeded C<sub>3</sub>S-based pastes.

In one hand, the seeding done with "pure" afwillite germs allowed the shift of C-S-H to afwillite in the cement-based pastes. Indeed, the rate of afwillite increased from 2% (initial seeding) to 20-45% during the first 7 days and kept going up stable or slowly up to 28 days. On the other hand, the growth of seeding seems to be limited to 26% (+/-3%) at ambient temperature whatever the composition and the granulometry of the OPC tested, as shown by the TGA results detailed in Figure 4.5.



Type of cement (factory)	Blaine (cm <sup>2</sup> /g)	W/C	Superplasticizer (ratio /Cement)	Curing temperature (°C)	Rate of afwillite (/theoretical maximum)	
					7 days	28 days
White OPC n°1 (Le Teil)	4600	0.70	None	20°C	24	Not measured
		0.50	Optima 203	20°C	26	Not measured
		0.50	Premia 196	20°C	29	Not measured
		0.50	None	20°C	23	25
		0.50	None	80°C	23	21
		0.35	None	20°C	26	Not measured
		0.35	Optima 203	20°C	26	29
		0.35	Optima203(0.01)	20°C	27	17
		0.35	Premia 196	20°C	28	19
		0.35	Premia 196	80°C	25	27
		0.30	Optima 203	20°C	23	20
White OPC (Le Teil) n°2	4600	0.50	None	20°C	19	13
		0.35	Premia 196	20°C	30	22
		0.35	Premia 196	80°C	22	23
Grey HTS OPC (Le Teil)	6000	0.50	None	80°C	29	Not measured
		0.35	Premia 196	20°C	30	17
Grey OPC (SPLC)	4600	0.70	None	20°C	32	Not measured
		0.50	Optima 203	20°C	32	Not measured
		0.50	Premia 196	20°C	31	Not measured
		0.50	None	20°C	31	28
		0.50	None	80°C	45	40
		0.35	None	20°C	34	Not measured
		0.35	Optima 203	20°C	27	28
		0.35	Premia 196	20°C	28	23
		0.30	Optima 203	20°C	27	29
Oil-well (Joppa)	3120	0.50	No	80°C	21	20
		0.35	Optima 203		17	22
		0.35	Premia 196		22	20
		0.30	Optima 203		27	29



Table 4.3. Comparison between the content of afwillite detected by TGA in cement-based pastes (with/without seeding, according to the W/C ratio). All the cement pastes were manufactured as reference or using the seed with afwillite germs (weight ratio/cement=0.002).

No specific influence of the W/C ratio or superplasticizers was highlighted according to the uncertainty of the quantification of the afwillite by TGA (due to the peak of calcium sulfoaluminate). Indeed, these results were in contradiction to those demonstrated by hydrating the slurries in the Turbula® (showing a higher increase of the contents of afwillite). They could highlight a positive effect of the continuous ball milling done into the Turbula®, which would clean the surface of afwillite during its growth and would remove the other "contaminants" contained into the alite or produced during hydration of calcium aluminates.

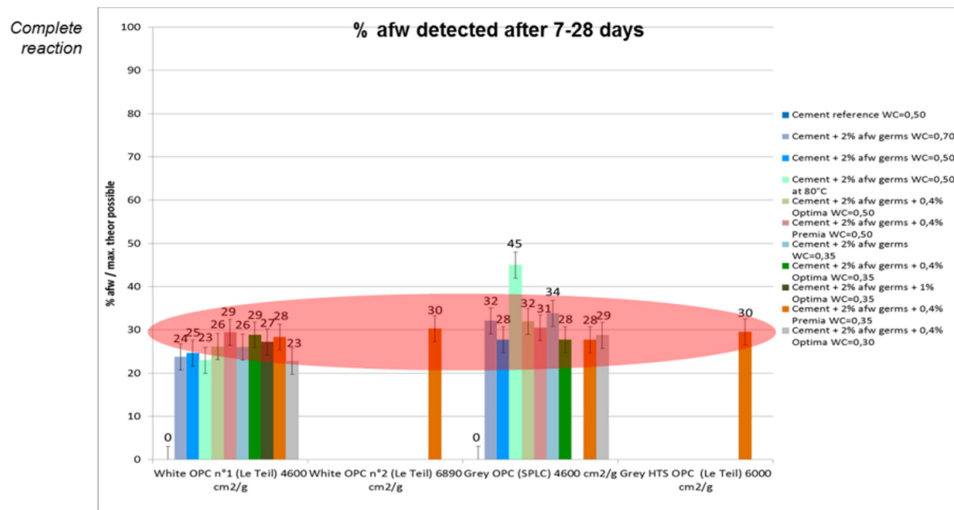


Figure 4.5. Influences of the type of cement, the W/C ratio and the use of PCP in cement pastes.

The effect of the curing temperature was also studied, supposing that afwillite would be more stable at higher temperature than C-S-H and because the oil well cement is commonly hydrated at higher temperature than OPC. The use of oil well cement seems to be a little less efficient to promote the growth of afwillite after 7 days of hydration. Maybe, the growth of afwillite would be delayed due to the specific composition and crystallography of this kind of cement (which contains



a high content of ferrite and where alite crystals are known to be bigger than the ones contained in OPC). Finally, the highest rate of afwillite (close to 40-45% of the maximum possible) was finally detected after hydration of grey OPC SPLC at 80°C, as shown in Figure 4.6, which was a too high temperature for a common use of this kind of OPC. This significant growth of afwillite after curing at 80°C could indicate a possible influence of the  $\text{Ca}(\text{SO}_4)_{1/2}$ .

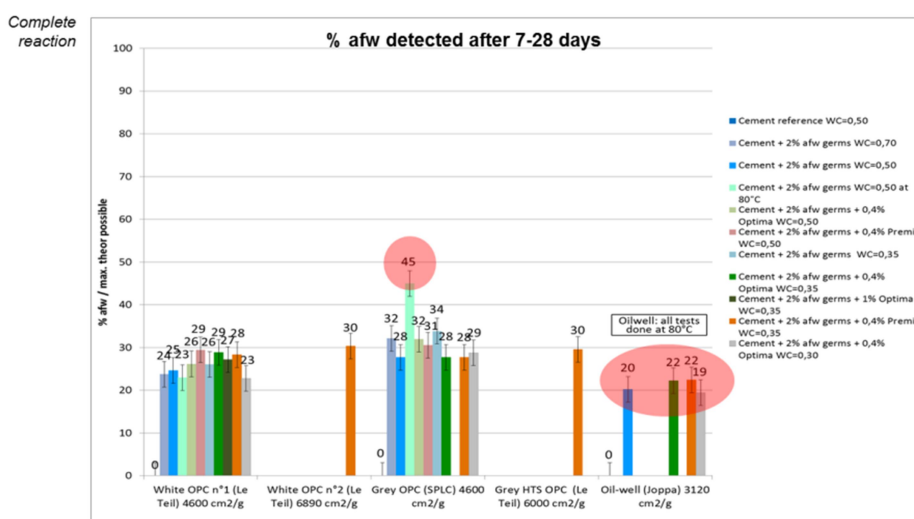


Figure 4.6. Influences of the curing temperature in cement pastes.

#### 4.4 Growth of afwillite in alite-based diluted slurry and $\text{C}_3\text{S}/\text{C}_3\text{A}$ pastes

##### 4.4.1 Maximum $\text{C}_3\text{A}$ percentage allowable to obtain afwillite

Figure 4.7 shows the maximum rate of afwillite measured by TGA after the seeding of alite-based slurry ( $\text{W/C}=9$ ), which was compared to the ones obtained with the slurries made of  $\text{C}_3\text{S}$  and white OPC n°1.

A maximum rate close to 72% of afwillite was measured after ball mill hydration of alite. This value is similar to the one obtained with white OPC n°1 but slightly lower than the one obtained with  $\text{C}_3\text{S}$ -based slurry. Indeed, even under the best conditions of hydration (using a Turbula®), the impurities contained into the microstructure of alite would affect the growth of afwillite and could explain the relative loss of reactivity



observed under ball-milling between C<sub>3</sub>S and white cement (for a same granulometry). This new result cannot explain by itself the low rate of afwillite detected using the seeded cement-based pastes.

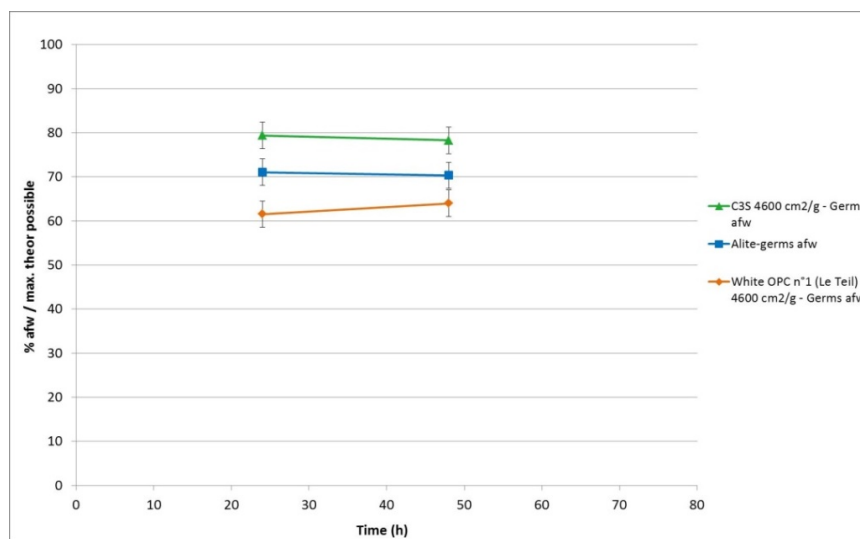


Figure 4.7. Growth of afwillite in seeded slurries made of C3S, alite and white OPC Le Teil n°1

#### 4.4.2 Different C<sub>3</sub>S ratios vs amount of afwillite

Other experiments were then done using specific seeded pastes (W/C=0.5) made of different ratios of C<sub>3</sub>S/C<sub>3</sub>A with the intention of study the influence of the calcium aluminate on the growth of afwillite.

As shown by Figure 4.8, the influence of mixing 1, 3 or 5% of C<sub>3</sub>A with C<sub>3</sub>S decreased significantly the growth of afwillite. The final contents of afwillite (close to 17 +/-2%) were non-negligible after 7 and 28 days in presence of C<sub>3</sub>A but significantly lower than the one measured with seeded C<sub>3</sub>S-based pastes (about 43% +/-2%). Indeed, the presence of calcium aluminate seems to affect the growth of afwillite, explaining why the final content of afwillite measured in seeded cement-based pastes did not exceed a value close to 25%.

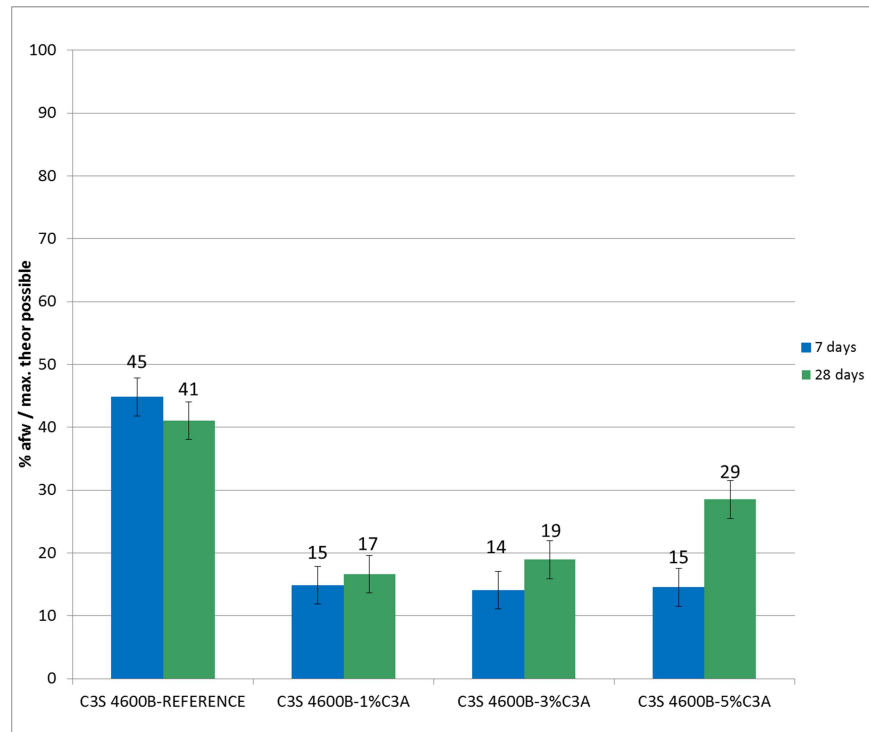


Figure 4.8. Growth of afwillite in seeded pastes made of various C<sub>3</sub>S/C<sub>3</sub>A ratios

As a conclusion, the tests done using seeded alite-based slurries and C<sub>3</sub>S+C<sub>3</sub>A based pastes highlights two potential inhibitors for the growth of afwillite: (i) the impure microstructure of alite and (ii) the presence of calcium aluminates.

#### 4.5 Drying shrinkage properties and porosity of seeded cement pastes

Even if the analyses did not show any significant growth of afwillite into the seeded pastes cured at 20°C (maximum close to 26% as shown in Table 4.3), the drying shrinkage properties were studied to check if a relative small growth of afwillite would be sufficient to induce a coarser microstructure (as already demonstrated with C<sub>3</sub>S-based paste). To determine the water desorption isotherm and the drying shrinkage at 50% of relative ambient humidity (RH), three cement cylinder pastes of each mixture were submitted to drying at constant temperature of (20±2)°C.



As shown by Table 4.4 and Figure 4.9, different cement-based pastes were casted in specific mould made of Teflon® and cured for 28 days at air (100% RH and temperature of 20°C ( $\pm 2$ )°C). Moreover, other seeded cement pastes were cured for 28 days in hot water (80°C) before being analysed. Starting at 100% RH, the RH was reduced to 50% and a corresponding equilibrium mass water contents, as well as the variations of dimensions (considered as drying shrinkage) were measured according to time (from 1 to 28 days after the cure). The mass water content, representing the ratio between the mass of water in the specimen and the mass of the dry specimen, was determined by weighing. The constant mass of the sample was assumed when the mass changes are smaller than 0.1% of the total mass in three subsequently conducted measurements. Each cylinder was equipped of two pads allowing the measurement of the variation of dimensions of the specimen according to the time of drying. Most of the experiments concerned cement-based pastes mixed with W/C ratio of 0.5 but certain ones were also done on pastes mixed with superplasticizer and using W/C ratio of 0.35.

a)



b)



Figure 4.9. Cement-based pastes done for shrinkage measurements:  
(a) three cement cylinder pastes of each mixture; (b) measurement of the variation of dimensions of each cylinder according to the time of drying.



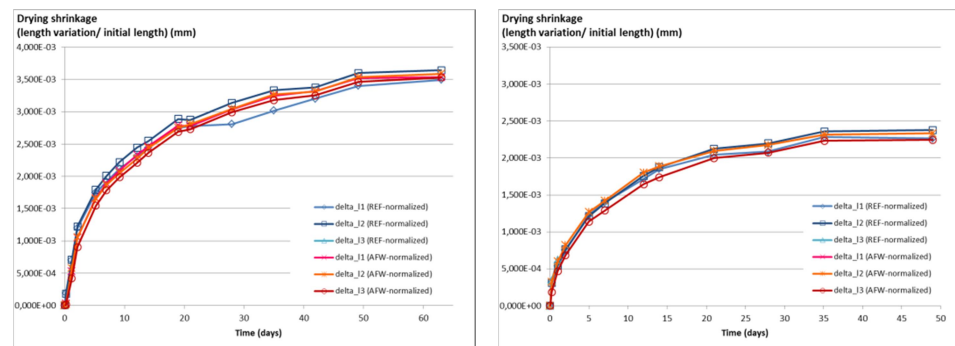
Type of cement (factory)	Blaine (cm <sup>2</sup> /g)	W/C	Seeding with afwillite germs (weight ratio/cement =0.02-0.04)	Superplasti-cizers (weight ratio/Cement =0.004)	Curing T <sup>a</sup> (°C)	Rate of afwillite (/theoretic al maximum)	Total porosity measured by MIP after 28 days (%)
White OPC n°1 (Le Teil)	4600	0.50	No	None	20°C	0	Not measured
		0.50	Yes (0.04)	None	20°C	Not measured	Not measured
		0.50	No	None	80°C	0	Not measured
		0.50	Yes (0.02)	None	80°C	30	Not measured
White OPC (Le Teil) n°2	6890	0.50	No	None	20°C	0	23,5
		0.50	Yes (0.02)	None	20°C	0	22,9
Grey OPC (SPLC)	4600	0.50	No	None	20°C	0	29,1
		0.50	Yes (0.02)	None	20°C	0	28,8
		0.50	No	None	80°C	0	Not measured
		0.50	Yes (0.02)	None	80°C	38	Not measured
		0.50	No	None	20°C	0	Not measured
		0.50	Yes (0.04)	None	20°C	Not measured	Not measured
		0.35	No	Premia 196	20°C	0	18,4
		0.35	Yes (0.02)	Premia 196	20°C	0	18,1
Oil-well (Joppa)	3120	0.50	No	None	80°C	0	Not measured
		0.50	Yes (0.02)	None	80°C	16	Not measured

Table 4.4. Samples done for shrinkage measurements (with/without seeding with afwillite germs, according to the W/C ratio) and the total porosity measured by MIP.

As shown by Figure 4.10, similar drying shrinkage results were measured with reference and seeded OPC-based pastes previously cured at 20°C during 28 days (whatever the W/C ratio used). No specific influence of the seeding with afwillite was highlighted about the variation of length according to the time of drying. Note also that other tests (not shown) done with white cement paste (OPC n°1) seeded with 4% of afwillite did not highlight better results in terms of reduction of the drying shrinkage.



(a) white OPC Le Teil n°2 (W/C=0.5)      (b) grey OPC SPLC (W/C=0.5)



(c) grey OPC SPLC (W/C=0.35)

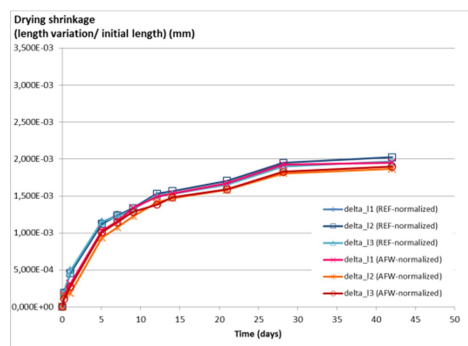


Figure 4.10. Drying shrinkage properties of reference and seeded cement pastes cured at 20°C

We also measured the total porosity by Mercury Intrusion Porosimetry technique (MIP), described in Chapter n°3. As shown in Table 4.5, we didn't observe any difference between the reference and seeded cement pastes, due to the absence of afwillite on these samples.

Sample	Porosity (%)
White OPC n°2 (Le Teil) 6890 Blaine - Reference WC=0,50	23.5
White OPC n°2 (Le Teil) 6890 Blaine +2%afw WC=0,50	22.9
Grey OPC (SPLC) 4600Blaine - Reference WC=0.50	29.1
Grey OPC (SPLC) 4600Blaine +2%afw WC=0.50	28.8
Grey OPC (SPLC) 4600Blaine + Premia 196 WC=0.35	18.4
Grey OPC (SPLC) 4600Blaine + Premia 196 +2%afw WC=0,35	18.1

Table 4.5. Total porosity measured by MIP.



As shown by Figure 4.11, the tests done on cement-based pastes (and more especially with oil-well cement) cured at 80°C during 28 days were not able to establish a possible reduction of the drying shrinkage due to afwillite: the complete hydration of each paste did not allow the measurement of length variations after 5 days of drying.

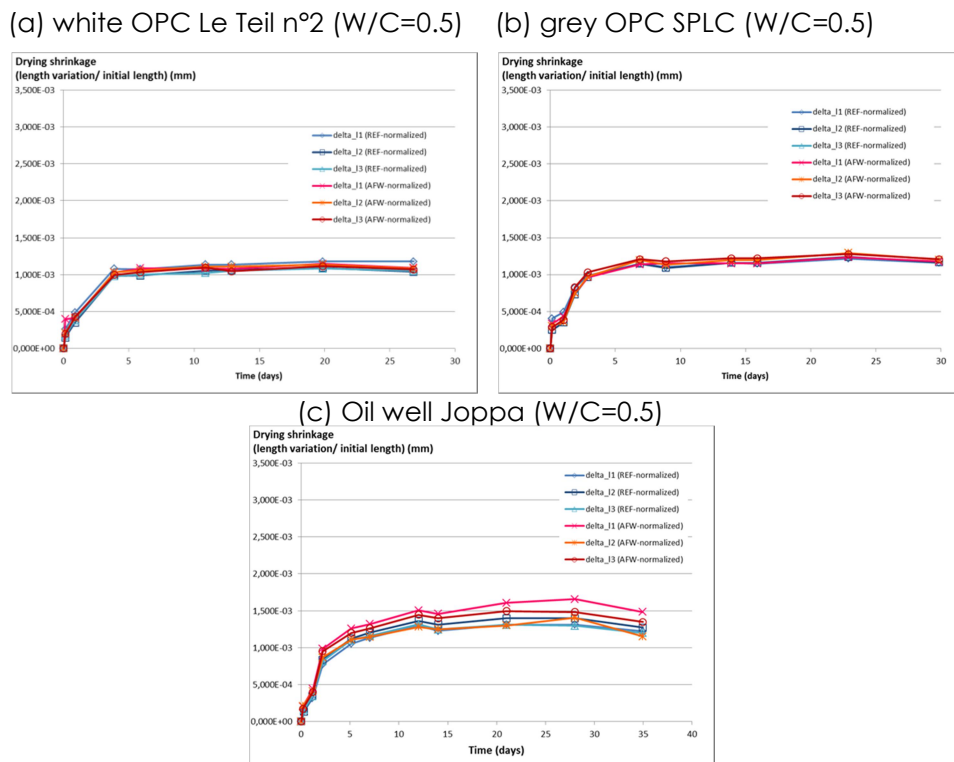


Figure 4.11. Drying shrinkage properties of reference and seeded cement pastes cured at 80°C

As a conclusion, no measurements done on seeded cement-based paste established a positive influence of the minor rate of afwillite (detected by TGA) in terms of reduction of the drying shrinkage. Only the seeded C<sub>3</sub>S pastes (where the afwillite rate reached to 50% of the maximum possible) showed a significant reduction of the drying shrinkage.

## **Capítulo 5**

---

**Obtención y caracterización de  
morteros aligerados estructurales  
fabricados con poliuretano  
reciclado**







## 5.1 Introducción

Hasta el momento, se han utilizado diferentes agregados poliméricos en morteros para alcanzar menores densidades y mejorar la trabajabilidad de los mismos,<sup>68</sup> aunque fabricados generalmente sin sustitución de árido o cemento, lo que provocaba que se alcanzaran radios agua/conglomerante más elevados que en morteros convencionales.<sup>69</sup>

El uso de residuos poliméricos en la fabricación de morteros y hormigones supone un importante beneficio medioambiental.<sup>70,71,72</sup> Concretamente la incorporación de espumas rígidas de poliuretano en el diseño y fabricación de morteros de cemento aligerados, para su utilización en construcción, ha sido ampliamente investigada, tanto en lo referido a caracterización de sus propiedades físicas como al estudio de su comportamiento mecánico.<sup>29,73</sup> El uso de estos morteros tiene las ventajas añadidas de reducir las cargas sobre las estructuras, abaratar el coste del transporte y mejorar las propiedades de aislamiento térmico.<sup>74,75,76</sup>

<sup>68</sup> Calderón V, Gutiérrez-González S, Rodriguez A, Hognies M. (2013). Study of the microstructure and pores distribution of lightweight mortar containing polymer waste aggregates. *WIT Transactions on Engineering Sciences*, 77: 263-272.

<sup>69</sup> Hamilton HR, Benmokrane B, Dolan W, Sprinkel MM. (2009) Polymer materials to enhance performance of concrete in civil infrastructure. *Journal of Macromolecular Science, Part C: Polymer Reviews*, 49:1-24.

<sup>70</sup> Dulsang N, Kasemsiri P, Posi P, Hiziroglu S, Chindaprasirt P. (2016) Characterization of an environment friendly lightweight concrete containing ethyl vinyl acetate waste. *Materials and Design*, 96:350-356.

<sup>71</sup> Ohama Y. (2010) Concrete-polymer composites-the past, present and future. *Key Engineering Materials*, 466, 1-14 and International Congress on Polymers in Concrete. ICPIC Madeira (Portugal).

<sup>72</sup> Ohama Y. (1998) Polymer-based admixtures. *Cement Concrete Composites*, 20(2-3): 189-212.

<sup>73</sup> Guide for structural lightweight aggregate concrete. (1987) ACI Manual of Concrete Practice, Part 1 Farmington Hills: American Concrete Institute.

<sup>74</sup> Ben Fraj A, Kismi M, Mounanga P. (2010) Valorization of coarse rigid polyurethane foam waste in lightweight aggregate concrete. *Construction Building Materials*, 24:1069-1077.

<sup>75</sup> Iucolano F, Liguori B, Caputo D, Colangelo F, Cioff R. (2013) Recycled plastic aggregate in mortars composition: effect on physical and mechanical properties. *Materials and Design*, 52:916-922.

<sup>76</sup> Corinaldesi V, Mazzoli A, Moriconi G. (2011) Mechanical behaviour and thermal conductivity of mortars containing waste rubber particles. *Materials and Design*, 32:1646-1650.



Todos los ensayos previos realizados sobre este tipo de morteros, incluidos los de durabilidad<sup>18</sup> han mostrado que son aptos para su empleo en obra, pues cumplen con la Normativa Europea aplicable para los morteros de enlucido y revoco y morteros de albañilería.<sup>77,78</sup>

Por otro lado, las espumas poliméricas son materiales ligeros potencialmente mucho más flexibles e hidrofóbicos que otros productos tradicionales, como la perlita expandida, el vidrio expandido o micro esferas que podrían ser útiles en el control del radio de absorción, lo que repercute de manera positiva en la durabilidad final.<sup>79,80</sup>

Aun así, las referencias específicas relativas a la obtención y la estabilidad a lo largo del tiempo en mezclas de áridos y polímeros reciclados son escasas.<sup>81,82,83</sup> En este sentido, hay estudios previos que han demostrado que una elevada porosidad puede estar relacionada con una menor densidad, unas resistencias mecánicas menores y un buen aislamiento térmico y conductividad térmica baja.<sup>84,85</sup>

Con el ánimo de avanzar en la investigación en este campo, se propone como objetivo de este capítulo reemplazar el uso de agregados tradicionales a través del empleo de poliuretano reciclado,

<sup>77</sup> Wu JW, Sung WF, Chu HS. (1999) Thermal conductivity of polyurethane foams. International Journal Heat Mass Transfer, 42:2211-2217.

<sup>78</sup> Verdolotti L, Di Maio E, Lavorgna M, Iannace S, Nicolais L. (2008) Polyurethane-cementbased foams: Characterization and potential uses. Journal Applied Polymer Science, 107(1): 1-8.

<sup>79</sup> Babu KG, Babu DS. (2003) Behaviour of lightweight expanded polystyrene concrete containing silica fume. Cement Concrete Research, 33 (5): 755-762.

<sup>80</sup> Peng JH, Chen MF, Zhang JX. (2002) Study on waste expanded polystyrene as lightweight aggregate for thermal insulating mortar. Jianzhu Cailliao Xuebao/Journal Building Materials, 5 (2):166.

<sup>81</sup> Wang R, Meyer C. (2012) Performance of cement mortar made with recycled high impact polystyrene. Cement Concrete Composites, 34 (9):975-981.

<sup>82</sup> Whinfield and Dickson. (1949) Improvements Relating to the Manufacture of Highly Polymeric Substances, British Patent 578,079, 1941; Polymeric Linear Terephthalic Esters, U.S. Patent 2,465,319.

<sup>83</sup> Reis JML, Carneiro EP. (2012) Evaluation of PET waste aggregates in polymer mortars. Construction Building Materials, 27 (1): 107-11.

<sup>84</sup> Van Gemert D, Czarnecki L, Maultzsch M, Schorn H, Beeldens A, Lukowski P, Knapen E. (2005) Cement concrete and concrete-polymer composites: Two merging worlds: A report from 11th ICPI Congress in Berlin, 2004. Cement Concrete Composites, 27 (9-10): 926-933.

<sup>85</sup> Ohama Y, Nishimura T, Hachisuka H. (1980) Strength properties of steel fiber reinforced polystyrene-impregnated concrete. Proceedings - Computer Networking Symposium, 3, 151-158.



para obtener materiales de construcción estructurales con propiedades mejoradas.<sup>86,87</sup>

Existen estudios relativos a la mejora del comportamiento mecánico y térmico de morteros de cemento mediante la adición de fibras de refuerzo y aditivos,<sup>88,89</sup> y prácticamente ningún trabajo de investigación en lo referente a los efectos de aditivos en morteros de cemento con polímeros. Ello ha llevado a realizar esta investigación que pretende ampliar el conocimiento en lo referido a la influencia del uso de surfactantes no iónicos en las propiedades mecánicas de los morteros de cemento aligerados con residuos de poliuretano. Este tipo de aditivos modifican la estructura del polímero después de la hidratación y promueven la adhesión de pigmentos sobre la superficie de estos morteros.

Por tanto, se compagina la sustitución de varias proporciones de árido por polímero y el empleo de surfactantes no iónicos con diferente balance hidrofilico-hidrofóbico, HLB. Esto proporciona una visión general de las variaciones de resistencias mecánicas a flexión y compresión, la densidad aparente, la porosidad y la microestructura que pueden alcanzarse en estos nuevos materiales aligerados con propiedades estructurales.

## 5.2 Caracterización de las materias primas

En este apartado se caracterizan las materias primas empleadas y los productos derivados que se obtienen, formados por una matriz de cemento, árido y agua, aligerada con residuos de poliuretano y reforzada mediante la incorporación de aditivos.

<sup>86</sup> Kismi M, Poullain P, Mounanga P. (2012) Transient Thermal Response of Lightweight Cementitious Composites Made with Polyurethane Foam Waste. International Journal Thermophysics, 1-20.

<sup>87</sup> Aulia TB. (2002) Effects of polypropylene fibres on the properties of high strength concretes. Lacer Vol. 7, 43-59.

<sup>88</sup> Abdollahnejad Z, Mastali M, Mastali M, Dalvand A. (2017) Comparative study on the effects of recycled glass-fiber on drying shrinkage rate and mechanical properties of the self-compacting mortar and fly ash-slag geopolymers mortar. Journal of Materials in Civil Engineering 29(8), 04017076.

<sup>89</sup> Dong X, Wang S, Gong C, Lu L. (2014) Effects of aggregate gradation and polymer modifiers on properties of cement-EPS/vitrified microsphere mortar. Construction Building Materials 73: 255-260.



### 5.2.1 Cemento

En la elaboración de los morteros para las propiedades en estado fresco y endurecido se han empleado dos tipos de cementos: tipo I y IV suministrado por la empresa Portland Valderrivas (Mataporquera, España), con al menos un 95% de clinker y un 5% de componentes minoritarios, una densidad de 3065 kg/m<sup>3</sup> y una superficie específica Blaine de 3500 cm<sup>2</sup>/g acorde a la norma EN 197-1.

### 5.2.2 Áridos

Los áridos utilizados, tanto en el mortero patrón de referencia como en las dosificaciones con sustitución de árido por poliuretano y aditivos son de carácter silíceo, denominados como “árido 0/4 silíceo rodado”, procedentes de una cantera a cielo abierto localizada en Cubillo del Campo, Burgos (España).

Según la cartografía geológica, la zona geográfica pertenece a la “Formación de Arenas de Utrillas” y está formada por conglomerados cuarcíticos, arenas caoliníferas y lutitas, situados en lechos sedimentarios en un terreno con una facies superficial que presenta importantes plegamientos.

La arena está compuesta casi totalmente por sílice, con más del 98% de granos de cuarzo y cuarcitas, así como por trazas de partículas micáceas y de areniscas.

En la Tabla 5.1 se recogen las características técnicas de la arena referidas a las Normas Europeas de valoración UNE-EN. Tras estos análisis, y ya determinadas las características referidas a las muestras de arena, podemos clasificarla como “Arena Cuarcífera”.



CARACTERÍSTICAS DE LA ARENA DE CUBILLO		
Ensayo:	Norma:	Resultado:
% Finos	UNE-EN 933-1:2012	0,78
Equivalente de arena	UNE-EN 933-1:2012	78
Densidad Real g/cm <sup>3</sup>	UNE-EN 1097-6:2001	2,619
Coeficiente de Absorción Normal %	UNE-EN 1097-6:2001	15,0 %
Densidad Real Saturada Sup. Seca g/cm <sup>3</sup>	UNE-EN 1097-6:2001	2,630
% Terrones de arcilla	UNE 7133:1958	0,01
% Partículas de bajo peso específico	UNE-EN 1744-1:1999	0,00
Coeficiente de forma del árido grueso	UNE-EN 933-4:2000	0,26
% Partículas blandas	UNE 7134:1958	0,93
% Contenido Total de Azufre (S)	UNE-EN 1744-1:2010	0,00
% Sulfatos solubles en ácidos (SO <sub>3</sub> )	UNE-EN 1744-1:2010	0,00
% Cloruros	UNE-EN 1744-1:2010	0,00
CLASIFICACIÓN DE LA ARENA	ARENA CUARCÍFERA	

Tabla 5.1 Características de la arena de Cubillo

Los áridos para morteros están regulados en la norma EN 13139. En esta norma se detallan las características de los áridos y del filler obtenidos por un proceso natural, materiales fabricados o reciclados y las mezclas de estos áridos para utilizarlos en morteros. Dichos áridos están formados por arenas naturales de depósitos sedimentarios a cielo abierto, lavadas y clasificadas o por arenas de machaqueo obtenidas por trituración y molturación, clasificadas por tamices y cedazos.

En esta arena también se ha comprobado la presencia de materia orgánica, con resultado negativo, y el contenido en arcillas que es despreciable. En general presenta una gran pureza ya que, como se ha comentado anteriormente, la mayoría es de naturaleza silícica y su aspecto es bastante fracturado pero adecuado para su uso en morteros.

Se ha llevado a cabo un estudio granulométrico para conocer la composición cuantitativa de la arena, así como su distribución en la serie de tamices según EN 933-2. La curva granulométrica se describe en



la Figura 5.1 y en la Tabla 5.2 en donde se muestra el porcentaje que pasa de la arena estudiada.

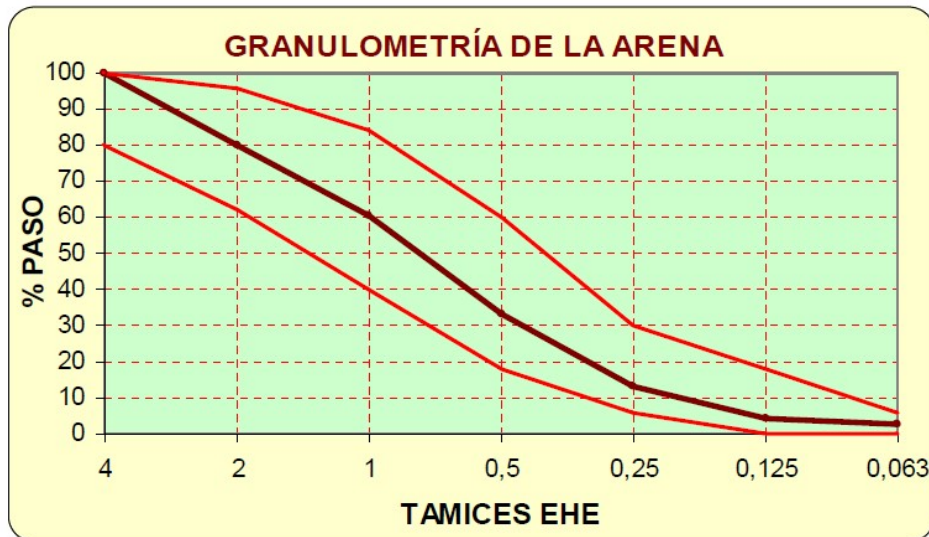


Figura 5.1 Curva granulométrica en la que se muestra el porcentaje de árido que pasa de la arena de Cubillo del Campo, Burgos, España

Tamaño	4	2	1	0,5	0,25	0,125	0,063
% Pasa	100	80,2	60,3	33,0	13,3	4,0	2,6

Tabla 5.2. Granulometría del árido silíceo.



Figura 5.2. Detalle de la arena de Cubillo del Campo, Burgos, España



### 5.2.3 Agua

El agua que se ha empleado para realizar los ensayos y elaborar las probetas procede de la red pública suministrada por Aguas de Burgos S.A. El análisis químico de esta agua se expresa en la Tabla 5.3.<sup>90</sup>

Parámetros	Unidades	Resultados	Valor Paramétrico
Físico-Químicos:			(Máx. permitido)
Olor	índice de dilución	1	3 a 25°C
Sabor	índice de dilución	1	3 a 25°C
Color	mg/l Pt/Co	5	15
pH	Uds. pH	8,01	6,5 < pH < 9,5
Turbidez	UNF	0,3	1
Conductividad	µS/cm	104,4	2.500
Nitratos	mg/l	<5,0	50
Nitritos	mg/l	<0,03	0,1
Amonio	mg/l	<0,25	0,50
Cloro libre residual	mg/l	0,44	1,0
Fluoruro	mg/l	<0,10	1,5
Sodio	mg/l	9,7	200
Cloruro	mg/l	21,3	250
Sulfato	mg/l	19,8	250
Calcio	mg/l	16,9	-
Dureza Total	°F	4,7	-
Bicarbonato	mg/l	54,9	-
Hierro	mg/l	<0,0001	0,2
Aluminio	mg/l	0,04	0,2
Cobre	mg/l	<0,001	2,0
Suma de trihalometanos	mg/l	<0,01	0,1
Índice de Langelier	-	-0,4	
Escherichia coli	UFC en 100ml.	0	0
Clostridium perfringens	UFC en 100ml.	0	0
Bacterias Coliformes	UFC en 100ml.	0	0
Recuento de colonias a 22°C	UFC en 1ml.	8	100

Tabla 5.3 Características del agua utilizada según R.D. 140/2003. 2016

<sup>90</sup>Análisis del agua tratada, media anual 2016.



El agua procedente de la red debe ser previamente almacenada en unos depósitos en el interior del taller hasta alcanzar una temperatura constante de unos  $23\pm2^{\circ}\text{C}$  para poder realizar los ensayos, debido a que la climatología extrema de esta zona hace que llegue a unas temperaturas mucho más bajas.

#### 5.2.4 Espuma triturada de poliuretano

Los residuos poliméricos que se han utilizado como aligerantes de los morteros son espumas de poliuretano de color gris, procedentes de la industria del automóvil. La espuma semirrígida gris procede del material que sobra en el proceso de fabricación de paneles aislantes para techos de automóviles en la fábrica Grupo Antolín, en Burgos. Las dimensiones de dichos paneles son aproximadamente de 1,60 m x 1,00 m y su espesor es de 1 cm. El material se tritura y tamiza mediante un Molino RETSCH SM100 y un tamiz de 4,00 mm de luz de malla tal y como se muestra en las Figuras 5.3 y 5.4 para su empleo como sustituto de diferentes porcentajes de árido, aligerando así los morteros.



Figura 5.3 Molino con tamizadora RESTCH SM100



Figura 5.4 Proceso de obtención de la espuma gris triturada

Mediante el método del picnómetro, se obtiene la densidad real de la espuma de poliuretano que es de  $1220 \text{ kg/m}^3$ , mientras que la densidad aparente es de  $68 \text{ kg/m}^3$ . Se han determinado los tamaños de partícula granulometría de difracción por rayos láser, indicados en la Tabla 5.4.

% de la muestra	Tamaño inferior ( $\mu\text{m}$ )
10	212,1
50	1.493,2
90	2.000,0

Tabla 5.4 Tamaño de partícula en el 10%, 50% y 90% de la muestra  
de la espuma de poliuretano gris

En el análisis elemental (CHNS) de carbono, hidrógeno y nitrógeno del poliuretano hallamos las proporciones indicadas en la Tabla 5.5. A través de microscopía electrónica de barrido (SEM) se puede observar en la Figura 5.5 su estructura celular, en la que se observan algunas celdas abiertas, posiblemente debido al proceso de triturado de dichos paneles de espuma, así como su proporción de oxígeno y calcio.

Elemento	C	H	N	S	O	Ca	Otros
%	65,50	6,20	7,20	0,00	19,00	1,00	1,10

Tabla 5.5 Resultados CHNS y SEM del residuo de espuma de poliuretano

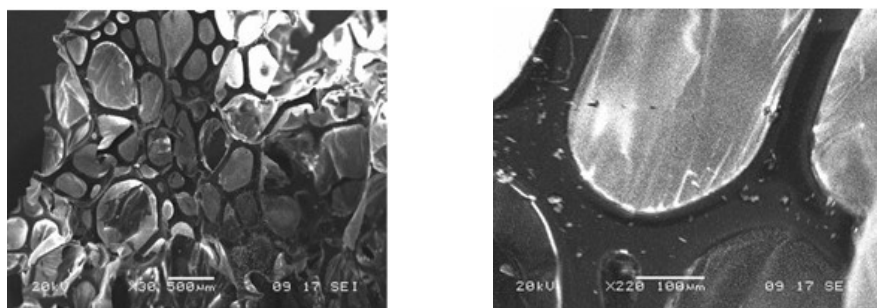


Figura 5.5 SEM del residuo de la espuma de poliuretano

### 5.2.5 Aditivos

Los aditivos utilizados en la fabricación de los morteros son superplastificantes, de manera que mejoran las propiedades de los morteros y reducen la cantidad de agua necesaria en las dosificaciones. Los aditivos utilizados se denominan T03 y XL40.

Se han empleado dos tipos diferentes de aditivos surfactantes no iónicos de tipo C13-oxo alcohol etoxilato, proporcionados por el grupo BASF empleados en estado líquido. Se caracterizan por su balance hidrofílico-lipofílico (HLB), descrito en la Tabla 5.6. El valor HLB se ha calculado utilizando el método de Griffin's:  $HLB = 20 M_h/M$ , donde  $M_h$  es la masa molecular de la parte hidrofílica de la molécula y  $M$  la masa molecular de la molécula completa.

Surfactante	Unidad hidrofóbica	Unidad hidrofílica	Valor HLB	Comentarios
T03	C13 = 200g	3 EO = 132g	6.1	Muy hidrofílico
XL40	C10 = 158g	4 EO = 176g	10.5	Poco hidrofílico pero con cadenas laterales

Tabla 5.6. Valores HLB para los diferentes surfactantes empleados



### 5.3 Dosificación

Se han fabricado morteros con dosificaciones de referencia sin residuos de poliuretano, y a partir de ahí se han ido sustituyendo en volumen porcentajes de árido por polímero en un 25%, 50%, 75% y un 100% de reemplazo, es decir, hasta obtener mortero sin áridos. En trabajos previos de este tipo se han estudiado este tipo de sustituciones en volumen de arena por poliuretano, aunque casi siempre con polímeros no termoestables<sup>91</sup>.

Cada una de las dosificaciones se ha ensayado con dos tipos diferentes de superplastificantes, T03 y XL40; con los dos tipos de cementos: tipo I y tipo IV; así como con relaciones [cemento/(árido+residuo de poliuretano)] de 1/3, 1/6 y 1/8. En todas ellas la relación [agua/cemento] ha sido de 0,5, excepto para la dosificación 1/8 en la que ha tenido que aumentarse a 0,6 para conseguir alcanzar una buena trabajabilidad acorde a la norma EN 1015-3, que determina la consistencia de los morteros frescos amasados por la mesa de sacudidas a través del valor del escurrimiento. La cantidad de aditivo añadido en todas las dosificaciones es de un 2% respecto a la masa de cemento.

Las mezclas empleadas y su nomenclatura se detallan a continuación en las Tablas 5.7, 5.8 y 5.9.

<sup>91</sup> Rocco JAFF, Lima JES, Lourenço VL, Batista NL, Botelho EC, Iha, K. (2012) Dynamic mechanical properties for polyurethane elastomers applied in elastomeric mortar. Journal Applied Polymer Science, 126(4): 1461-1467



<b>Relación cemento/ (árido+residuo de poliuretano)</b>	1/3
	1/6
	1/8
<b>Referencia (R) o sustitución de árido por poliuretano (PU)</b>	R
	PU
	25
<b>Porcentaje de sustitución de árido por poliuretano</b>	50
	75
	100
<b>Aditivo</b>	T03
	XL40
<b>Tipo de cemento</b>	I
	IV

Tabla 5.7. Nomenclatura de las distintas dosificaciones utilizadas en la fabricación de los morteros



Cemento empleado	Relación en volumen cemento/(árido+residuo de poliuretano)	Aditivo	Nomenclatura de cada dosificación
Cemento tipo I	1/3	T03	3PU100T03I 3PU75T03I 3PU50T03I 3PU25T03I 3RT03I
			3PU100XL40I 3PU75XL40I 3PU50XL40I 3PU25XL40I 3RXL40I
			6PU100T03I 6PU75T03I 6PU50T03I 6PU25T03I 6RT03I
			6PU100XL40I 6PU75XL40I 6PU50XL40I 6PU25XL40I 6RXL40I
			8PU100T03I 8PU75T03I 8PU50T03I 8PU25T03I 8RT03I
	1/6	T03	8PU100XL40I 8PU75XL40I 8PU50XL40I 8PU25XL40I 8RXL40I
			8PU100T03I 8PU75T03I 8PU50T03I 8PU25T03I 8RT03I
			8PU100XL40I 8PU75XL40I 8PU50XL40I 8PU25XL40I 8RXL40I
			8PU100T03I 8PU75T03I 8PU50T03I 8PU25T03I 8RT03I
			8PU100XL40I 8PU75XL40I 8PU50XL40I 8PU25XL40I 8RXL40I

Tabla 5.8. Dosificaciones utilizadas en morteros con cemento tipo I



Cemento empleado	Relación en volumen cemento/(árido+residuo de poliuretano)	Aditivo	Nomenclatura de cada dosificación
Cemento tipo IV	1/3	T03	3PU100T03IV 3PU75T03IV 3PU50T03IV 3PU25T03IV 3RT03IV
			3PU100XL40IV 3PU75XL40IV 3PU50XL40IV 3PU25XL40IV 3RXL40IV
			6PU100T03IV 6PU75T03IV 6PU50T03IV 6PU25T03IV 6RT03IV
			6PU100XL40IV 6PU75XL40IV 6PU50XL40IV 6PU25XL40IV 6RXL40IV
			8PU100T03IV 8PU75T03IV 8PU50T03IV 8PU25T03IV 8RT03IV
		XL40	8PU100XL40IV 8PU75XL40IV 8PU50XL40IV 8PU25XL40IV 8RXL40IV

Tabla 5.9. Dosificaciones utilizadas en morteros con cemento tipo IV

Los criterios que se han tenido en cuenta para la elección de dichas dosificaciones son, por un lado la norma UNE 1015-11, que determina las resistencias a flexión y a compresión del mortero endurecido y, por otro,



criterios medioambientales, ya que se ha tratado de sustituir la mayor cantidad de árido por poliuretano posible para tratar de eliminar en mayor medida este residuo, siempre cumpliendo los requisitos que determina la norma mencionada anteriormente.

Para la obtención de las mezclas, el procedimiento operatorio que se ha llevado a cabo consiste en la adición progresiva de espuma de poliuretano triturada, sustituyendo los diferentes porcentajes de árido por poliuretano en volumen. Tras realizar la dosificación en volumen de las proporciones de cemento, árido, residuo de poliuretano, agua y aditivo de cada una de las dosificaciones anteriores, se mezclaron los componentes en varias fases.

Por una parte se mezcla el cemento con el árido en seco hasta conseguir una mezcla homogénea, y por otra parte, se mezcla el agua con el aditivo. Se añade el residuo de poliuretano en polvo a la mezcla de agua con aditivo y agita durante 1 minuto de forma manual. Esto se hace para conseguir la máxima dispersión posible del polímero, e intentar optimizar sus propiedades. Posteriormente, se añade la fase sólida del cemento con el árido, mezclando mecánicamente siguiendo la norma EN 1015-2. Finalmente se vierte la mezcla en distintos moldes, en función del ensayo que se vaya a realizar, y se procede a su endurecimiento mediante las técnicas habituales de curado de morteros.

## 5.4 Caracterización en estado fresco y en estado endurecido

### 5.4.1 Densidad aparente del mortero fresco

La densidad aparente del mortero fresco se determinó siguiendo los criterios descritos por la norma EN 1015-6. Para ello se ha empleado el mismo recipiente que se utiliza en el ensayo para determinar el aire que contiene el mortero fresco, descrito en la norma EN 1015-7. La capacidad de este recipiente es de un litro por lo que, al llenarlo tal y como indica la norma, y determinar su masa con la balanza, se obtiene directamente la densidad del mortero. El mortero se amasa acorde a las prescripciones de la EN 1015-2 con la relación agua/conglomerante óptima. Como se trata de un mortero de consistencia plástica, se empleará el método de llenado y compactado por el método de



sacudidas. Para ello se introduce con la cuchara el mortero en el recipiente hasta la mitad, se bascula de un lado a otro desde una altura de unos 30 mm y se deja caer 10 veces sobre una placa sólida y rígida de una masa superior a los 25 kg. Como se llena en dos tongadas, se realiza lo mismo una vez se ha llenado hasta desbordar y se enrasa con una regla, de modo que la superficie del mortero esté plana y nivelada con el borde superior del recipiente. Se limpia después el borde con un paño húmedo. Se pesa en una balanza para determinar la masa total del recipiente lleno, calculando el valor de la densidad aparente del mortero fresco según la expresión 5.1. Dicho proceso se realiza dos veces, determinando el valor medio de dos ensayos, en kilogramos por metro cúbico. Los resultados obtenidos en las dosificaciones ensayadas son los que se muestran a continuación en la Tablas 5.10 y 5.11.

$$\rho_m = \frac{m_2 - m_1}{V_v}$$

Eq. (5.1)

**$m_1$**  : masa del recipiente vacío

**$m_2$**  : masa del recipiente lleno de mortero

**$V_v$**  : volumen del recipiente (1L)



Tipo de cemento	Relación en volumen cemento/(árido+PU)	Aditivo	Nomenclatura de cada dosificación	Densidad aparente (kg/m <sup>3</sup> )
Cemento tipo I	1/3	T03	3PU100T03I	1760
			3PU75T03I	1940
			3PU50T03I	2080
			3PU25T03I	2120
			3RT03I	1980
		XL40	3PU100XL40I	1740
			3PU75XL40I	1940
			3PU50XL40I	2020
			3PU25XL40I	2110
			3RXL40I	2030
	1/6	T03	6PU100T03I	1740
			6PU75T03I	2030
			6PU50T03I	2010
			6PU25T03I	2040
			6RT03I	2080
		XL40	6PU100XL40I	1750
			6PU75XL40I	2040
			6PU50XL40I	1880
			6PU25XL40I	1760
			6RXL40I	1750
	1/8	T03	8PU100T03I	1590
			8PU75T03I	1970
			8PU50T03I	1680
			8PU25T03I	1730
			8RT03I	1770
		XL40	8PU100XL40I	1600
			8PU75XL40I	1940
			8PU50XL40I	1990
			8PU25XL40I	1990
			8RXL40I	1830

Tabla 5.10. Densidades aparentes de las dosificaciones con cemento tipo I



Tipo de cemento	Relación en volumen cemento/(árido+PU)	Aditivo	Nomenclatura de cada dosificación	Densidad aparente (kg/m <sup>3</sup> )
Cemento tipo IV	1/3	T03	3PU100T03IV	1700
			3PU75T03IV	1850
			3PU50T03IV	1950
			3PU25T03IV	2090
			3RT03IV	2060
	1/6	XL40	3PU100XL40IV	1680
			3PU75XL40IV	1850
			3PU50XL40IV	1960
			3PU25XL40IV	2110
			3RXL40IV	2150
	1/8	T03	6PU100T03IV	1670
			6PU75T03IV	2160
			6PU50T03IV	2020
			6PU25T03IV	1770
			6RT03IV	1910
		XL40	6PU100XL40IV	1650
			6PU75XL40IV	1940
			6PU50XL40IV	1880
			6PU25XL40IV	1860
			6RXL40IV	1920
		T03	8PU100T03IV	1580
			8PU75T03IV	1960
			8PU50T03IV	1780
			8PU25T03IV	1890
			8RT03IV	1890
		XL40	8PU100XL40IV	1550
			8PU75XL40IV	1920
			8PU50XL40IV	1800
			8PU25XL40IV	1820
			8RXL40IV	1760

Tabla 5.11. Densidades aparentes de las dosificaciones con cemento tipo IV

A partir de los resultados obtenidos en la Tablas 5.10 y 5.11 se observa que, en el caso del cemento tipo I, generalmente, la densidad del material disminuye conforme aumenta la cantidad de árido sustituido por poliuretano. Este comportamiento puede deberse a la menor densidad del residuo de poliuretano comparada con el árido al que



sustituye, o bien al incremento de la porosidad del material ya que estamos introduciendo un polímero de estructura celular. Sin embargo, no tenemos ese comportamiento en todos los casos, ya que para el caso de relación en volumen [cemento/(árido+residuo de poliuretano)] de 1/3, en las dosificaciones en las que se sustituye un 25% y un 50% de árido por poliuretano, la densidad aumenta, tal vez debido al efecto del aditivo surfactante. Lo mismo ocurre en el caso de relación [cemento/(árido+residuo de poliuretano)] 1/6 para la sustitución del 75% y en el caso de relación [cemento/(árido+residuo de poliuretano)] de 1/8 para la sustitución del 75% en el aditivo T03 y 25%, 50% y 75% para el aditivo XL40.

Tal y como se puede observar en la Figura 5.7, en el caso de dosificación [cemento/(árido+residuo de poliuretano)] de 1/3, apenas hay diferencia en cuanto al aditivo empleado se refiere, sin embargo en el caso 1/6 sí que varía en las primeras sustituciones, siendo menos densas aquellas dosificaciones con el aditivo tipo XL40. Lo contrario ocurre en el caso de dosificación 1/8, ya que en este caso es de menor densidad las dosificaciones en las que se ha empleado el aditivo tipo T03.

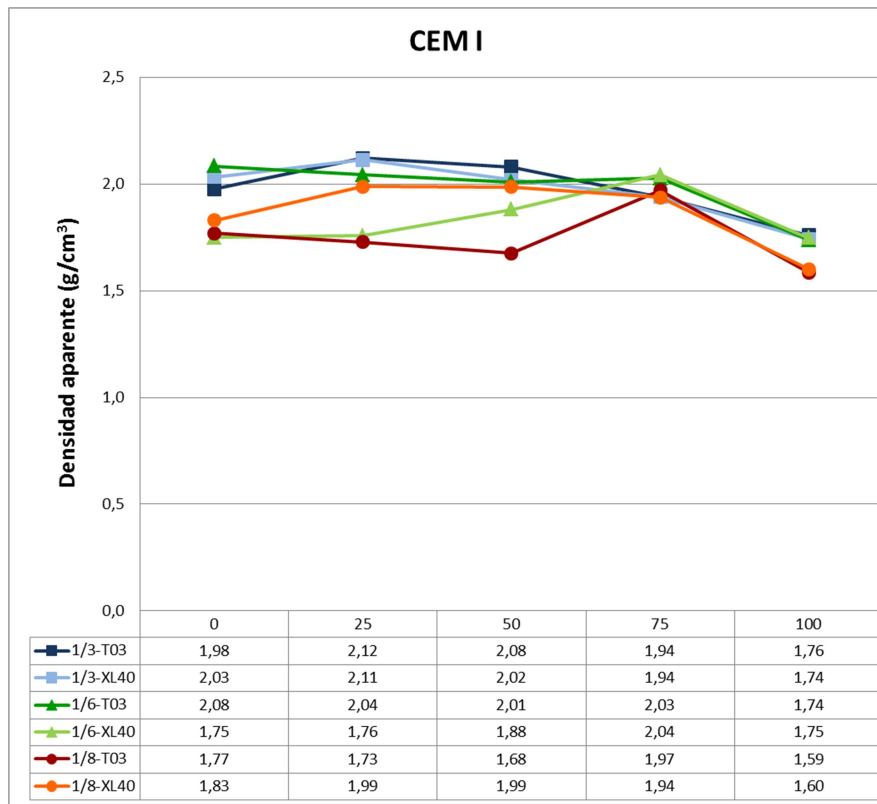


Figura 5.7. Densidades aparentes de las dosificaciones según los diferentes porcentajes de árido sustituido por poliuretano con cemento tipo I

En caso del cemento tipo IV, las densidades son similares a las del cemento tipo I, ya que, generalmente, según aumenta la cantidad de árido sustituido por poliuretano, la densidad tiende a disminuir debido a su menor densidad comparada con el árido al que sustituye, o bien al incremento de la porosidad del material por ser un polímero de estructura celular. No obstante, tampoco sucede esto siempre ya que para el caso de relación en volumen [cemento/(árido+residuo de poliuretano)] de 1/3 y aditivo T03, al sustituir un 25%, la densidad aumenta ligeramente, al igual que en el caso 1/6 al sustituir un 50% y el 75% con ambos aditivos. Asimismo, este comportamiento se repite en relaciones 1/8 para el 25% en el XL40 y para el 75% en ambos casos.

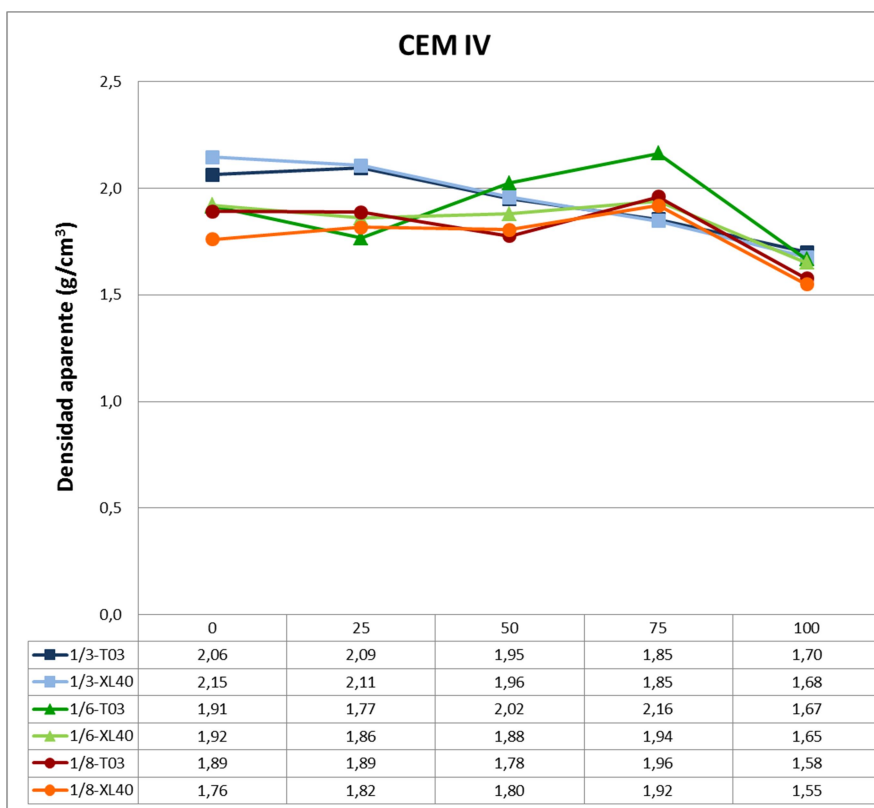


Figura 5.8. Densidades aparentes de las dosificaciones según los diferentes porcentajes de árido sustituido por poliuretano con cemento tipo IV

Las densidades son prácticamente iguales para la misma relación [cemento/(árido+residuo de poliuretano)], Figura 5.8, exceptuando la de referencia en la que es algo menor al emplear el aditivo tipo T03. En los casos en los que la relación [cemento/(árido+residuo de poliuretano)] es 1/6 y 1/8, la densidad es generalmente menor cuando se emplea el aditivo XL40.

#### 5.4.2 Determinación del contenido de aire del mortero fresco

Para calcular el contenido de aire del mortero fresco se siguen los criterios que se describen en la Norma Europea UNE-EN 1015-7. Esta norma describe dos métodos para determinar el contenido de aire en los morteros frescos, incluyendo aquellos que contienen conglomerantes minerales y a la vez áridos pesados y ligeros. De estos dos métodos, elegiremos realizar este ensayo por el método de presión, ya que el método de alcohol sólo se debe utilizar en morteros cuyo contenido en



aire sea igual o superior al 20% y en nuestro caso dicho contenido será menor.

Para calcular el contenido de aire en el mortero se coloca un volumen de mortero en un recipiente de medida especificada, se vierte agua en su superficie y, aplicando una presión de aire, se fuerza la introducción de agua en el mortero desplazando el aire que contienen los poros. La disminución del nivel de agua refleja el volumen de aire extraído del mortero.

Para realizar el ensayo, el mortero se amasa según las prescripciones de la UNE-EN 1015-2. El recipiente se llena por completo con mortero en cuatro capas, aproximadamente iguales, compactando cada capa con 10 golpes cortos del pisón, regularmente distribuidos, de manera que se obtenga una superficie del mortero plana. Se elimina el exceso de mortero con la regla para enrasar de manera que se obtenga una superficie del mortero plana y nivelada con el borde superior del recipiente. Posteriormente se limpia el exterior del recipiente de modo que este además de limpio seco, y se fija la tapa firmemente en el recipiente. A continuación se cierra la válvula principal de aireación situada entre la cámara de aire y el recipiente para la muestra, se llena el espacio de aire que se encuentra debajo de la cubierta y encima del mortero, con agua inyectada por una válvula A, manteniendo la otra válvula B abierta hasta que todo el aire que se encuentra encima de la superficie del mortero se haya eliminado. Después se inyecta aire en la cámara de aire hasta que haya alcanzado una presión estable igual a la de calibración. Se cierran las válvulas A y B, y se abre la que está situada entre la cámara de aire y el recipiente para la muestra. Una vez realizado el equilibrio, se lee el contenido de aire en el manómetro y se anota ese valor que es el porcentaje de aire ocluido (Figura 5.9). Se toma el valor del contenido de aire como el valor medio de dos valores individuales de cada muestra de mortero.

Los resultados obtenidos son los que se muestran en la Tabla 5.12.



Figura 5.9. Medida del contenido de aire del mortero fresco



Dosificación	Contenido en aire (%)	Dosificación	Contenido en aire (%)
3PU100T03I	2,4	3PU100T03IV	2,8
3PU75T03I	2,0	3PU75T03IV	6,0
3PU50T03I	2,6	3PU50T03IV	6,5
3PU25T03I	3,0	3PU25T03IV	5,8
3RT03I	3,4	3RT03IV	9,2
3PU100XL40I	3,3	3PU100XL40IV	3,9
3PU75XL40I	5,8	3PU75XL40IV	6,8
3PU50XL40I	7,5	3PU50XL40IV	7,6
3PU25XL40I	6,4	3PU25XL40IV	5,4
3RXL40I	12,0	3RXL40IV	5,3
6PU100T03I	3,8	6PU100T03IV	4,1
6PU75T03I	6,4	6PU75T03IV	6,8
6PU50T03I	10,1	6PU50T03IV	6,6
6PU25T03I	6,2	6PU25T03IV	8,8
6RT03I	5,2	6RT03IV	13,5
6PU100XL40I	3,4	6PU100XL40IV	4,4
6PU75XL40I	6,4	6PU75XL40IV	6,8
6PU50XL40I	13,5	6PU50XL40IV	13,5
6PU25XL40I	19,0	6PU25XL40IV	13,0
6RXL40I	19,5	6RXL40IV	14,5
8PU100T03I	4,8	8PU100T03IV	4,9
8PU75T03I	6,2	8PU75T03IV	6,1
8PU50T03I	13,5	8PU50T03IV	18,0
8PU25T03I	19,5	8PU25T03IV	14,8
8RT03I	20,1	8RT03IV	12,6
8PU100XL40I	4,6	8PU100XL40IV	4,7
8PU75XL40I	8,1	8PU75XL40IV	8,0
8PU50XL40I	9,8	8PU50XL40IV	19,5
8PU25XL40I	9,5	8PU25XL40IV	17,3
8RXL40I	18,0	8RXL40IV	16,5

Tabla 5.12. Contenido en aire ocluido de las diferentes dosificaciones

Tal y como se puede ver en la Tabla 5.12, en el cemento tipo I, en general la porosidad disminuye conforme aumenta la cantidad de árido sustituido por poliuretano debido al menor tamaño de partícula de éste comparado con el de los áridos.

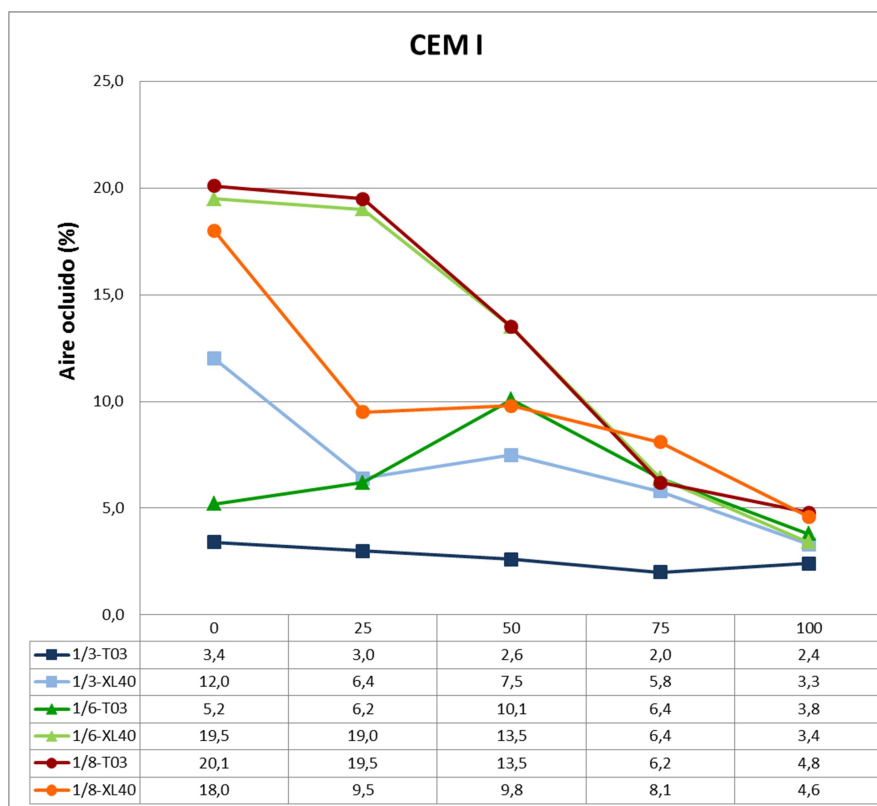


Figura 5.10. Contenido en aire de las dosificaciones con cemento tipo I

En la Figura 5.10 se pueden apreciar los diferentes valores de aire ocluido obtenidos. En general y tal como se ha comentado anteriormente, los valores tienden a disminuir conforme sustituimos árido por poliuretano. Para las dosificaciones 1/3 y 1/6, el contenido en general de aire ocluido es menor cuando se emplea el aditivo T03, aunque para la dosificación 1/8 sucede al contrario, quizás debido a la diferente cantidad de agua/cemento que hace que la reacción con los aditivos sea diferente.

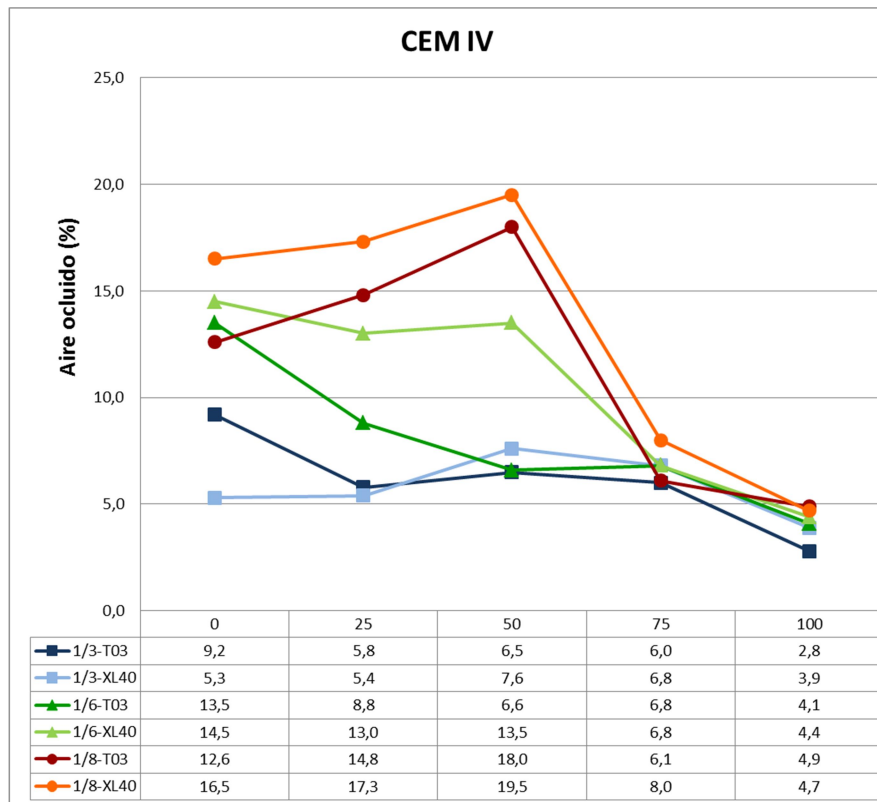


Figura 5.11. Contenido en aire de las dosificaciones con cemento tipo IV

En el caso del cemento tipo IV, la tendencia final también es a disminuir si la comparamos con la dosificación inicial, aunque se producen algunos pocos comunes en las dosificaciones con sustitución del 25% y del 50%. Dichos picos quizás puedan ser debidos a que, al mezclar dos materiales diferentes como el árido y el poliuretano con distinto tamaño de partícula, se produzcan más huecos que cuando empleamos tan sólo uno de esos materiales. A pesar de obtener distintas cantidades de aire ocluido inicialmente sin poliuretano, como podemos ver en la Figura 5.11, finalmente en la sustitución del 100%, los valores de aire ocluido están muy próximas entre ellos. La mayor cantidad de aire ocluido la obtenemos en la dosificación 1/8 debido también al empleo de mayor cantidad de agua y de árido en comparación con las demás dosificaciones, lo que conlleva mayor número de huecos. Eso también justifica porqué el menor contenido en aire ocluido se da en la dosificación 1/3, con menor cantidad de árido y poliuretano en comparación con la de cemento.



### 5.4.3 Densidad aparente en seco del mortero endurecido

La densidad aparente en seco se calcula siguiendo las prescripciones de la Norma Europea UNE-EN 1015-2, con la relación agua/cemento descrita anteriormente para cada dosificación. Los recipientes empleados son los mismos moldes prismáticos de 160 mm x 40 mm x 40 mm que se utilizan posteriormente para calcular las propiedades mecánicas de los morteros, descritos en la Norma Europea UNE-EN 1015-11.

Se rellenan dichos moldes con mortero en dos capas similares compactando cada una de ellas con 25 golpes del pistón distribuidos de forma regular y se enrasta, eliminando el exceso con una regla, para obtener una superficie del mortero plana y nivelada con el borde superior del molde.

Las probetas se secan hasta masa constante, anotando su valor, y, dividiéndolo entre el volumen de cada probeta se obtiene su densidad. Para cada dosificación se realizan seis probetas, y el valor final se calcula hallando la media entre cada una de dichas medidas. Los resultados obtenidos se muestran a continuación en la Tabla 5.13.



Dosificación	Densidad aparente (kg/m <sub>3</sub> )	Dosificación	Densidad aparente (kg/m <sub>3</sub> )
3PU100T03I	1750	3PU100T03IV	1640
3PU75T03I	1980	3PU75T03IV	1860
3PU50T03I	2140	3PU50T03IV	1950
3PU25T03I	2190	3PU25T03IV	2090
3RT03I	2130	3RT03IV	2100
3PU100XL40I	1680	3PU100XL40IV	1610
3PU75XL40I	1920	3PU75XL40IV	1820
3PU50XL40I	2050	3PU50XL40IV	1980
3PU25XL40I	2150	3PU25XL40IV	2090
3RXL40I	2150	3RXL40IV	2130
6PU100T03I	1680	6PU100T03IV	1570
6PU75T03I	2060	6PU75T03IV	1990
6PU50T03I	2070	6PU50T03IV	2000
6PU25T03I	1980	6PU25T03IV	1890
6RT03I	2030	6RT03IV	2050
6PU100XL40I	1690	6PU100XL40IV	1590
6PU75XL40I	2070	6PU75XL40IV	1940
6PU50XL40I	1990	6PU50XL40IV	2090
6PU25XL40I	1950	6PU25XL40IV	2030
6RXL40I	1840	6RXL40IV	2010
8PU100T03I	1510	8PU100T03IV	1460
8PU75T03I	2020	8PU75T03IV	2000
8PU50T03I	2030	8PU50T03IV	2010
8PU25T03I	1670	8PU25T03IV	2010
8RT03I	1920	8RT03IV	2060
8PU100XL40I	1570	8PU100XL40IV	1390
8PU75XL40I	2010	8PU75XL40IV	2000
8PU50XL40I	2110	8PU50XL40IV	2050
8PU25XL40I	2100	8PU25XL40IV	2020
8RXL40I	1990	8RXL40IV	2060

Tabla 5.13. Densidad aparente en seco del mortero endurecido de las diferentes dosificaciones

Las densidades aparentes del mortero con cemento tipo I disminuyen conforme aumenta la cantidad de árido que sustituimos por poliuretano (Figura 5.12). En general se mantienen similares hasta la sustitución del 50%, a partir de la cual comienzan a descender, exceptuando la dosificación 1/8 con aditivo T03 y sustitución del 25%, en la que la densidad desciende más de lo que lo hace en las otras dosificaciones,



tal vez por la mayor proporción agua/cemento y su reacción con el aditivo T03. Aun así, no se consideran morteros ligero para albañilería, ya que las densidades son mayores de 1300 kg/m<sup>3</sup>, pero sí aligerados respecto a materiales de referencia.

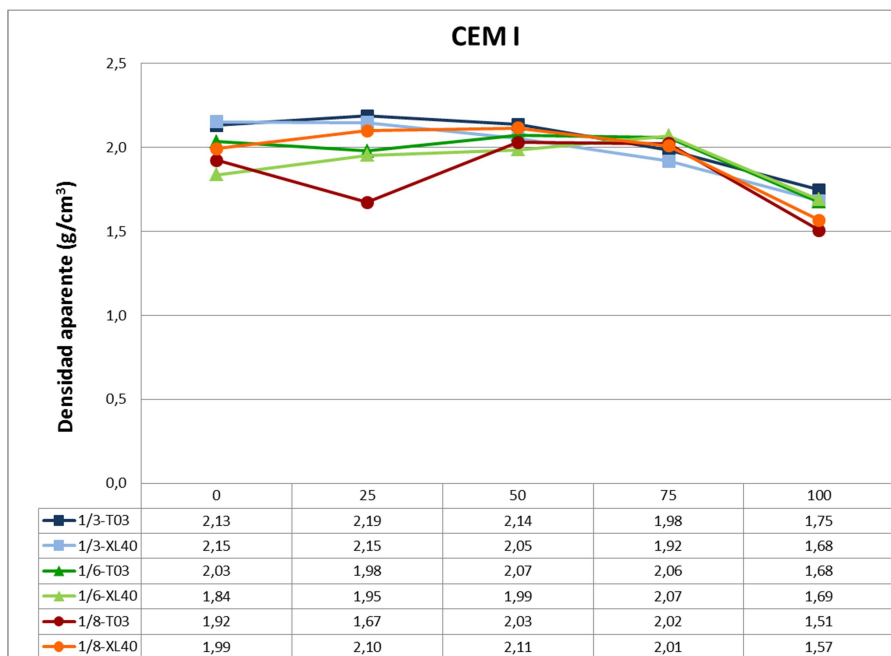


Figura 5.12 Densidades aparentes en seco para el cemento tipo I

Similares resultados se obtienen en el caso del cemento tipo IV (Figura 5.13) en el que las densidades disminuyen cuando aumenta la cantidad de árido que sustituimos por poliuretano. Los valores en este caso son más similares en todas las dosificaciones, pero, tal y como sucedía en el cemento tipo I.

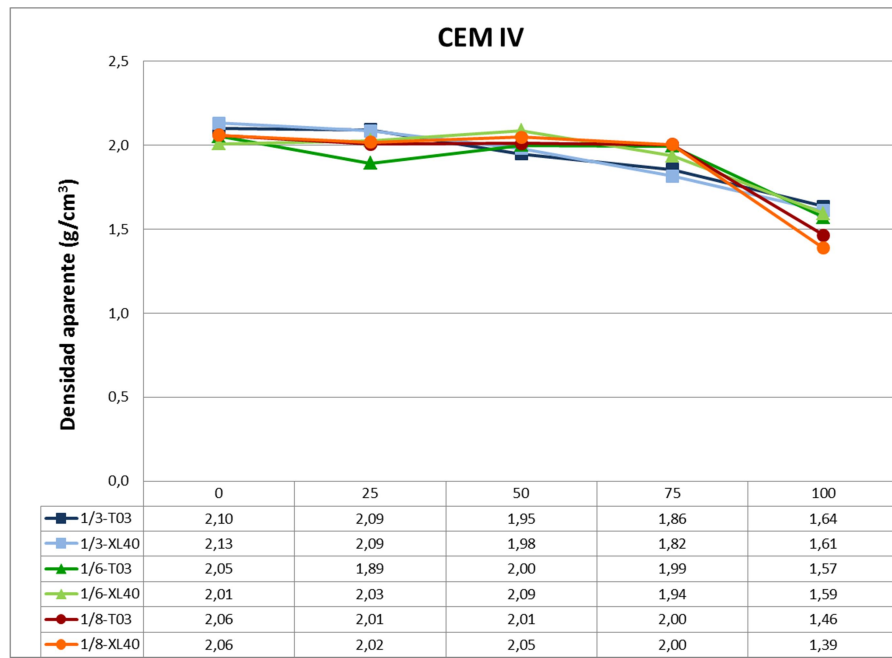


Figura 5.13. Densidades aparentes en seco para el cemento tipo IV

## 5.5 Resistencias mecánicas

Las resistencias a flexión y a compresión de probetas de mortero endurecido se determinan siguiendo los pasos descritos en la UNE-EN 1015-11 y EN 1015-2, con probetas prismáticas de dimensiones 40mm x 40mmx160 mm.

### 5.5.1 Resistencias mecánicas a flexión

Después de amasar, se llenan los moldes con el material fresco en dos capas similares, y se compacta cada una de ellas con 25 golpes del pistón. Se elimina el exceso de mortero con la regla de forma que quede enrasado y así obtener una superficie del mortero plana y nivelada con el borde superior del molde. Posteriormente, el molde se coloca en una cámara húmeda a una temperatura constante de 20 °C ± 2 °C con 95% ± 5% de humedad relativa durante 2 días en el molde, después durante 2 días una vez retirado el molde y finalmente 21 días una vez retirado el molde a una humedad relativa del 65% ± 5%.



Las probetas se ensayan 7 y 28 días después de su confección e inmediatamente después de haberla retirado de su medio de conservación. Las superficies de contacto de los rodillos y las caras de la probeta se limpian con un paño limpio con el fin de eliminar las partículas o cualquier otro material no adherido. Una de las caras de la probeta que haya estado en contacto con las paredes del molde se coloca sobre los rodillos de apoyo.

Para calcular la resistencia a flexión del mortero se aplica una carga en tres puntos de los prismas de mortero endurecido hasta su rotura, y la resistencia a compresión del mortero se determina en cada una de las dos mitades (semiprismas) resultantes del ensayo de resistencia a flexión.

Las resistencias a flexión ( $f$ ) se calculan por medio de la expresión 5.2., y los resultados son los que se muestran en las Tablas 5.14 y 5.15.

$$f = 1,5 \cdot \frac{F \cdot l}{b \cdot d^2}$$

Eq. (5.2)

**f** : resistencia a flexión en N/mm<sup>2</sup>

**b, d** : dimensiones interiores del molde, en mm

**F** : carga máxima aplicada en la probeta, en N

**l** : distancia entre los ejes de los rodillos de apoyo, en mm



Dosificación	Resistencia a flexión a 7 días (MPa)	Resistencia a flexión a 28 días (MPa)
3PU100T03I	2,39	2,67
3PU75T03I	3,75	4,30
3PU50T03I	4,56	4,07
3PU25T03I	5,15	4,32
3RT03I	4,63	4,37
3PU100XL40I	2,05	4,14
3PU75XL40I	3,81	6,20
3PU50XL40I	4,34	6,84
3PU25XL40I	5,16	6,93
3RXL40I	4,82	8,23
6PU100T03I	2,57	3,20
6PU75T03I	4,69	5,76
6PU50T03I	3,81	6,45
6PU25T03I	3,00	5,82
6RT03I	3,21	5,38
6PU100XL40I	3,06	4,27
6PU75XL40I	4,70	6,75
6PU50XL40I	4,75	5,73
6PU25XL40I	3,67	4,23
6RXL40I	1,64	3,94
8PU100T03I	3,00	3,10
8PU75T03I	4,02	5,32
8PU50T03I	3,17	4,45
8PU25T03I	2,75	4,01
8RT03I	1,68	3,19
8PU100XL40I	3,42	2,15
8PU75XL40I	4,62	5,73
8PU50XL40I	4,59	5,90
8PU25XL40I	3,38	6,27
8RXL40I	2,45	5,50

Tabla 5.14. Resistencias mecánicas a flexión tras 7 y 28 días de curado para las dosificaciones con cemento tipo I.



Dosificación	Resistencia a flexión a 7 días (MPa)	Resistencia a flexión a 28 días (MPa)
3PU100T03IV	3,17	2,22
3PU75T03IV	3,87	3,37
3PU50T03IV	3,76	3,42
3PU25T03IV	4,28	4,57
3RT03IV	4,73	5,37
3PU100XL40IV	3,03	2,80
3PU75XL40IV	3,63	3,16
3PU50XL40IV	4,07	4,94
3PU25XL40IV	4,32	6,58
3RXL40IV	4,37	7,37
6PU100T03IV	3,07	2,48
6PU75T03IV	4,02	6,48
6PU50T03IV	2,61	3,79
6PU25T03IV	2,07	2,69
6RT03IV	3,17	4,73
6PU100XL40IV	3,67	3,00
6PU75XL40IV	3,99	5,81
6PU50XL40IV	4,45	6,07
6PU25XL40IV	3,21	4,79
6RXL40IV	2,96	3,74
8PU100T03IV	2,22	4,23
8PU75T03IV	3,45	5,41
8PU50T03IV	2,95	4,28
8PU25T03IV	1,38	2,60
8RT03IV	0,15	2,05
8PU100XL40IV	0,00	3,04
8PU75XL40IV	3,07	5,06
8PU50XL40IV	3,01	4,80
8PU25XL40IV	2,00	3,92
8RXL40IV	1,44	2,93

Tabla 5.15. Resistencias mecánicas a flexión tras 7 y 28 días de curado para las dosificaciones con cemento tipo IV.



En las Figuras 5.14 y 5.15 se representan las resistencias a flexión de las probetas tras 7 y 28 días de curado. Como es lógico, las resistencias aumentan a lo largo del tiempo. A los 7 días, las dosificaciones con mayores resistencias son las de la relación [cemento/(árido+residuo de poliuretano)] 1/3, independientemente del aditivo empleado, ya que tienen resistencias en torno a los 4,5-5 MPa. El máximo lo adquiere en la sustitución del 25%, llegando a los 5,15-5,16 MPa (según el aditivo, T03 o XL40 respectivamente). Posteriormente, disminuye progresivamente conforme vamos sustituyendo árido por polímero. Para la dosificación 1/6, las resistencias comienzan siendo menores de las anteriormente descritas, especialmente con el aditivo XL40, pero alcanzan su máximo en la sustitución del 75% para ambos aditivos con valores de 4,69-4,70 MPa. Para la dosificación 1/8, las resistencias comienzan en torno a los 1,6-2,5 MPa para aumentar posteriormente hasta alcanzar su máximo en la sustitución del 75% para ambos aditivos, siendo siempre mayor en el caso del aditivo XL40 (4,62 MPa) frente al T03 (4,02 MPa).

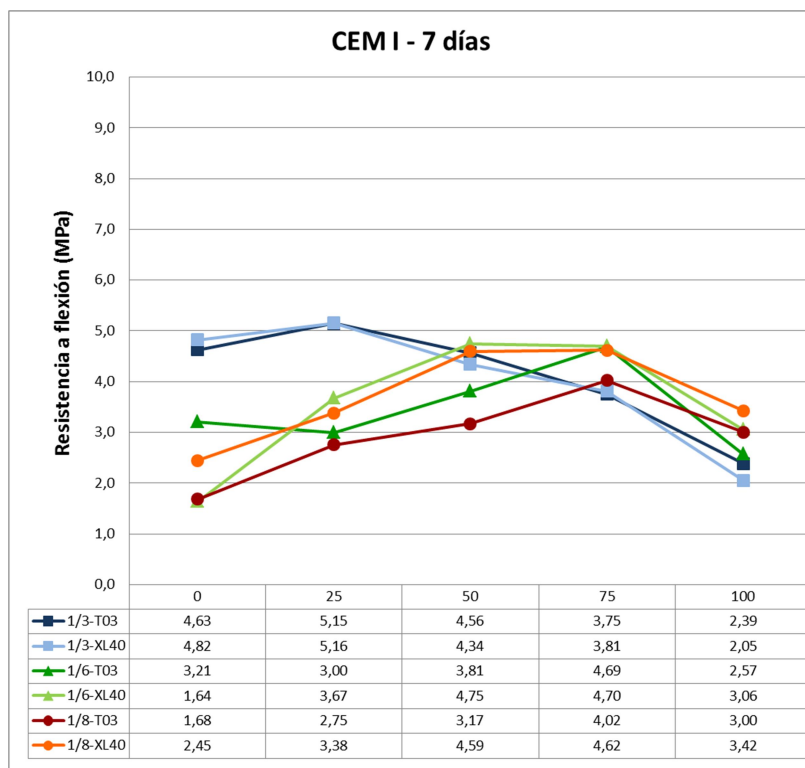


Figura 5.14. Resistencias mecánicas a flexión del cemento tipo I a 7 días

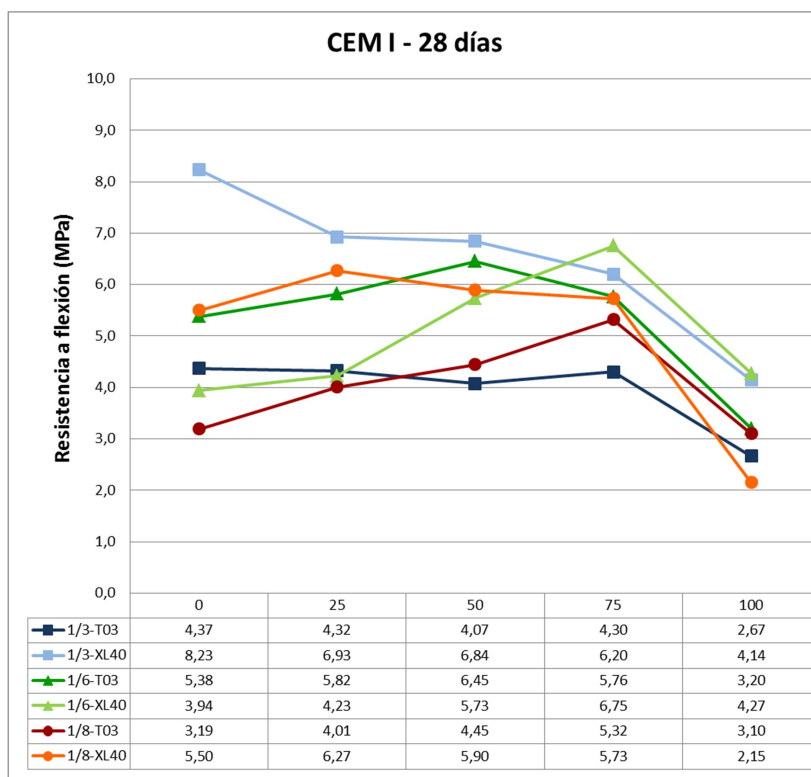


Figura 5.15. Resistencias mecánicas a flexión del cemento tipo I a 28 días

Tras 28 días de curado, el mayor dato alcanzado se obtiene con la relación cemento/[árido+residuo de poliuretano] 1/3 y el aditivo XL 40, ya que llegamos a alcanzar los 8,2 MPa, disminuyendo de forma progresiva conforme aumenta la cantidad de árido que sustituimos por poliuretano. En el caso del aditivo T03 el comportamiento es similar aunque los valores son algo menores, ya que van de los 4,4 MPa iniciales hasta los 2,7 MPa finales. Para la dosificación 1/6, los valores son en general mayores para el aditivo T03, con la mayor resistencia en la sustitución del 50% al llegar a los 6,5 MPa, pero el máximo lo alcanza el aditivo XL40 en la sustitución del 75% con 6,8 MPa. Para la dosificación 1/8, las resistencias a flexión son mucho mayores en el caso del aditivo XL40, comparado con el T03, llegando a ser de hasta 6,3 MPa en la sustitución del 25%. En general, los valores finales en la mayoría de las dosificaciones son mucho menores que los iniciales, ya que se ha sustituido todo el árido por poliuretano, reduciendo por tanto la capacidad de las probetas a resistir los esfuerzos de flexión.

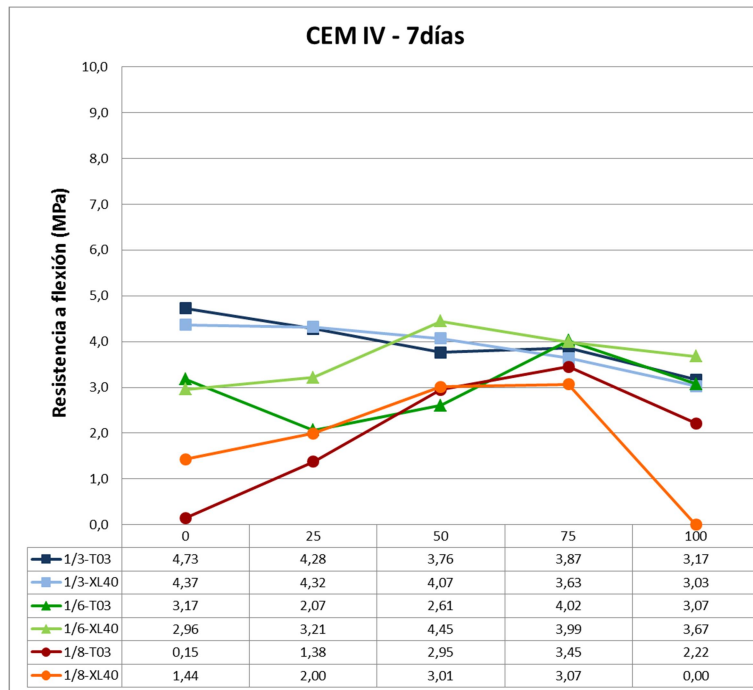


Figura 5.16. Resistencias mecánicas a flexión del cemento tipo IV a los 7 días de curado para las diferentes dosificaciones

En las Figuras 5.16 y 5.17 se muestran las resistencias a flexión de las probetas de cemento tipo IV tras 7 y 28 días de curado. En general, las resistencias son menores que para el cemento tipo I, ya que este cemento contiene más impurezas que repercuten en las propiedades finales. A los 7 días, las dosificaciones con mayores resistencias son las mezclas con mayor cantidad de cemento, es decir las relaciones 1/3, en las probetas de referencia, con un valor de 4,7 MPa para el aditivo T03, disminuyendo posteriormente progresivamente conforme vamos sustituyendo árido por poliuretano. Para la dosificación 1/6, las mayores resistencias se registran en la sustitución del 50% para el aditivo XL40 con un valor de 4,5 MPa, y de 4,02 MPa para el aditivo T03 en la sustitución del 75%. Sin embargo, en esta dosificación con aditivo XL40, las resistencias son mayores en la sustitución del 100% que en las probetas de referencia. Para la dosificación 1/8, las resistencias son las menores, comenzando entre 0 y 1,5 MPa para el aditivo T03 y XL40 respectivamente, hasta alcanzar el máximo en la sustitución del 75% con valores de 3,5-3,1 MPa.

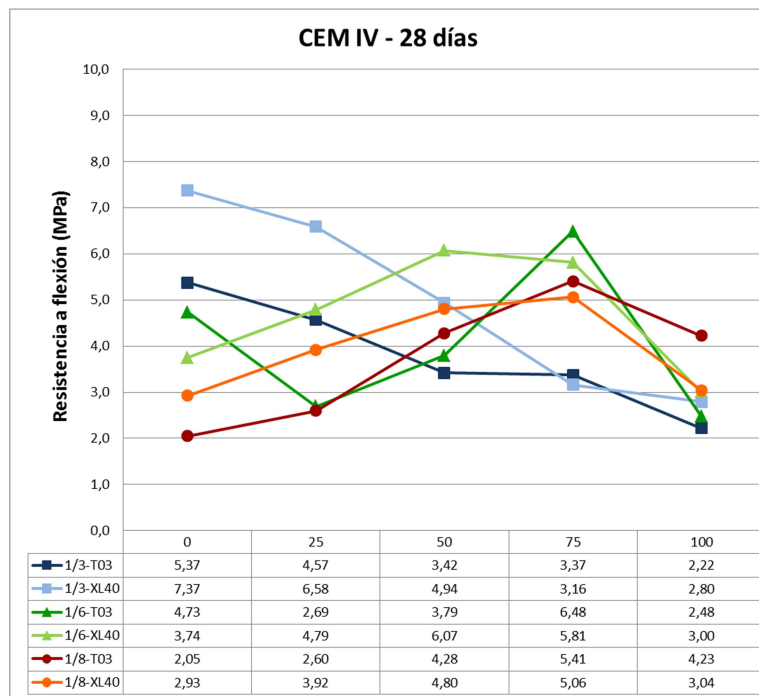


Figura 5.17 Resistencias mecánicas a flexión del cemento tipo IV a los 28 días de curado para las diferentes dosificaciones

A los 28 días, se obtienen mejores resultados con el aditivo XL40, donde se alcanza el máximo valor de 7,4 MPa en materiales de referencia, e igualmente disminuye a continuación de forma progresiva según aumenta la cantidad de árido que sustituimos por polímero. Para el aditivo T03 obtenemos el mismo comportamiento pero con menores valores, de 5,4 MPa iniciales a los 2,2 MPa que obtenemos al final. En la dosificación 1/6, los valores iniciales son menores a los anteriores pero posteriormente las resistencias a flexión aumentan hasta los 6,5 MPa que alcanzan en la sustitución del 75% para el T03 y los 6,1 MPa que se obtienen en la sustitución del 50% con el XL40. En el caso de la dosificación 1/8, los valores iniciales son los menores de todas las dosificaciones, entre los 2 MPa y 3 MPa, aumentando posteriormente conforme aumenta la cantidad de árido que se sustituye por poliuretano hasta un máximo de 5,4 MPa en el caso del aditivo T03 y de 5,1 MPa en el aditivo XL 40, ambos en la sustitución del 75%. Por lo tanto, en estas dos dosificaciones finales (1/6 y 1/8) el efecto de la sustitución de árido por poliuretano es positivo, ya que conseguimos un aumento



de las resistencias mecánicas de flexión en comparación con las de referencia, con máximos en las dosificaciones de 50% y 75% de sustitución.

### 5.5.2 Resistencias mecánicas a compresión

Estos materiales se ensayan a compresión después de 7 y 28 días de curado. Se eliminan las partículas o cualquier otro material no adherido de la superficie de las probetas, y se limpia la superficie de carga de la máquina de ensayo así como los platos de apoyo y el adaptador de ensayo. La resistencia a compresión ( $c$ ) se calcula dividiendo la carga máxima soportada por la probeta por su sección transversal, tal y como se muestra en la expresión 5.3. Los resultados de ambos ensayos tras 7 y 28 días se muestran en las Tabla 5.16 y 5.17.

$$c = \frac{F}{S} \quad \text{Eq. (5.3)}$$

**c** : resistencia a compresión en N/mm<sup>2</sup>

**F** : carga máxima aplicada en la probeta, en N

**S** : sección transversal en mm<sup>2</sup>



Dosificación	Resistencia a compresión a 7 días (MPa)	Resistencia a compresión a 28 días (MPa)
3PU100T03I	21,21	27,83
3PU75T03I	22,43	27,96
3PU50T03I	25,03	30,67
3PU25T03I	24,21	33,40
3RT03I	25,56	31,57
3PU100XL40I	21,91	29,57
3PU75XL40I	21,31	30,20
3PU50XL40I	23,58	33,16
3PU25XL40I	23,30	32,01
3RXL40I	26,81	31,27
6PU100T03I	19,95	25,32
6PU75T03I	24,96	31,72
6PU50T03I	17,18	25,70
6PU25T03I	12,63	16,40
6RT03I	9,71	15,80
6PU100XL40I	20,11	24,70
6PU75XL40I	26,36	33,93
6PU50XL40I	19,11	26,65
6PU25XL40I	12,05	16,65
6RXL40I	5,83	14,11
8PU100T03I	11,25	16,62
8PU75T03I	16,12	25,30
8PU50T03I	11,17	17,65
8PU25T03I	7,83	15,48
8RT03I	5,44	11,58
8PU100XL40I	12,89	18,27
8PU75XL40I	15,31	23,91
8PU50XL40I	16,91	27,77
8PU25XL40I	10,94	18,53
8RXL40I	7,49	14,64

Tabla 5.16. Resistencias mecánicas a compresión tras 7 y 28 días de curado para las dosificaciones con cemento tipo I.



Dosificación	Resistencia a compresión a 7 días (MPa)	Resistencia a compresión a 28 días (MPa)
3PU100T03IV	11,77	17,51
3PU75T03IV	13,09	18,80
3PU50T03IV	14,26	18,78
3PU25T03IV	16,91	26,06
3RT03IV	15,38	25,73
3PU100XL40IV	11,97	20,30
3PU75XL40IV	12,94	21,87
3PU50XL40IV	14,79	27,61
3PU25XL40IV	15,12	25,87
3RXL40IV	17,15	23,61
6PU100T03IV	11,62	17,10
6PU75T03IV	15,72	25,70
6PU50T03IV	8,26	17,85
6PU25T03IV	5,29	8,10
6RT03IV	9,14	15,59
6PU100XL40IV	10,56	19,75
6PU75XL40IV	14,26	24,73
6PU50XL40IV	14,24	24,72
6PU25XL40IV	7,21	15,47
6RXL40IV	5,75	12,63
8PU100T03IV	7,53	15,69
8PU75T03IV	10,64	21,02
8PU50T03IV	9,25	16,12
8PU25T03IV	4,55	8,83
8RT03IV	2,94	7,74
8PU100XL40IV	6,58	11,17
8PU75XL40IV	9,27	15,93
8PU50XL40IV	9,21	18,89
8PU25XL40IV	5,32	12,45
8RXL40IV	2,95	8,55

Tabla 5.17. Resistencias mecánicas a compresión tras 7 y 28 días de curado para las dosificaciones con cemento tipo IV.



A los 7 días, las dosificaciones con las que obtenemos mayores resistencias son las de la relación [cemento/(árido+residuo de poliuretano)] de 1/3, para los dos aditivos empleados (Figura 5.17). Posteriormente las resistencias mecánicas a compresión disminuyen progresivamente conforme vamos sustituyendo árido por poliuretano hasta unos valores de unos 21,2-21,9 MPa, según el tipo de aditivo empleado (T03 y XL40 respectivamente). Aun así, este último valor para la sustitución del 100% de árido por poliuretano sigue siendo mayor de 20 N/mm<sup>2</sup> por lo que incluso en este caso se podría considerar como un mortero M20.

En el caso de la dosificación 1/6, las resistencias iniciales son mucho menores a las anteriores, en torno a los 5,8-9,7 MPa, según los aditivos empleados (XL40 y T03 respectivamente) pero posteriormente aumentan hasta llegar a un máximo para la sustitución del 75% con el aditivo XL40 de 26,4 MPa y con el aditivo T03 de 25 MPa. En la sustitución del 100% de árido por poliuretano disminuye, quedándose en torno a los 20 MPa de resistencia. Para la última dosificación de 1/8 sucede lo mismo que en esta anterior, en la que comenzamos inicialmente con resistencias menores que en la primera dosificación de 1/3, en torno a los 5,4-7,5 MPa, según los aditivos empleados (T03 y TXL40 respectivamente) pero posteriormente sucede algo similar al caso anterior, ya que aumentan hasta llegar a un máximo para la sustitución del 50% con el aditivo XL40 de 16,9 MPa, y con el aditivo T03 la mayor resistencia se da en la sustitución del 75% con 16,1 MPa. En este caso por lo tanto, para la dosificación 1/3, al sustituir árido por poliuretano las resistencias disminuyen en comparación con la de referencia, pero incluso en el menor de los valores obtenidos (sustitución 100%), el mortero alcanza valores mayores de 20MPa, pudiéndolo considerar un mortero M20. En el resto de las dosificaciones, la sustitución de árido por poliuretano hace que las resistencias mecánicas a compresión se incrementen, por lo que el efecto que tiene el reemplazo de residuo de polímero por arena es muy positivo, ya que en algún caso tenemos morteros también con resistencias mayores a 20 MPa para la sustitución 1/6, siendo valores muy elevados para este tipo de morteros.

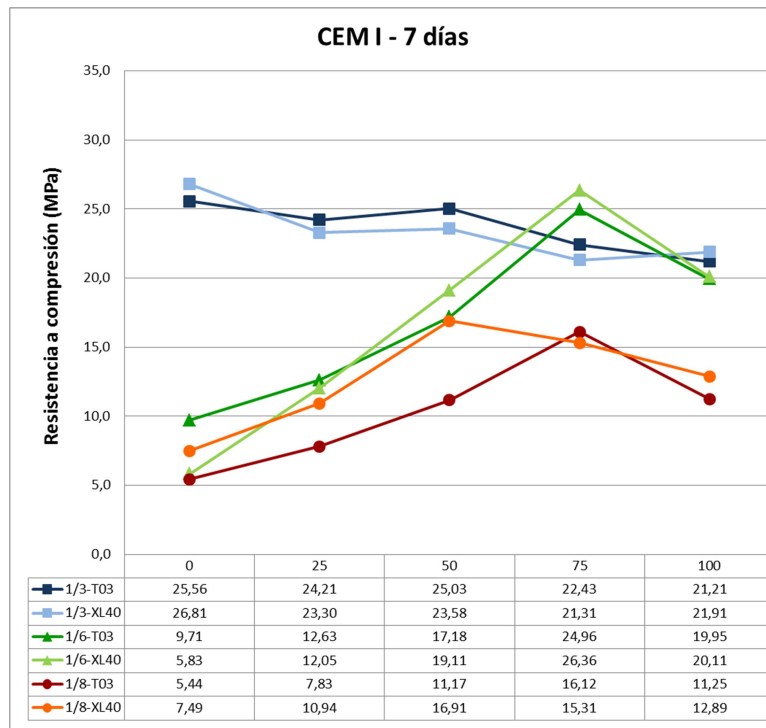


Figura 5.17 Resistencias mecánicas a compresión del cemento tipo I a los 7 días de curado para las diferentes dosificaciones

A los 28 días (Figura 5.18) sucede algo similar, ya que los valores se van incrementando a medida que aumentamos la sustitución de árido por PU. Mientras que las probetas de referencia alcanzan unos valores de 31,3-31,6 MPa según el aditivo empleado (XL40 y T03 respectivamente), llegan a alcanzar 33,4 MPa para el aditivo T03 y sustitución del 25%, y 33,2 MPa para el aditivo XL40 y sustitución del 50%. Posteriormente los valores disminuyen ligeramente, con mínimos de 27,8-29,6 MPa en la sustitución del 100% de árido por poliuretano. En caso de la dosificación 1/6, las resistencias de los morteros iniciales de referencia son relativamente menores, alrededor de los 14,1-15,8 MPa. A medida que se incorporan cantidades mayores de residuo las resistencias aumentan, hasta alcanzar el máximo en ambos aditivos en la sustitución del 75% con valores de 33,9 MPa y 31,7 MPa para el aditivo XL40 y T03 respectivamente.

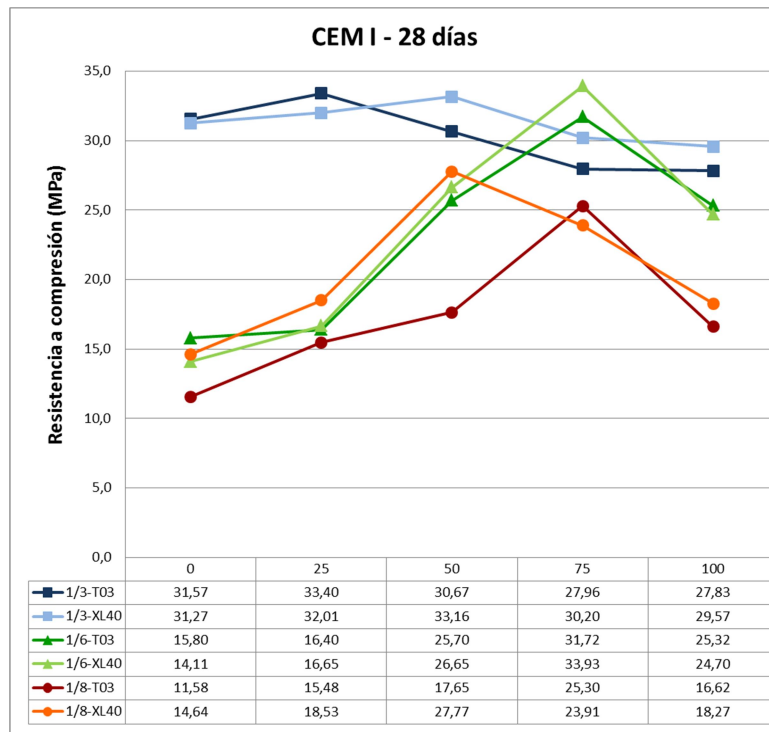


Figura 5.18 Resistencias mecánicas a compresión del cemento tipo IV a los 28 días de curado para las diferentes dosificaciones

La dosificación de relación cemento/[árido+residuo de poliuretano]] 1/8 tiene un comportamiento parecido a la anterior, aunque las resistencias mecánicas que alcanza son algo menores. Inicialmente, en las probetas de referencia se parte de unas resistencias mecánicas de entre 11,6-14,6 MPa para los aditivos T03 y XL40, que aumentan hasta un máximo de 27,8 MPa en la sustitución del 50% con el aditivo XL40, y 23,9 MPa para la sustitución del 75% con el T03. En ambos casos, las resistencias mecánicas son mayores a 20 MPa, por lo que también se podría considerar mortero tipo M20. Las demás son menores pero casi siempre (excepto la de referencia con aditivo T03) están por encima de los 15 MPa, por lo que la resistencia que tienen a compresión sigue siendo elevada.

Se puede concluir que se alcanzan máximos de resistencia al reemplazar árido por residuo de poliuretano triturado, por lo que esta sustitución tiene un efecto beneficioso para las resistencias mecánicas. Los valores de referencia aumentan un 6% y oscilan en torno a los 33 MPa, valores muy elevados y suficientes para morteros de tipo



estructural. Por ejemplo, para la dosificación 1/6 aumenta las resistencias iniciales un 200% con el aditivo T03, y un 240% con el XL40. Para las muestras con relación 1/8 se obtienen resultados muy similares, con un 218% c y un 190%, respectivamente.

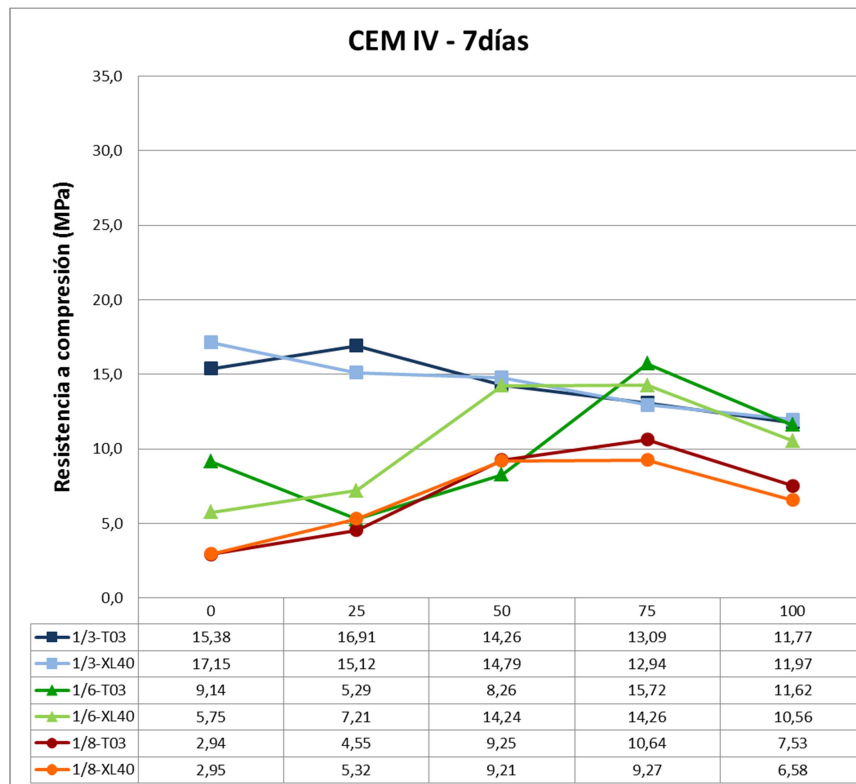


Figura 5.19 Resistencias mecánicas a compresión del cemento tipo IV a los 7 días de curado para las diferentes dosificaciones

En las Figuras 5.19 y 5.20 se comprueban las resistencias de las probetas de cemento tipo IV tras 7 y 28 días de curado. Los resultados son similares a los obtenidos con cemento tipo I aunque con valores menores debido a la naturaleza del conglomerante utilizado.

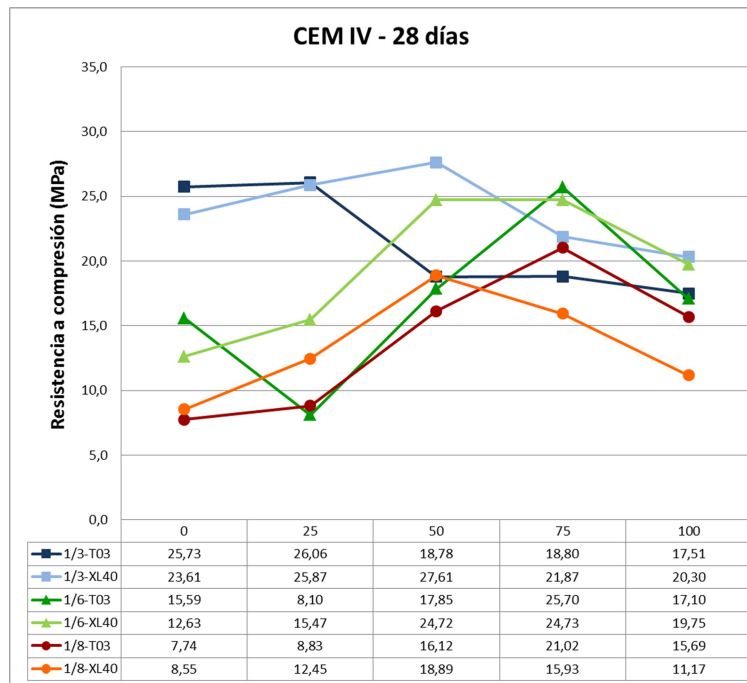


Figura 5.20 Resistencias mecánicas a compresión del cemento tipo IV a los 28 días de curado para las diferentes dosificaciones

En general, y salvo en el caso de la dosificación 1/3 y aditivo XL40 en la que las resistencias a 7 días disminuyen hasta un 30% en la sustitución del 100% pero con valores siempre mayores a los 10MPa, el efecto de la sustitución de árido por poliuretano resulta ventajoso en cuanto a las resistencias mecánicas se refiere, ya que aumentan considerablemente respecto de las dosificaciones de referencia.

En caso de la dosificación 1/6 las resistencias llegan hasta valores de 15,6 MPa y crecen progresivamente hasta alcanzar el máximo en la sustitución del 75% con valores de 25,7 MPa y 24,7 MPa para los aditivos T03 y XL40, respectivamente.

Para la dosificación 1/8, se parte de resistencias iniciales no muy elevadas, de 7,7 MPa y de 8,6 MPa, que posteriormente se desarrollan hasta un máximo de 21 MPa en la sustitución del 75% con el aditivo T03, y 18,9 MPa para la sustitución del 50% con el aditivo XL40.



## 5.6. Retracción

La retracción se ha determinado mediante la fabricación de probetas de pastas de cemento cilíndricas con moldes de Teflon®, tal y como se muestra en la Figura 5.21a),b). Una vez desmoldadas, se curan durante 28 días al aire, a una humedad relativa del 100% y a una temperatura de  $20\pm2^{\circ}\text{C}$ . Los cementos empleados son cemento gris OPC (SPLC) tipos I, II y IV, fabricando 3 probetas cilíndricas con cemento de referencia y otras 3 probetas con poliuretano, con las dosificaciones descritas en la Tabla 5.18.

Previo al proceso de curado, las probetas se dejan 24 horas girando continuamente para evitar que haya poros, tal y como se muestra en la Figura 5.21c).

Las probetas se mantienen 28 días al 100% de humedad relativa, reduciendo a continuación dicha humedad al 50%, lo que supone una disminución del contenido de agua, que a su vez conlleva un descenso de sus dimensiones (fenómeno conocido como retracción). La variación de longitud de las probetas se realizó durante 28 días tras el tiempo de curado con un equipo de medida de la retracción (Figura 5.21d).

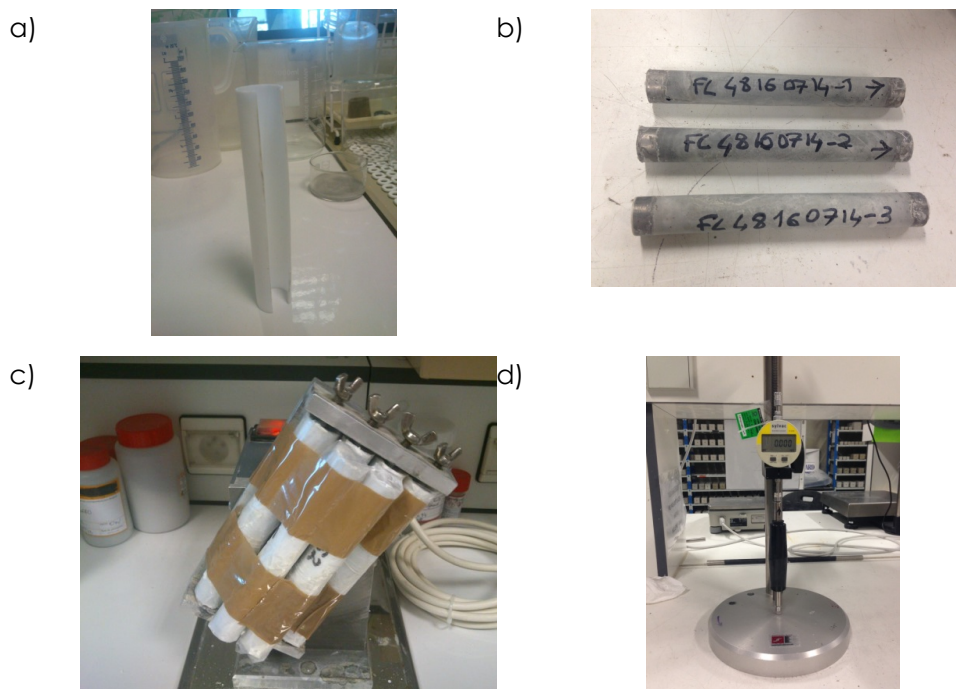


Figura 5.21. Ensayo de retracción. a),b) Molde cilíndrico de Teflon® empleado para la fabricación de las probetas; c) Las probetas giran continuamente durante 24h para evitar poros; d) Aparato empleado para medir la retracción, determinando la variación de longitud de las probetas.

Tipo de cemento	Relación agua/cemento	Incluye PU	Dosificación
Cemento gris OPC (SPLC) tipo I	0,45	no	REF-CEM1
		sí	CEM1+PU
Cemento gris OPC (SPLC) tipo II	0,45	no	REF-CEM2
		sí	CEM2+PU
Cemento gris OPC (SPLC) tipo IV	0,45	no	REF-CEM4
		sí	CEM4+PU

Tabla 5.18. Tipos de cementos y mezclas empleadas para los ensayos de retracción.



El contenido de masa de agua, que representa el ratio entre la masa de agua que hay en la muestra y la masa seca, se obtiene pesando las probetas. Cuando las variaciones de masa de las muestras son menores al 0,1% en tres pesadas continuas, se considera masa constante. Cada cilindro incluye dos pastillas cilíndricas en cada extremo para permitir medir las variaciones de dimensiones de cada probeta en función del tiempo. Los resultados obtenidos para los cementos tipo I, II, y IV son los que se muestran en las Figuras 5.22, 5.23 y 5.24, respectivamente.

Los resultados obtenidos para el cemento tipo I (Figura 5.22) muestran cómo los valores para probetas de referencia y aquellas que contienen poliuretano son muy similares, por lo que en este tipo de cemento no se puede considerar que la adición de poliuretano al cemento influya en la retracción.

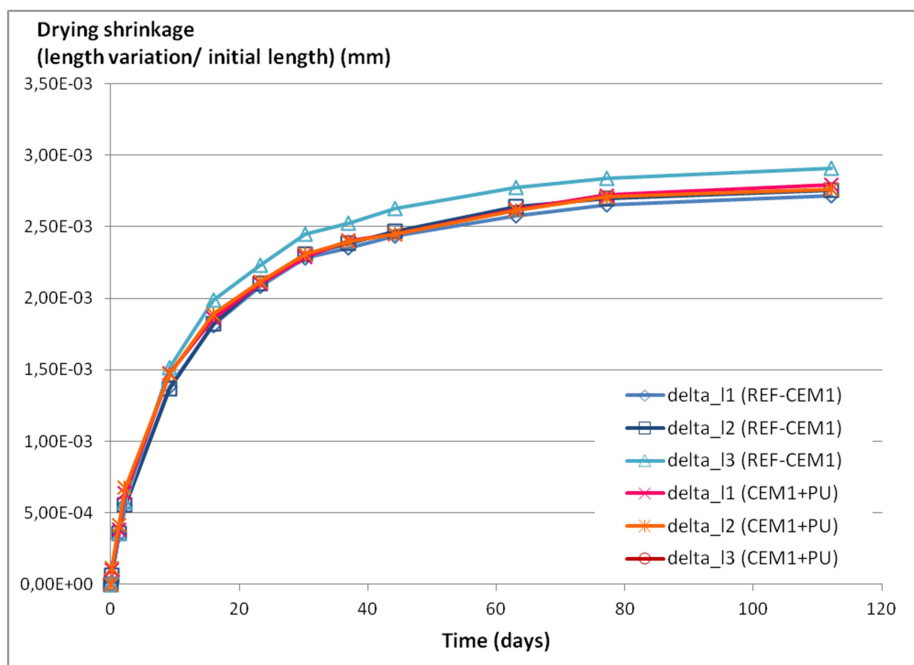


Figura 5.22. Resultados de los ensayos de retracción para cemento tipo I, de referencia y con poliuretano.

En el caso del cemento tipo II (Figura 5.23), hay dos probetas cuyos valores son ligeramente mayores a los de la media. Aunque se obtienen algunos resultados donde la retracción es algo mayor de la media, en términos generales, la mayoría de ellos arrojan valores muy similares, por



lo que en este caso tampoco se podría considerar que añadir poliuretano al cemento pueda modificar la retracción.

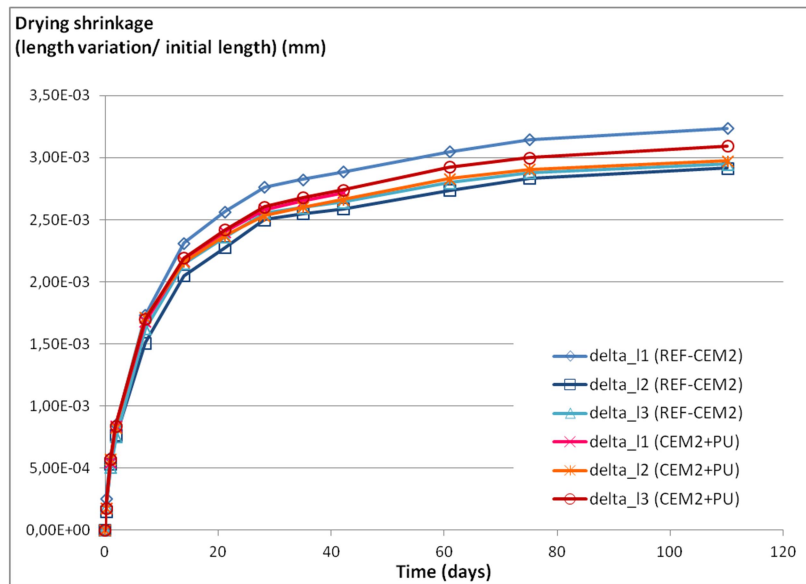


Figura 5.23. Resultados de los ensayos de retracción para cemento tipo II de referencia y con poliuretano.

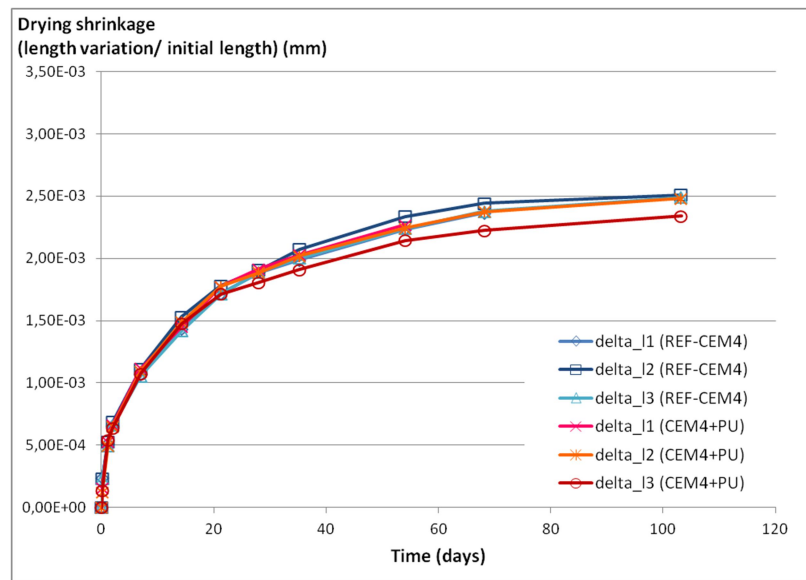


Figura 5.24. Resultados de los ensayos de retracción para cemento tipo IV de referencia y con poliuretano.



En el caso de una de las probetas de referencia realizadas con cemento tipo IV (Figura 5.24), se obtienen valores de retracción sensiblemente mayores a los de la media. Por el contrario, una de las muestras que incluye poliuretano, alcanza valores inferiores a la media. Estos datos tampoco son significativos por lo que no se considera que el poliuretano tenga influencia en la retracción.

Las diferencias en cuanto a los valores finales de retracción se debe al distinto tipo de cemento empleado y a sus distintos componentes especificados en el apartado 5.2.1, que es lo que provoca que los valores finales sean diferentes.

## **Capítulo 6**

---

**Otras propiedades de los  
morteros aligerados con  
capacidades estructurales**





Con la intención de completar el análisis y la viabilidad a largo plazo de estos materiales con propiedades estructurales, se han llevado a cabo otros ensayos de caracterización que, aun no siendo habituales en procesos de verificación para la puesta en obra, contribuyen a un mejor conocimiento del comportamiento de este tipo de morteros con poliuretano reciclado.

### 6.1. Microscopia electrónica de barrido (SEM)

Los morteros de cemento y las pastas de C<sub>3</sub>S se han caracterizado utilizando un microscopio electrónico de barrido, que emplea un haz de electrones para formar imágenes de alta resolución. De este modo se puede enfocar a la vez una gran parte de la muestra y observar así su estructura a pequeña escala. Para los morteros de cemento se emplea un microscopio electrónico de barrido JEOL JSM-6460LV con sistema INCA de análisis elemental por rayos X, tal y como se puede ver en la Figura 6.1, mientras que las pastas de C<sub>3</sub>S con o sin afwillita se analizan con un equipo SEM FEG Quanta 400 de la compañía FEI, USA; con un voltaje de aceleración de 15 keV y una intensidad de corriente de 1 nA. SEM/EDS ayudo a identificar las fases de la sección pulida de la pasta, midiendo el ratio molar Ca/Si.



Figura 6.1. Microscopio electrónico de barrido JEOL JSM-6460LV (SEM)

En el caso de la relación 1/3 en la dosificación de referencia se puede observar el cemento con el árido y el efecto del aditivo T03, que compacta la matriz respecto a las mismas mezclas a pesar de la presencia del poliuretano espumado (Figura 6.2).

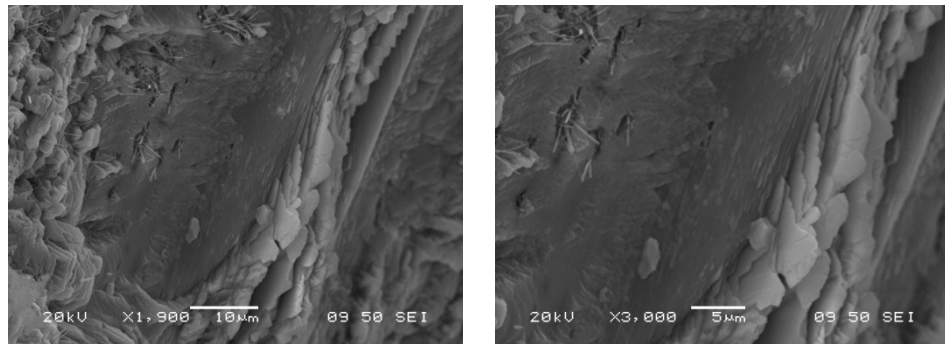


Figura 6.2. Imágenes para la dosificación 3RT03I

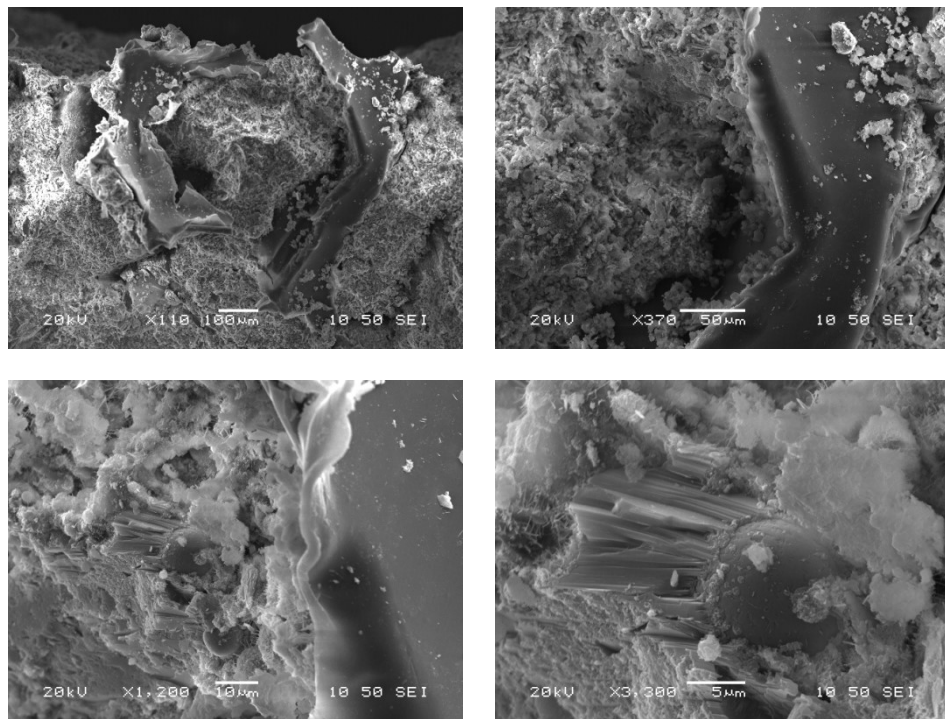


Figura 6.3. Imágenes para la dosificación 3PU75XL40

En esta misma relación 1/3, cuando se sustituye el 75% de árido por poliuretano empleando aditivos, es decir, para las mezclas 3PU75T03 y 3PU75XL40, se obtienen las imágenes mostradas en las Figura 6.3 y 6.4 respectivamente, donde se observa una capacidad similar a la muestra de referencia, a pesar de la inclusión de residuo de poliuretano que



introduciría una mayor porosidad a priori. Esta mayor compacidad viene dada por el efecto del surfactante.

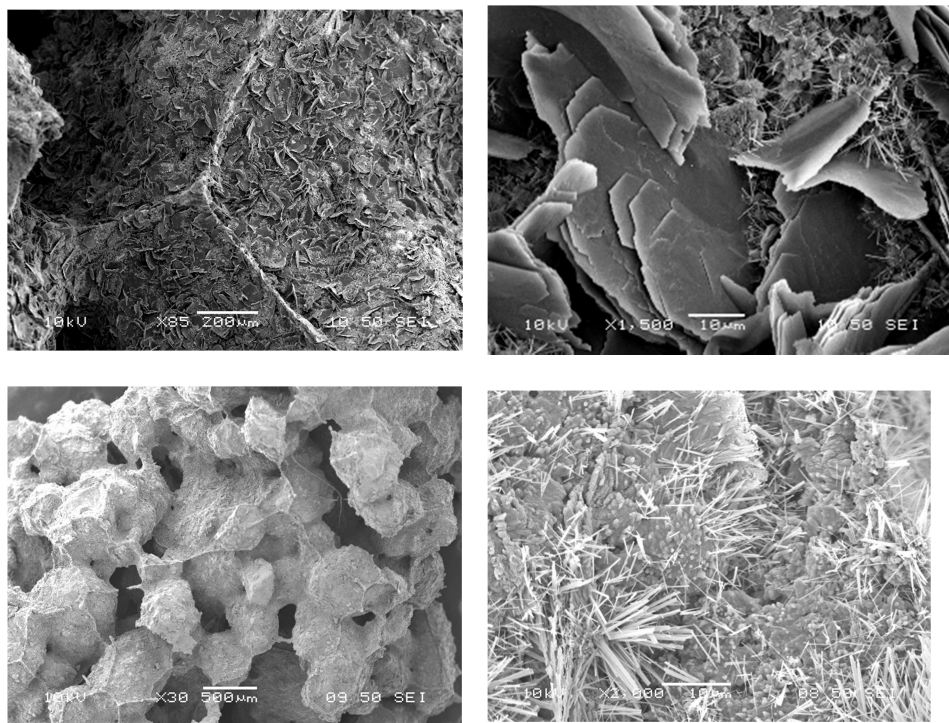


Figura 6.4. Imágenes para la dosificación 3PU75T03

Si ampliamos el estudio a la dosificación 3PU100T03I, con 100% de sustitución, se obtienen las imágenes de la Figura 6.5, en la que se aprecia el aditivo T03 en forma de hilos uniendo las partículas de poliuretano con el cemento y ayudando a formar una estructura más compacta, evitando de este modo que las partículas de poliuretano se disgreguen.

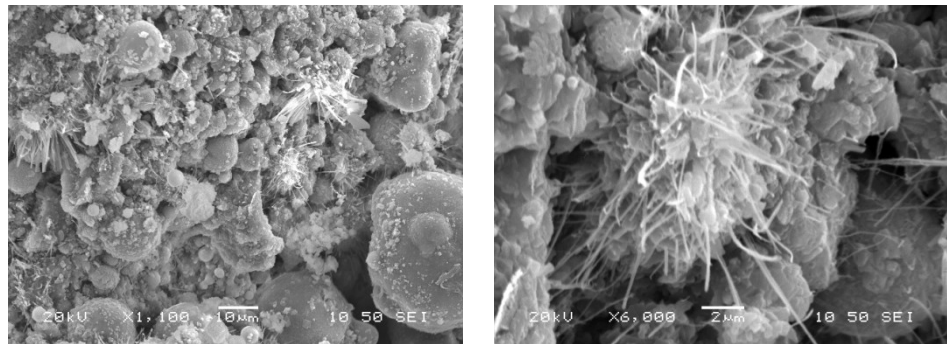


Figura 6.5. Imágenes para la dosificación 3PU100T03I

Ampliando el estudio a relaciones [cemento/(árido+residuo de poliuretano)] de 1/6 y de 1/8, también se aprecian los cambios en la matriz cementante a través de una compactación, provocada por el efecto surfactante del aditivo. En el caso de la 6RT03I, es decir, la relación 1/6 en el mortero de referencia en el que sólo hay cemento tipo I, árido y aditivo T03, se puede observar la unión de las partículas a través del aditivo T03 mediante hilos, lo cual confiere una estructura más compacta y resistente que si no se empleara este último. (Figura 6.6)

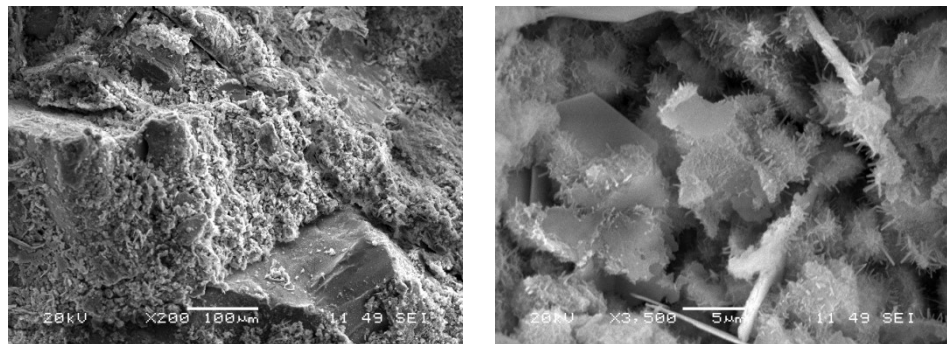


Figura 6.6. Imágenes para la dosificación 6RT03I

Para la relación 1/8 se ha visualizado mediante microscopio electrónico la sustitución del 75% de árido por poliuretano con aditivo T03 (Figura 6.7).

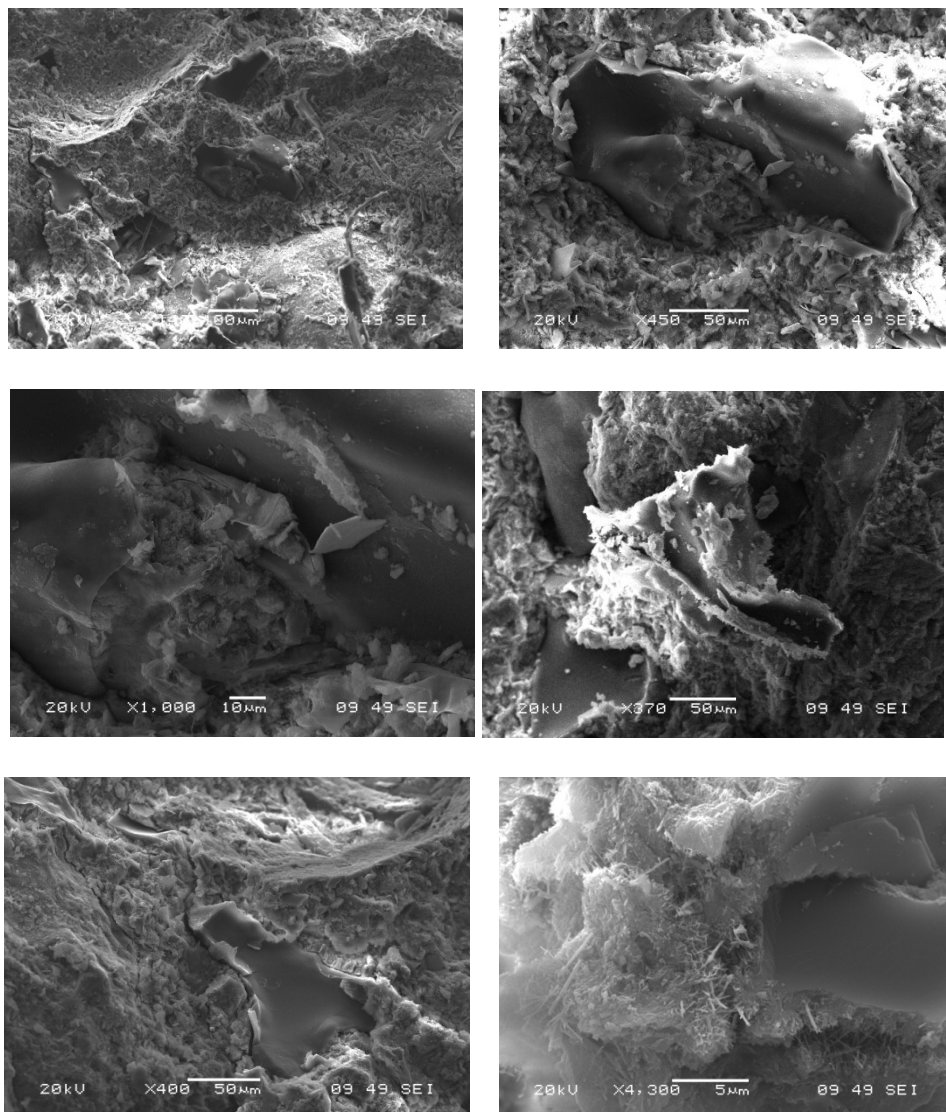


Figura 6.7. Imágenes para la dosificación 8PU75T03

Asimismo, se ha analizado mediante el microscopio electrónico la sustitución del 100% de árido por poliuretano con aditivo T03, en esta misma relación 1/8. En la Figura 6.8, se puede observar con gran nitidez la unión de poliuretano al cemento mediante este aditivo empleado, que es lo que contribuye a que el mortero tenga una mayor consistencia y por tanto mayor resistencia mecánica.

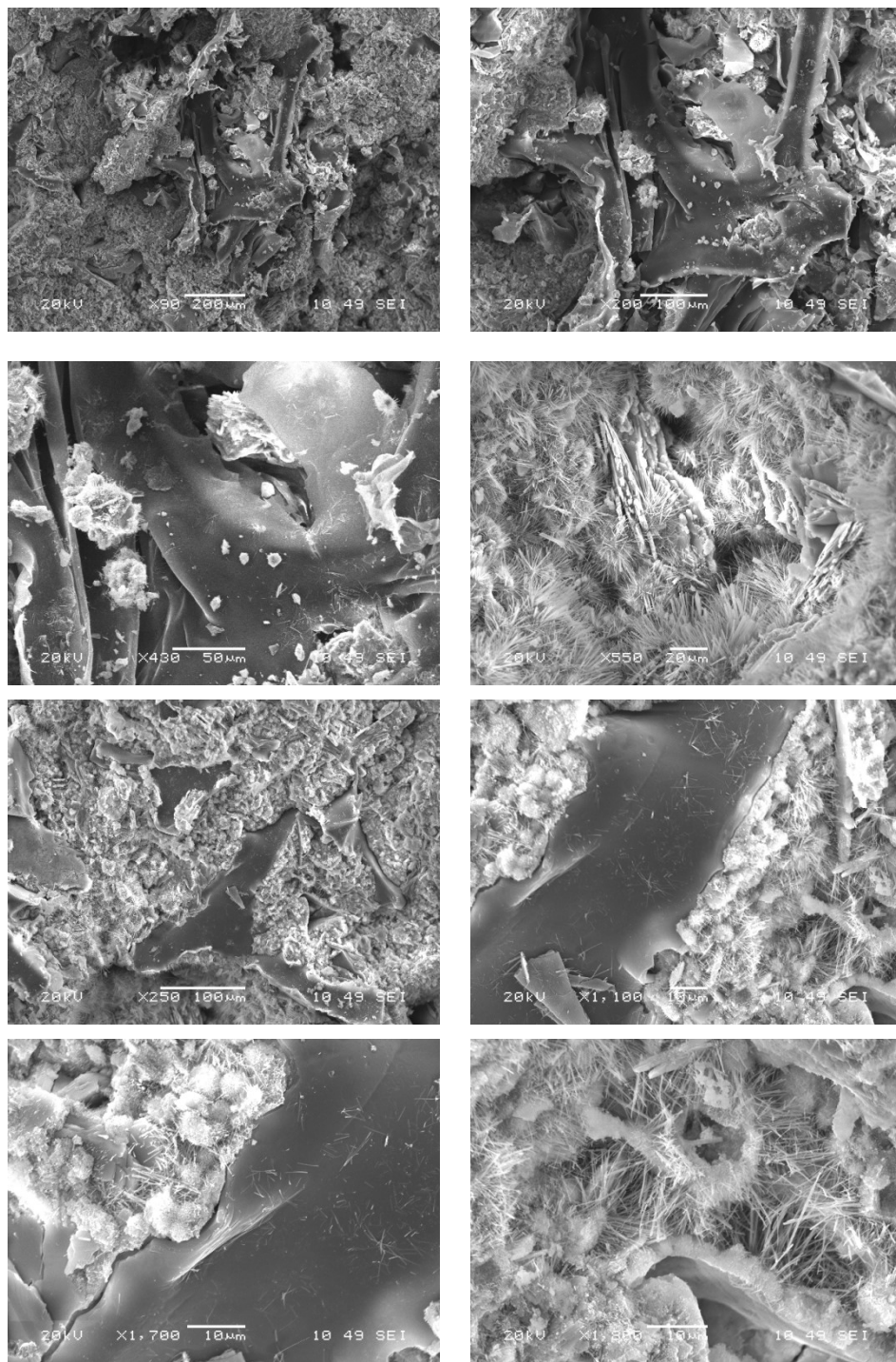


Figura 6.8. Imágenes para la dosificación 8PU100T03I



En el caso de las pastas de  $\text{C}_3\text{S}$ , se ha realizado una comparación entre las pastas de referencia tras 7 y 28 días de curado y las pastas en las que se siembran semillas de afwillita para ver la estructura que adquieren dichas pastas y las modificaciones que la afwillita realiza en la microestructura de  $\text{C}_3\text{S}$ .

En la Figura 6.9 se muestra la distribución de las partículas de afwillita que han sido empleadas para sembrar la pasta de  $\text{C}_3\text{S}$  así como su tamaño, comprendido entre 3 y 5  $\mu\text{m}$ . La microestructura de la pasta sembrada con afwillita es más gruesa que la de referencia. El gel de C-S-H no desaparece del todo ya que recubre los cristales de afwillita. La microestructura que se forma en el caso de añadir afwillita al  $\text{C}_3\text{S}$  es más porosa que la red formada tan solo por gel C-S-H. En el caso de la pasta de referencia, los poros son menores de 0,1  $\mu\text{m}$  mientras que la pasta sembrada incluye también poros de mayor tamaño.

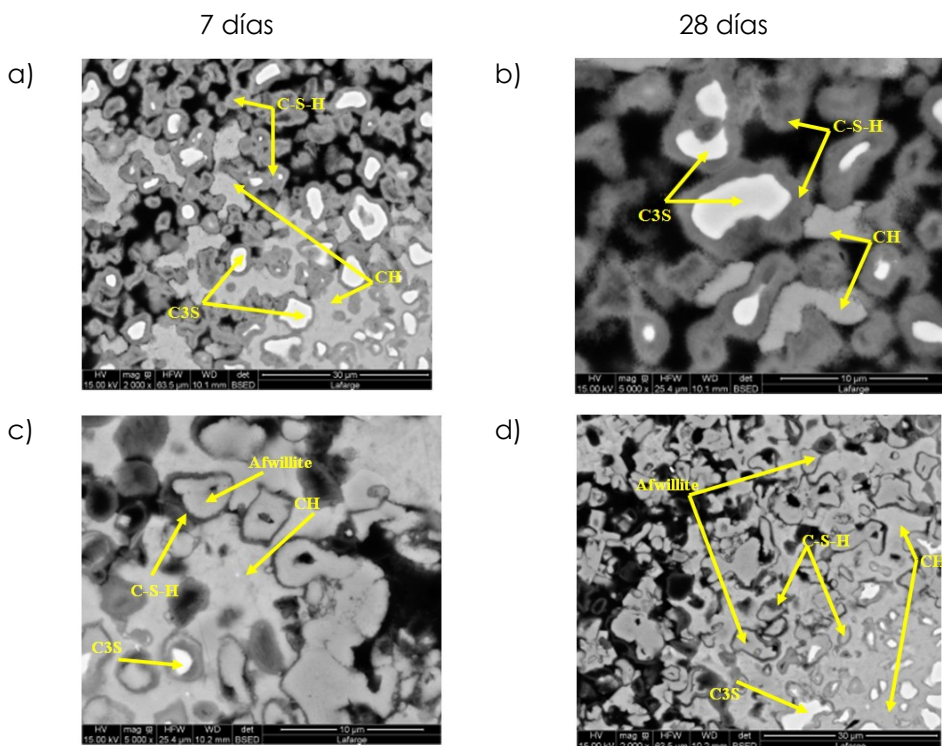


Figura 6.9. Imágenes SEM (en modo BSED) de las pastas de  $\text{C}_3\text{S}$  tras 7 y 28 días de curado: (a,b) pastas de referencia; (c,d) pastas sembradas con afwillita (ratio afwillita/ $\text{C}_3\text{S}$ =0,02).

En la Figura 6.10 se puede observar la afwillita, con forma prismática, rodeada de C-S-H, formada por pequeños hilos, y la microestructura



que forman en la pasta de  $\text{C}_3\text{S}$ . Como se puede observar en la pasta sembrada con afwillita, dichos cristales sustituyen al gel de C-S-H. Por otro lado, la Figura 6.11 recoge imágenes de semillas de afwillita pura.

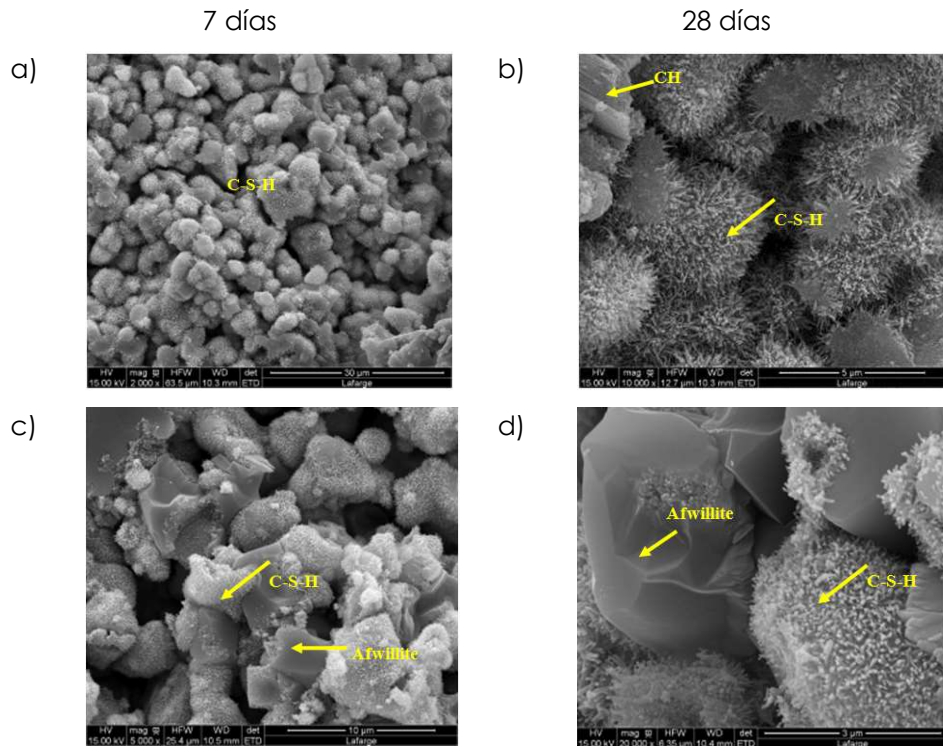


Figura 6.10. (b) Imágenes SEM (en modo SE) de las pastas de  $\text{C}_3\text{S}$  tras 7 y 28 días de curado: (a,b) pastas de referencia; (c,d) pastas sembradas con afwillita (ratio afwillita/ $\text{C}_3\text{S}=0,02$ ).

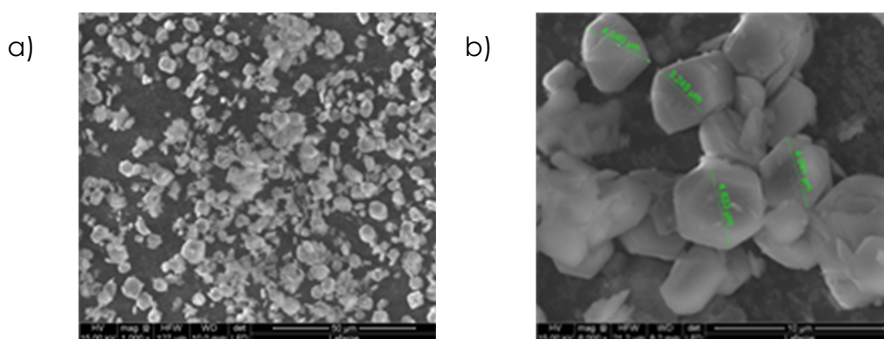


Figura 6.11. Imágenes SEM de semillas puras de afwillita: (a) distribución de las semillas; (b) tamaño y forma prismática de los cristales de 3-5  $\mu\text{m}$ .



## 6.2. Porosidad

Para analizar la porosidad de manera cuantitativa se combinan dos técnicas complementarias, la porosimetría de intrusión de mercurio (MIP, que nos indica la microporosidad) y la Tomografía Axial Computarizada (CAT, que proporciona la macroporosidad).

### 6.2.1. Porosimetría de intrusión de mercurio (MIP)

Para estudiar la estructura de poros de la pasta de  $C_3S$  se ha empleado la técnica de Porosimetría de Intrusión de Mercurio (mediante el Autopore IV de Micrometrics). El rango de presión del porosímetro abarca desde la presión ambiental hasta 400 MPa, cubriendo un rango de diámetro de poros de entre 360  $\mu\text{m}$  hasta 3 nm. Se llevaron a cabo ensayos en muestras de  $(5 \times 5 \times 5)$  mm<sup>3</sup> obtenidas del interior de las probetas. Las muestras se secaron en un horno a 45°C durante 24h antes de ser ensayadas. El ángulo de contacto para el avance o retroceso empleado fue de 130°, tal y como recomienda Taylor<sup>53</sup>para muestras de cemento ordinario. Las muestras de cemento ensayadas aparecen en la Tabla 6.1.

Tipo de cemento	Poliuretano	Afwillita	Nomenclatura
Cemento blanco Lafarge White OPC n°1 (Le Teil)	-	-	Cemento blanco I (Lafarge) - Ref
	100% de sustitución de árido por poliuretano	-	Cemento blanco I (Lafarge) + PU
	100% de sustitución de árido por poliuretano	2%	Cemento blanco I (Lafarge) + PU + afw
Cemento I (Burgos)	-	-	Cemento I (Burgos) - Ref
	100% de sustitución de árido por poliuretano	-	Cemento I (Burgos) + PU
Cemento II (Burgos)	-	-	Cemento II (Burgos) - Ref
	100% de sustitución de árido por poliuretano	-	Cemento II (Burgos) + PU

Tabla 6.1 Dosificación de las muestras de cemento ensayadas con Porosimetría de Intrusión de Mercurio (MIP)

Los resultados tras 28 días de curado se pueden ver en la Figura 6.12. En un principio la siembra de afwillita en la pasta de  $C_3S$  sí que parecía influir en la porosidad, aumentando el tamaño de poros, tal y como se ha demostrado en el Capítulo 3. Sin embargo, al realizar los ensayos de



porosimetría en las pastas de cemento con afwillita y con poliuretano, la porosidad apenas varía respecto de las pastas de referencia, por lo que se demuestra de este modo que la adición de poliuretano a las pastas de cemento no afecta a la porosidad.

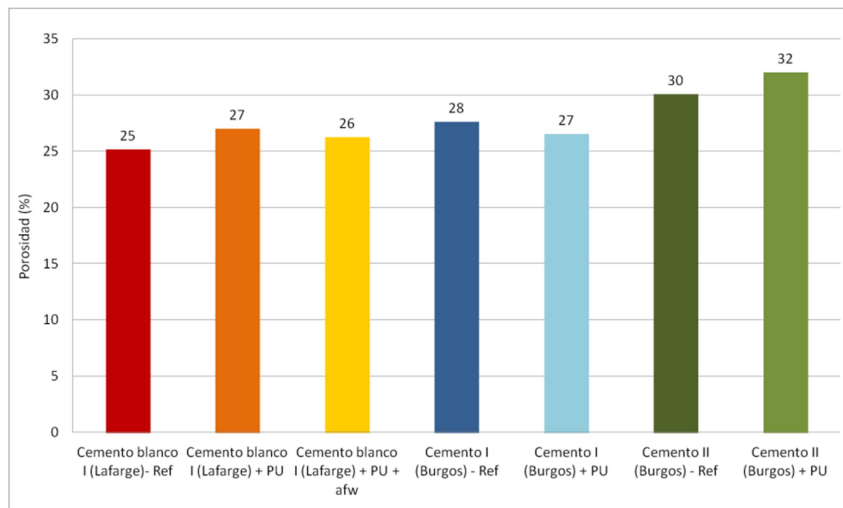


Figura 6.12. Resultados de porosidad en porcentaje de las diferentes dosificaciones ensayadas mediante Porosimetría de Intrusión de Mercurio (MIP)

Además, se ha llevado a cabo análisis de microporosimetría de las muestras de morteros de cemento con diferentes porcentajes de sustitución de árido por poliuretano aditivadas. Tal y como se describe en la Tabla 6.2, el carácter surfactante T03 o XL40, provoca una compactación que produce un incremento en la microporosidad del mortero al aumentar el porcentaje de residuo de poliuretano.

En la Tabla 6.2 se observa una disminución de la macroporosidad de los morteros mezclados con aditivos tensoactivos T03 y XL40 con el aumento de la tasa de sustitución de arena por los residuos de poliuretano. Podría plantearse la hipótesis de que los aditivos tensoactivos no iónicos con valores bajos de balance hidrófilo-lipófilo (HBL), como son el T03 y XL40, ayudan a una mejor dispersión de las partículas de cemento en el agua y mejoran la cohesión de los agregados (arena y/o residuos de poliuretano).



### 6.2.2. Tomografía axial computarizada (TAC)

Para determinar de forma cuantitativa la macroporosidad de estos morteros reciclados, se ha empleado Tomografía Axial Computarizada (CAT), que conlleva el análisis de tamaños de poro mayores de 200  $\mu\text{m}$ .<sup>92,93</sup> El equipo consiste en un sistema de rayos X con un tubo Yxlon de 225 kV / 30 mA y una cabina metálica de acero-plomo-acero, de forma que, operando con una radiación máxima de 225 kV/30 mA dentro de la cabina, las dosis máximas de radiación a una distancia de 100 mm en la superficie externa no exceden los 2,5  $\mu\text{Sv}/\text{h}$ . El procesado de datos se ha llevado a cabo con el software Mimics 10.0. Los porcentajes cuantitativos de macroporosidad se reflejan en la Tabla 6.2, junto con los valores de microporosidad y la porosidad total.

Tipo de muestra	Microporosidad (MIP) (%)	Macroporosidad (TAC) (%)	Porosidad total (%)
RTO3I	19,4	3,4	<b>22,8</b>
PU25TO3I	17,4	3,0	<b>21,9</b>
PU50TO3I	18,9	2,6	<b>20,0</b>
PU75TO3I	20,3	2,4	<b>22,7</b>
PU100TO3I	24,0	2,0	<b>26,0</b>
RXL40I	18,6	12,0	<b>30,6</b>
PU25XL40I	18,1	7,5	<b>25,6</b>
PU50XL40I	19,5	6,4	<b>25,9</b>
PU75XL40I	27,6	5,8	<b>33,4</b>
PU100XL40I	29,6	3,3	<b>32,9</b>

Tabla 6.2 Porosidades calculadas con MIP con poros entre 200  $\mu\text{m}$  y 3 nm, y TAC para cubrir el diámetro de poros mayor de 200  $\mu\text{m}$ , de varias muestras de mortero, según el tensoactivo utilizado y la tasa de sustitución de arena por PU.

El programa de reconstrucción identifica las densidades de los diferentes materiales por colores. Así, en la Figura 6.13 se puede observar la sección axial de cada probeta, siendo el color negro el menos denso y por lo tanto, el correspondiente a los poros, y el blanco

<sup>92</sup> Manso JM, Rodríguez A, Aragón A, González JJ. (2011). The durability of masonry mortars made with ladle furnace slag. Construction and Building Materials, 25, 3508-3519.

<sup>93</sup> Grangeat P. (2002) La Tomographie, Hermes Science, Traité IC2, Paris.



el más denso. Entre ambos, hay una escala de colores cuyo pixelado corresponde al resto de materiales.

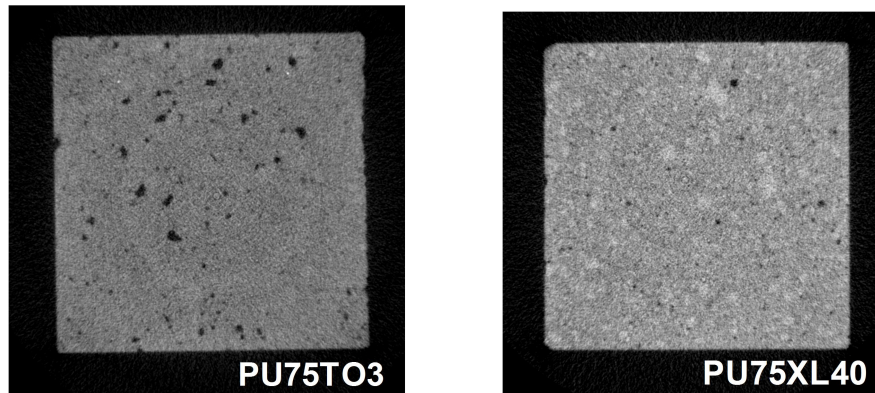


Figura 6.13. Sección axial de las dosificaciones con 75% de polímero

Con este método, se consigue observar la estructura interna de los materiales a escala real, lo que permite un estudio más exacto de los procesos que ocurren dentro del mortero. En las Figura 6.14 se muestran las distribuciones de materias primas y poros en una reconstrucción 3D.

Estas reconstrucciones tridimensionales confirman que el porcentaje de poros aumenta con la cantidad de poliuretano en la composición, que implica que el residuo incorpora cada vez mayores cantidades de aire en el material.

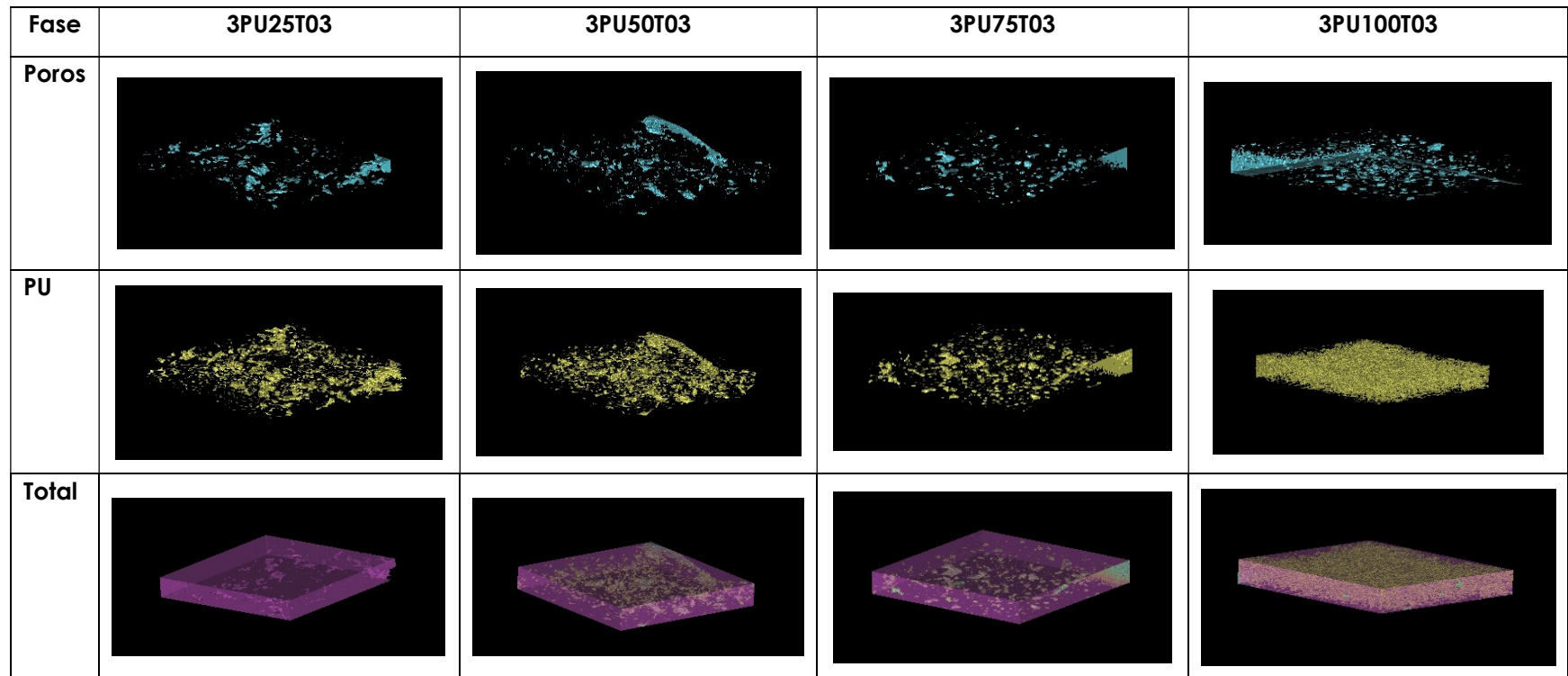


Figura 6.14. Reconstrucción 3D mediante tomografía axial computarizada de los morteros 1/3 con poliuretano y aditivo T03.



### 6.3. Termogravimetría

Se ha utilizado la termogravimetría (TGA) para observar la deshidratación de las muestras y comprobar su degradación en función de la temperatura. El aparato empleado es un TGA-DSC-DTA modelo TA Instruments con doble brazo, uno para la muestra, de la que se emplean unos 15 mg, y otro para la referencia. El programa está basado en la evolución de la temperatura en atmósfera de nitrógeno, con una rampa de temperatura de 10°C/min desde temperatura ambiente hasta los 800°C.

En las Figuras 6.15, 6.16 y 6.17 se muestran los resultados de TGA representando la pérdida de masa medida en tanto por ciento respecto de la temperatura. Las relaciones ensayadas son las dosificaciones de cemento/(árido+residuo de poliuretano) de 1/3, 1/6 y 1/8, empleando para ello cemento tipo I y aditivo T03.

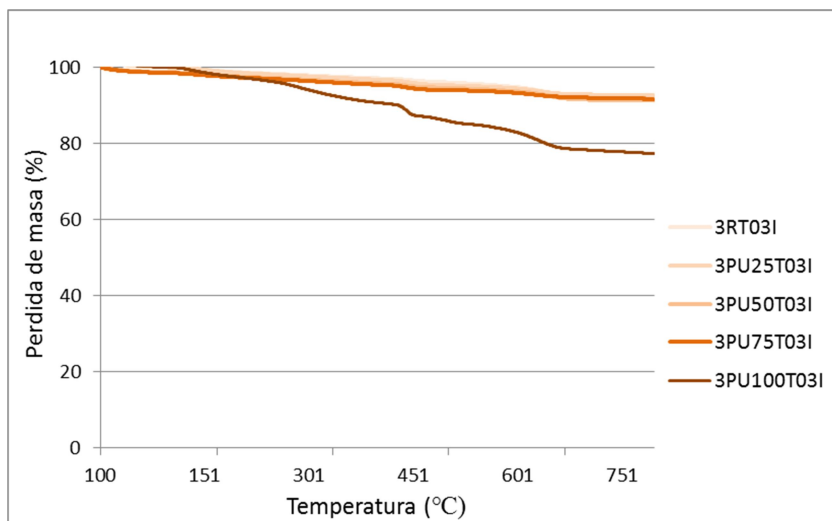


Figura 6.15. Resultados de TGA para las diferentes dosificaciones con relación 1/3 y con aditivo T03.

Tal y como se puede ver en estas gráficas, en todos los casos la pérdida de masa es mayor cuanto mayor porcentaje de árido se sustituye por poliuretano, como era de esperar. Se puede observar cómo la pérdida de masa tiene valores similares desde los morteros de referencia hasta la sustitución del 50%, y es a partir de ese porcentaje de



sustitución cuando la pérdida de masa aumenta hasta alcanzar la sustitución del 100% de árido por poliuretano. En cualquier caso, en esta última mezcla, los valores son similares para todas las dosificaciones ensayadas.

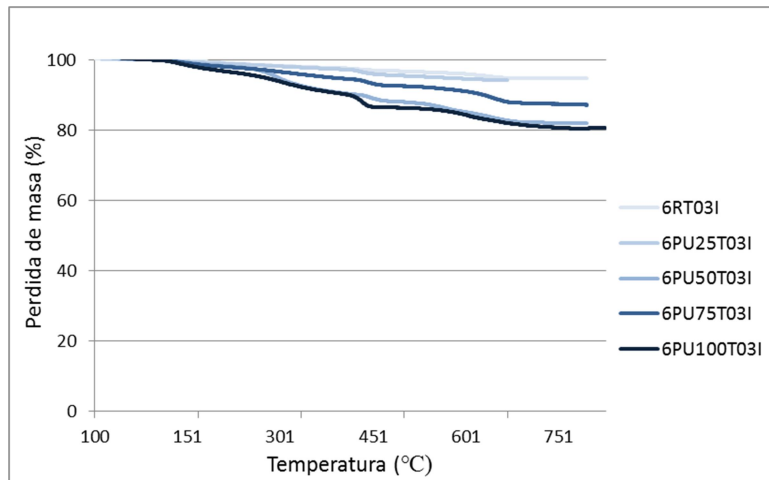


Figura 6.16. Resultados de TGA para las diferentes dosificaciones con relación 1/6 y con aditivo T03.

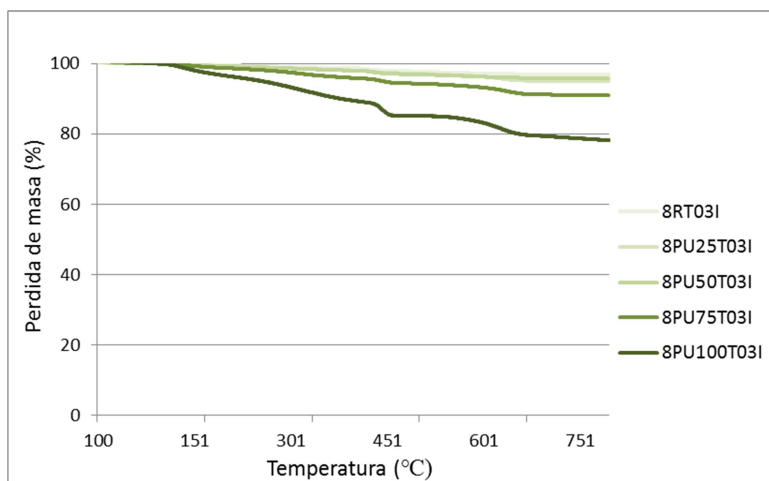


Figura 6.17. Resultados de TGA para las diferentes dosificaciones con relación 1/8 y con aditivo T03.



## 6.4. Reacción al fuego

En este ensayo se determina el comportamiento de los morteros frente a la combustión de distintas dosificaciones, para ver así como contribuye al desarrollo al fuego. El ensayo se realiza en el Laboratorio de Reacción al Fuego AFITI LICOF en Toledo según la Norma UNE-EN ISO 1182 *Ensayos de reacción al fuego de productos. Ensayo de no combustibilidad.*<sup>94</sup> Estos resultados no son los únicos criterios de evaluación del potencial riesgo de incendio que conlleva el uso de estos productos, pero dan una idea de comportamiento que se puede extrapolar a una situación real.

Para el acondicionamiento de las muestras, se ha empleado la Norma UNE-EN ISO 13238. *Ensayos de reacción al fuego para productos de combustión. Procedimiento de acondicionamiento y reglas generales para la selección de sustratos.*<sup>95</sup>

En la Figura 6.18 se muestra el horno vertical empleado para evaluar el comportamiento de las muestras a altas temperaturas, diseñado de acuerdo con la norma UNE EN ISO 1182. Este dispositivo está compuesto por un espacio cilíndrico de 75 mm de diámetro y 150 mm de altura en el que se colocan las muestras. La temperatura dentro del horno se mide mediante un termopar situado a media altura y a 10 mm de la pared. La forma de la muestra introducida en el horno era cilíndrica, con un diámetro de 40 mm y una altura de 50 mm. Durante la preparación de las muestras, con la mezcla aún fresca, se introdujo dentro de éstas un termopar a través del eje de simetría de forma que la punta del termopar se situaba en el centro geométrico de los cilindros. Además de los dos anteriores, se empleó un tercer termopar en contacto con la superficie de las muestras, situado diametralmente opuesto al termopar que está dentro del horno. Tanto el horno como los termopares de superficie se protegieron con campanas de acero inoxidable. A continuación, la temperatura del horno se elevó de la temperatura ambiente a 750°C en 2 horas y luego se mantuvo a 750°C durante 60 minutos. Se registraron las temperaturas de superficie y del centro de la muestra cada 10 segundos.

<sup>94</sup> UNE-EN ISO 1182 Ensayos de reacción al fuego de productos. Ensayo de no combustibilidad

<sup>95</sup> UNE-EN ISO 13238. Ensayos de reacción al fuego para productos de combustión. Procedimiento de acondicionamiento y reglas generales para la selección de sustratos.



La combustión potencial de la muestra de ensayo se registró cuando las temperaturas subieron y/o las llamas se hicieron visibles. La pérdida de masa de la muestra de ensayo se calculó después de la prueba.

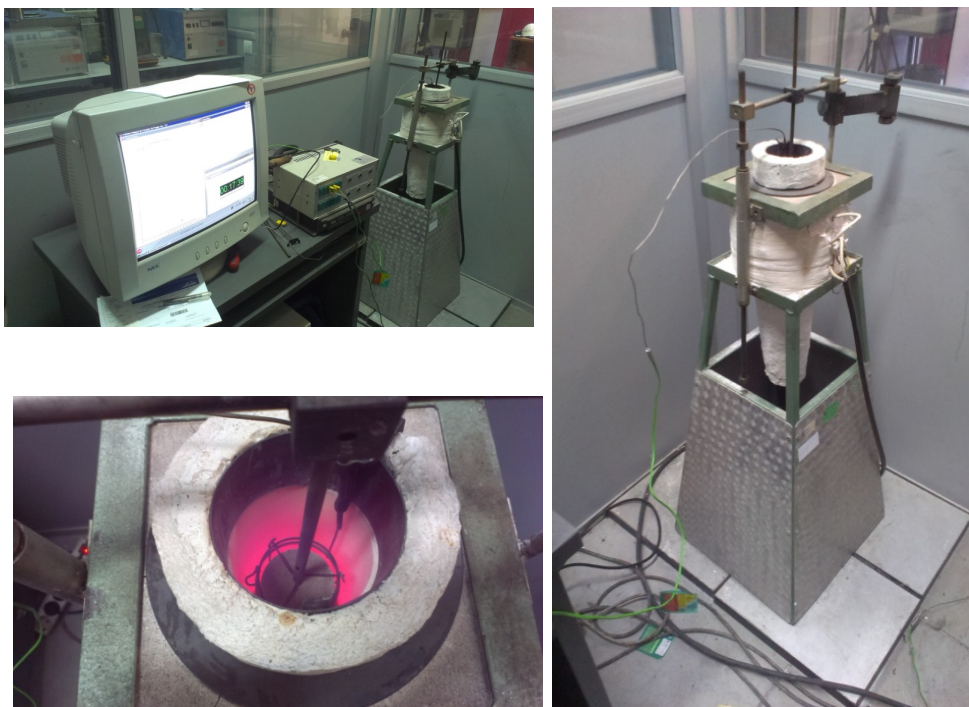


Figura 6.18 Horno de no combustibilidad en funcionamiento con una muestra en el interior, según la norma UNE-EN ISO 1182

Aunque se obtienen conclusiones muy interesantes que permiten determinar el comportamiento respecto a la temperatura de las mezclas, dando una idea de la contribución al desarrollo del fuego del material, estos resultados no constituyen el único criterio de valoración del riesgo potencial de incendio que puede conllevar el uso del producto, pero a partir de ellos se puede extrapolar el comportamiento a una situación real.<sup>96</sup>

En términos cualitativos, se observó que la pérdida de masa aumentó a medida que el árido fue reemplazado por poliuretano. Aun así la pérdida de masa no es significativa.

<sup>96</sup> Ciudad A, Lacasta AM, Haurie L, Formosa J, Chimenos J.M. (2011) Improvement of passive fire protection in a gypsum panel by adding inorganic fillers: Experiment and theory. Applied Thermal Engineering, 31:3971-3978.



En la Tabla 6.3 se muestran los resultados de este ensayo, que confirman la buena reacción al fuego de los morteros con distinto porcentaje de sustitución de árido por poliuretano. Ninguna de las muestras presentó propiedades inflamables y su uso podría considerarse aceptable.

La muestra en la que se sustituye un 50% de árido por poliuretano muestra un tiempo de inflamación menor a los 20 segundos especificado en el estándar y un incremento en la temperatura del horno de 3,8°C, muy por debajo de los 50°C límite especificados en la norma. En la muestra con un 75% de poliuretano el tiempo de inflamación se corresponde con 502 segundos, notablemente mayor que en el caso anterior. La temperatura del horno incrementa en este caso 14,2°C, también por debajo de los 50°C que especifica la norma.

Muestra	Incremento de la temperatura del horno (°C)	Persistencia de la inflamación (s)	Pérdida de masa (%)
3PU50T03	3,8	-	17,94
3PU75T03	14,2	502	29,71

Tabla 6.3 Resultados de la reacción al fuego tras la prueba de no combustibilidad

En cuanto a la pérdida de masa, en ambos casos se obtienen valores relativamente bajos, con una pérdida de masa en el caso de sustitución del 50 % de árido por poliuretano de 17,94 % del material, y una pérdida de masa de 29,71 % del material en el caso de la muestra con 75% de polímero.

Teniendo en cuenta únicamente su contribución a la inflamabilidad de los materiales, estos resultados indican que los materiales pueden clasificarse como fuego Euroclass A2, es decir, no combustible, sin aportación al fuego, según la EN 13501-1 + A1.<sup>97</sup>

<sup>97</sup> UNE- EN 13501-1:2007+A1:2010. Fire classification of construction products and building elements - Part 1: Classification using data from reaction to fire tests.



## 6.5. Carbonatación

Entre los factores que afectan a la durabilidad de los morteros y hormigones destacan los procesos de corrosión de las armaduras. Considerando que estos materiales tienen propiedades estructurales y que podrían estar en contacto con materiales de naturaleza metálica, la realización de este ensayo resulta muy interesante.

La carbonatación que lleva posteriormente a la corrosión tiene lugar cuando se altera la capa de pasivación formada en la interfase hormigón-acero o mortero-acero. Esta capa pasivante se genera en unas condiciones de alcalinidad determinadas, con pH básicos comprendidos entre 12,5 y 13,5. Cuando estas condiciones cambian desaparece el efecto de protección sobre el acero que recubre. Las alteración de la alcalinidad de la capa pasivante se puede producir por la presencia de iones tipo cloruros, o por procesos de carbonatación, reduciéndose los pH (Figura 6.19).

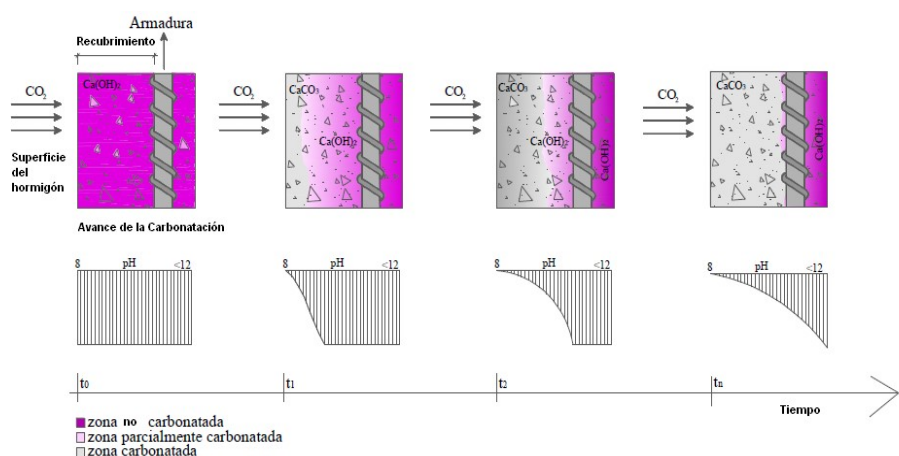


Figura 6.19. Representación del avance del frente de carbonatación y alteración del pH de morteros y hormigones en el tiempo.

La carbonatación propiamente dicha se produce al reaccionar el CO<sub>2</sub> atmosférico con el Ca(OH)<sub>2</sub>. Este proceso afecta tanto a la fase líquida como a la fase sólida del mortero u hormigón. Los procesos de carbonatación son generalmente muy lentos a causa del bajo contenido en CO<sub>2</sub> de la atmósfera, produciéndose alteraciones muy bajas, del orden de 0,04% en volumen, de forma que los efectos de este



fenómeno pueden no aparecer hasta pasados varios años.<sup>98</sup> Por ello, se han diseñado métodos normalizados en los que los materiales se exponen a altas concentraciones de CO<sub>2</sub>, simulando situaciones reales con procesos acelerados que permiten predecir su comportamiento a largo plazo.

La velocidad de la carbonatación es la variación de la profundidad del frente carbonatado con el tiempo en el interior del mortero u hormigón. Esta velocidad está condicionada por el contenido en cemento de la mezcla, por la porosidad y por el grado de saturación de agua en el interior de los poros.

Las técnicas para caracterizar la carbonatación son muy variadas, en esta investigación se ha utilizado el método de análisis del indicador de pH fenolftaleína, que permite diferenciar tres zonas de pH mediante el color. (Figura 6.20) Para valores de PH inferiores a 8 la disolución se vuelve incolora, entre 8 y 9,5 adquiere una tonalidad rosa suave y para valores superiores a 9,5 adquiere un color púrpura intenso.

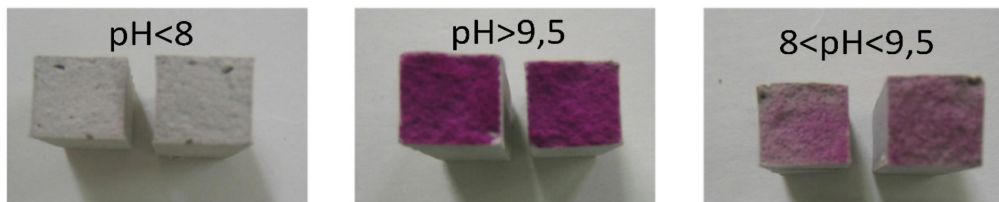


Figura 6.20. Tonalidades de la fenolftaleína.

Para la realización del ensayo se fabrican 3 probetas normalizadas de (40x40x160) mm<sup>3</sup>, y se curan en cámara húmeda durante 28 días. A continuación, las probetas se secan en una estufa hasta peso constante a una temperatura de (65±5)°C. De las tres probetas, dos se utilizaron para realizar el ensayo y una se reserva como referencia para cada uno de los morteros.

El proceso de carbonatación acelerada se realiza en una cámara estanca sellada (Figura 6.21), en la que se introducen 30 litros de CO<sub>2</sub> mediante un regulador de caudal y un sistema de purga de aire, lo que significa el 20% del volumen total de la cámara (140 litros). Mediante una sonda se comprueba que la concentración de CO<sub>2</sub> en el interior de

<sup>98</sup> Moreno El. (1999) Carbonation of blended cement concretes, University of South Florida.



la cámara supera siempre el 5%. Las mediciones de humedad y temperatura se realizaron mediante termómetro-higrómetro digital.

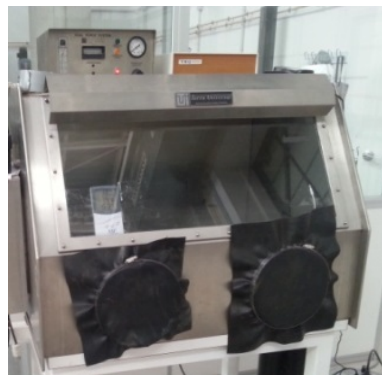


Figura 6.21. Cámara estanca empleada en el ensayo de carbonatación.

Las probetas permanecen 28 días en el interior de la cámara, renovando cada semana la atmósfera interior retirando el gas mediante una purga y añadiendo un volumen adicional de CO<sub>2</sub>.

Finalizado el tiempo de exposición se comprueba el efecto del CO<sub>2</sub> sobre el mortero mediante la valoración de la medida de la profundidad de la carbonatación y variaciones de las resistencias mecánicas.

La medición de la profundidad media de la carbonatación se realiza aplicando sobre las probetas rotas a flexión una impregnación de fenolftaleína al 1%. Se retira el polvo residual de la misma y se pulveriza la disolución de fenolftaleína. Las áreas carbonatadas del mortero no cambiarán de color, mientras que las áreas con un pH mayor de 9 que no han sufrido cambios adquirirán un color rosáceo.

Los morteros más porosos facilitan la difusión del CO<sub>2</sub> en el interior del material. Diversos estudios corroboran este comportamiento.<sup>99</sup> Esto se corresponde con los resultados obtenidos en términos cualitativos (Figura 6.22, Tabla 6.4), donde se aprecia claramente que las probetas que incorporan más cantidad de polímero reciclado alcanzan un frente

<sup>99</sup> Gaspar Tebar D, Muñoz Plaza M. (1991) Acción del CO<sub>2</sub> sobre un cemento portland: influencia sobre las características química y fisicomecánicas. Materiales de Construcción, 611: 37-53.



mayor de carbonatación, siendo prácticamente total en el caso de un reemplazo de árido por poliuretano del 100%.

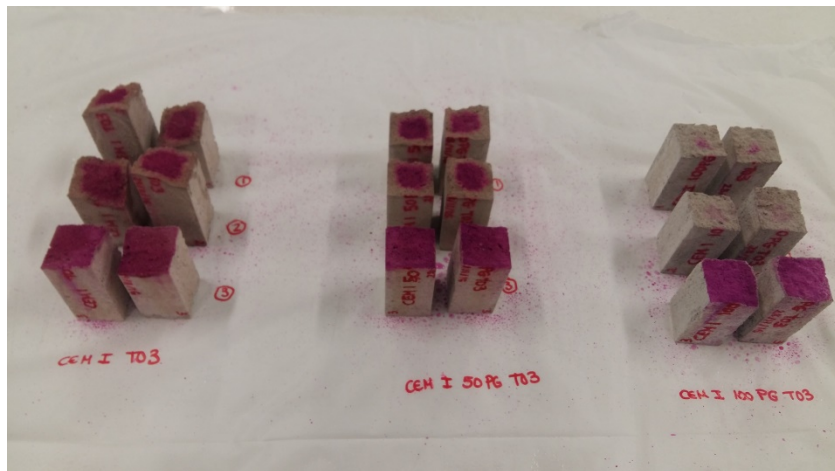


Figura 6.22. Frente de carbonatación para las probetas de dosificación 3PURTO3 (izquierda), 3PU50T03 (central) y 3PU100T03 (derecha). La probeta de delante es la muestra que no se ensaya, el color rosa en toda la superficie indica que no ha sufrido el proceso de carbonatación acelerada.

Hay que tener en cuenta que estos productos reciclados incluyen proporciones muy elevadas de residuo, lo que sin duda puede afectar a las propiedades finales de durabilidad, como en este caso de carbonatación acelerada. En todo caso, y ateniéndonos a los resultados obtenidos, se estima que podrían ser adecuados para soportar procesos de carbonatación con inclusión de polímero de hasta un 50%.

Las resistencias mecánicas obtenidas (Tabla 6.4) muestran resultados con un comportamiento contrario a los encontrados en la bibliografía consultada, donde generalmente aumentan con la carbonatación.<sup>100</sup> Por el contrario, excepto el mortero de referencia (3PURTO3), el resto de materiales registran pérdidas de resistencia, aunque no demasiado significativas.

<sup>100</sup> Hornain H. (1976) Carbonatación del Concreto. RILEM. Wexham-Springs. Inglaterra.



Dosificación	Flexión media (MPa)	Compresión media (MPa)	Penetración media CO <sub>2</sub> (mm)
3PURTO3	4,45	29,43	6,5
	(*) 8,60	(*) 31,14	(*) completa
3PU50T03	3,32	22,11	8,0
	(*) 4,76	(*) 20,90	(*) completa
3PU100T03	3,19	9,63	completa
	(*) 3,18	(*) 9,18	(*) completa

Tabla 6.4. Resultados medios después del ensayo de carbonatación.

\*Probeta referencia que no se somete al ensayo.



## **Chapter 7**

---

## **Conclusions**





In this chapter the conclusions of this Doctoral Thesis are presented in agreement with the objectives initially proposed.

The first part of the research was focused on the synthesis of afwillite and its introduction in C<sub>3</sub>S pastes, grouts and hardened cement pastes. The conclusions drawn from this research are described below.

- Afwillite crystals (Ca<sub>3</sub>Si<sub>2</sub>O<sub>7</sub>.3H<sub>2</sub>O) can be synthesized from highly diluted C<sub>3</sub>S slurry agitated with stainless steel balls in Turbula®. With appropriate amount of balls used, addition of afwillite germs and superplasticizer, weight percentage of afwillite in the mixture reaches 40-50% after 2-3 days of reaction, which represents 65-90% of the theoretical maximum possible. It has been obtained a purity of afwillite close to 90-100%, confirmed by XRD.
- Those afwillite crystals synthesized by such a method, once seeded in C<sub>3</sub>S paste, do induce afwillite growth in the paste under conventional hydration conditions. Starting from 2% afwillite seeding, weight percentage of afwillite in the C<sub>3</sub>S paste would reach 25-45% after 7-28 days of hydration, respectively.
- Paste seeded with afwillite shows very different properties compared with reference C<sub>3</sub>S paste. First, rate of hydration is considerably accelerated after seeding with 2% afwillite germs (compared to C<sub>3</sub>S weight), that is closely shortened from 28 days to 7 days. Second, the total porosity after 28 days of hydration becomes 30% higher after seeding with afwillite and mean pore size becomes larger.
- SEM images show the presence of afwillite crystals of 3-5 µm in size close to remaining C-S-H. The microstructure depicted is then coarsened since afwillite assemblage replaces C-S-H gel as the frame.
- Increasing the pore size leads to decrease of capillary tension and drying shrinkage. Although higher porosity with greater pore size implies easier water evaporation when being dried, drying shrinkage is significantly reduced (at least by a factor of 2.5 after 100 days of measurements and using W/C=0.5 and C<sub>3</sub>S Blaine of 4600 cm<sup>2</sup>/g).
- The coarse microstructure and the higher porosity are responsible for a significant decrease of the mechanical resistance after 28 days



of hydration. This decrease seems to depend on the total afwillite formed at 28 days, which is reduced at W/C=0.35 (and/or using superplasticizers).

- The drying shrinkage is closely related to capillary tension within cement paste, which can be reduced by increasing the capillary pore radius. The experiments were done to check if the growth of afwillite was possible according to the composition of cement, the water/cement ratio, the use of certain superplasticizers and for two curing temperatures (20 and 80°C). The results obtained after ball mill hydration of the slurries showed that:
  - The growth of afwillite was first governed by the content of alite
  - The interstitial phases (made of tri-calcium aluminate and ferrite) may poison the afwillite growing from the surface of alite
  - The granulometry may be only considered such as a second order parameter that may boost the growth of afwillite
  - The addition of superplasticizers helped in growing afwillite in Portland cement containing the lowest contents of alite
  - The synergy consisting in pre-seeding with afwillite and superplasticizers helped in growing afwillite in oil-well and Portland cement.
- The growth of afwillite in cement-based paste was clearly demonstrated after seeding with pure germs of afwillite (purity >90%), effective whatever the type of cement. However, all the maximum contents of afwillite detected reached only to 20-30% after 28 days of hydration. These lowest rates of afwillite detected in pastes (compared what happened using seeded slurries) would highlight the positive effect induced by a continuous ball milling in Turbula®, which would be able to clean the crystals of afwillite under growing and to remove the "impurities" released from alite and/or from the hydration of calcium aluminates.
- This hypothesis was confirmed by seeding alite-based slurries and C<sub>3</sub>S+C<sub>3</sub>A pastes; these last tests showing that a minor part of C<sub>3</sub>A was enough to inhibit significantly the growth of afwillite in pastes.



However, a relative high content of afwillite (close to 45-50%) was detected by curing grey OPC SPLC at 80°C, which is not a common temperature for this kind of cement but could open a new area of research about the growth of afwillite using Portland cements.

- All the experiments done on various seeded cement-based (previously cured 28 days at 100% relative humidity and 20 or 80°C) established no specific reduction of the drying shrinkage and no difference in total porosity whatever the type of Portland/oil-well cements and W/C ratio used, certainly due to a too low content of afwillite after hydration.

The second part of this Thesis deals with the properties of a new range of structural and lightweight mortars, containing a low fraction of soluble non-ionic surfactant, and manufactured with several substitution rates of sand by the polyurethane wastes.

- All mortars have been made with Portland cement, water, sand and PU foam wastes, and including non-ionic surfactants with different hydrolysis grade were mainly examined. A 1/3, 1/6 and 1/8 cement/aggregate ratio was dosed, where the aggregate was the sum of sand plus polymer wastes. Sand was substituted by the PU foam wastes in rates that varied 25%, 50%, 75% and 100% in volume. In addition, reference samples were fabricated, with the intention to carry out a comparative study of their properties.
- A specific dosage of 2% of non-ionic surfactants XL40 and T03 by weight of cement was used. It has been demonstrated that the incorporation of certain surfactant rates in designed mortars allowed fixing the water/cement ratio to 0.5 or 0.6, ensuring an appropriate consistency, good workability and a plastic state in mixtures.
- The progressive substitution of sand by the PU wastes logically induced a proportional reduction in density, yielding finally a lightweight mortar.
- However, this influence on the density had no effect on mechanical strength, which was not only maintained, but even increased with regard to the reference specimen RTO3. Mortar with a total substitution of sand by the PU wastes showed compressive strengths of over 38 MPa. One explanation might be related to the



positive effect of the mixture of the both polymeric types, such as the hydrophilic characteristics of the surfactants used and the recycled polyurethane. Therefore, one of the most innovative aspects of these materials lies in the improvement of the behavior with regard compressive strength with very low densities, aspect that could be reached by means of different surfactants to modify the cement hydration properties.

- The mechanical strengths increased using larger rates of PU wastes, reaching an optimal substitution of sand around 50%. At higher substitution rates, the mechanical properties seem to be stabilised at very high values, according to the evolution of the bulk density of the specimens.
- The microporosity (covering the pore diameter range from about 200 µm to 3 nm) was measured by MIP and the macroporosity (with pore diameter range bigger than 200 µm) was obtained with the analysis of the 3D reconstruction images, following Computarized Tomography tests (CAT). The microporosity in the mortar increased with the increase of the substitution rate of sand by the PU wastes, whereas the macroporosity, measured in terms of entrained air, decreased. One would hypothesize that the non-ionic surfactants showing low HLB values that contribute to a better dispersion of the cement particles in water and can improve the cohesion between the aggregates (sand and/or PU wastes), resulting in an increase of the microporosity but a decrease of the large-size porosity, finally leading to an improvement of the mechanical properties.
- Additionally, the non-ionic surfactant also contributed to the hydration of mortar, which was observed with the presence of ettringite and portlandite crystals in the early stages of material hydration. SEM micrographs of the fractured surfaces and the portions of the interfacial transition zone, a significant amount of hexagonal crystals of portlandite and needle-shaped crystals, which were probably caused by the formation of ettringite, were detected around the PU wastes when non-ionic surfactants such as TO3 and XL40 were used in the mix.
- The microstructure analysis confirms that the particles were homogeneously dispersed in the mineral matrix, and remained smooth and spherical in the experimental conditions studied. The SEM images of the polished sections of mortar also showed that the



addition of PU wastes entails a good interfacial transition zone, due to the size of the polymer-based aggregate and, alternatively, a larger transition region produced by the water released by the polymer wastes, which initially absorbs a large amount of water. The additives help the structure that is formed to be more compact, avoiding the disintegration of the polyurethane particles and helping to improve the mechanical resistance.

- The HLB value is a key-parameter to establish which type of surfactants can enhance the compressive and flexural strengths of mortars manufactured with a high substitution rate of sand by PU wastes. The characterization of the mortars by several methods (MIP, SEM, CAT) established that non-ionic surfactants with low HLB values are the more useful to improve adhesion between the PU wastes and cement paste, generate an homogenous distribution of aggregates, and guarantee a lightweight but structurally resistant microstructure (even if 50% to 100% of sand is substituted by PU wastes).
- The loss of mass measured by thermogravimetry (TGA) is greater by increasing the amount of polyurethane. Up to 50% substitution has similar values while bigger proportions of polymer increase the loss of mass in all cases, regardless of the ratio [cement / (arid + polyurethane residue)], cement used or added additive.
- For the non-combustibility test, a greater loss of mass was observed with the progressive replacement of sand by polyurethane, although the mass loss was scarcely significant. The samples don't exhibit flammable properties and their use can be considered acceptable, being classified as Euroclass A2.
- Is clearly appreciated that the specimens incorporating bigger amount of recycled polymer reach a higher carbonation front, being practically total in the case of a 100% replacement. The mechanical strengths obtained after carbonation show results where they decrease with carbonation, although not excessively significant.
- As a conclusion, this new range of materials containing polymer wastes complies with the principle of the sustainable development and contributes to a greener business model within the building sector.



## **Capítulo 8**

---

### **Líneas futuras de investigación**





Tras las investigaciones realizadas en esta Tesis Doctoral y las conclusiones obtenidas, se proponen las siguientes líneas de investigación futuras:

- Estudiar en detalle el crecimiento de afwillita en cementos Portland para confirmar los últimos resultados con un contenido relativamente alto de afwillita, a través del curado de todo tipo de cementos a 80°C.
- Completar los ensayos en los que se introduzcan gérmenes de afwillita en cemento con poliuretano y aditivos superplastificantes en diferentes cantidades, con el objetivo de determinar la influencia de éstos en la porosidad y en las resistencias mecánicas.
- Proponer nuevos ensayos de durabilidad para corroborar si los morteros obtenidos morteros son aptos para su uso en construcción, y por lo tanto se considera factible el uso de estos residuos de poliuretano con arreglo a la normativa vigente.
- Ampliar la influencia y el mecanismo de activación de otro tipo de aditivos, así como el empleo en otras clases de polímeros en pastas de cemento para dar salida a este tipo de residuos.
- Emplear estos materiales con propiedades mecánicas mejoradas para aligerar prefabricados en construcción. Para ello, y en base al conocimiento adquirido en este trabajo, se propone analizar mezclas de cemento tipo IV, relación [cemento/(árido+residuo de poliuretano)] 1/8, con sustitución del 100% de árido por poliuretano y aditivo XL40.





**Anexo 1**

---

**Bibliografía**





AENOR. (1999) Norma UNE-EN 1015-3. Métodos de ensayo para morteros de albañilería. Parte 3: Determinación de la consistencia del mortero fresco (por la mesa de sacudidas).

AENOR. (1999) Norma UNE-EN 1015-6. Métodos de ensayo de los morteros para albañilería. Parte 6: Determinación de la densidad aparente del mortero fresco.

AENOR. (1999) Norma UNE-EN 1015-7. Métodos de ensayo de los morteros para albañilería. Parte 7: Determinación del contenido en aire en el mortero fresco.

AENOR. (1999) Norma UNE-EN 933-2/1M. Ensayos para determinar las propiedades geométricas de los áridos. Parte 2: Determinación de la granulometría de las partículas. Tamices de ensayo, tamaño nominal de las aberturas.

AENOR. (2000) Norma UNE-EN 1015-10. Métodos de ensayo de los morteros para albañilería. Parte 10: Determinación de la densidad aparente en seco del mortero endurecido.

AENOR. (2000) Norma UNE-EN 1015-11. Métodos de ensayo de los morteros para albañilería. Parte 11: Determinación de la resistencia a flexión y a compresión del mortero endurecido.

AENOR. (2000) Norma UNE-EN 1015-9. Métodos de ensayo de los morteros para albañilería. Parte 9: Determinación del periodo de trabajabilidad y del tiempo abierto del mortero fresco.

AENOR. (2003) Norma UNE-EN 13139. Áridos para morteros.

AENOR. (2004) Norma UNE-EN 13139/AC. Áridos para morteros.

AENOR. (2005) Norma UNE-EN 1015-3:2000/A1. Métodos de ensayo para morteros de albañilería. Parte 3: Determinación de la consistencia del mortero fresco (por la mesa de sacudidas).

AENOR. (2007) Norma UNE-EN 1015-10:2000/A1. Métodos de ensayo de los morteros para albañilería. Parte 10: Determinación de la densidad aparente en seco del mortero endurecido.

AENOR. (2007) Norma UNE-EN 1015-11:2000/A1. Métodos de ensayo de los morteros para albañilería. Parte 11: Determinación de la resistencia a flexión y a compresión del mortero endurecido.



AENOR. (2007) Norma UNE-EN 1015-2:1999/A1. Métodos de ensayo de los morteros para albañilería. Parte 2: Toma de muestra total de morteros y preparación de los morteros para ensayo.

AENOR. (2007) Norma UNE-EN 1015-3:2000/A2. Métodos de ensayo para morteros de albañilería. Parte 3: Determinación de la consistencia del mortero fresco (por la mesa de sacudidas).

AENOR. (2007) Norma UNE-EN 1015-6:1999/A1. Métodos de ensayo de los morteros para albañilería. Parte 6: Determinación de la densidad aparente del mortero fresco.

AENOR. (2007) Norma UNE-EN 1015-9:2000/A1. Métodos de ensayo de los morteros para albañilería. Parte 9: Determinación del periodo de trabajabilidad y del tiempo abierto del mortero fresco.

AENOR. (2010) Norma UNE-EN 13501-1:2007+A1. Clasificación en función del comportamiento frente al fuego de los productos de construcción y elementos para la edificación. Parte 1: Clasificación a partir de datos obtenidos en ensayos de reacción al fuego.

AENOR. (2011) Norma UNE-EN ISO 1182. Ensayos de reacción al fuego de productos. Ensayo de no combustibilidad.

AENOR. (2011) Norma UNE-EN ISO 13238. Ensayos de reacción al fuego para productos de combustión. Procedimiento de acondicionamiento y reglas generales para la selección de sustratos.

AENOR. (2012) Norma UNE-EN 998-2. Especificaciones de los morteros para albañilería. Parte 2: Morteros para albañilería.

AENOR (2007) Norma UNE-EN 13501-1. Fire classification of construction products and building elements - Part 1: Classification using data from reaction to fire tests.

Abdollahnejad Z, Mastali M, Mastali M, Dalvand A. (2017) Comparative study on the effects of recycled glass-fiber on drying shrinkage rate and mechanical properties of the self-compacting mortar and fly ash-slag geopolymers mortar. Journal of Materials in Civil Engineering 29(8), 04017076.

Acker P, Ulm FJ. (2001) Creep and shrinkage of concrete: physical origins and practical measurements, Nuclear Engineering and Design 203, 143-158.

Alameda L, Calderón V, Junco C, Rodríguez A, Gadea J, Gutiérrez-González S. (2016) Characterization of gypsum plasterboard with



polyurethane foam waste reinforced with polypropylene fibers. *Materiales de Construcción*, 66,100.

Allen AJ, Thomas JJ, Jennings HM. (2007) Composition and density of nanoscale calcium-silicate-hydrate in cement. *Nature Materials*, 6:311-316.

Aulia TB. (2002) Effects of polypropylene fibres on the properties of high strength concretes. *Lacer Vol.* 7, 43-59.

Babu KG, Babu DS. (2003) Behaviour of lightweight expanded polystyrene concrete containing silica fume. *Cement Concrete Research*, 33 (5): 755-762.

Baroghel-Bouny V, Godin J. (2001) Experimental study on drying shrinkage of ordinary and high-performance cementitious materials, *Concrete Science Engineering*, 3: 13-22.

Ben Fraj A, Kismi M, Mounanga P. (2010) Valorization of coarse rigid polyurethane foam waste in lightweight aggregate concrete. *Construction Building Materials*, 24:1069-1077.

Bignozzi MC, Saccani A, Sandrolini F. (2000) New polymer mortars containing polymeric wastes. Part 1. Microstructure and mechanical properties. *Composites Part A: Applied Science Manufacturing*, 31 (2): 97-106.

Calderón V, Gutiérrez-González S, Rodriguez A, Hognies M. (2013). Study of the microstructure and pores distribution of lightweight mortar containing polymer waste aggregates. *WIT Transactions on Engineering Sciences*, 77: 263-272.

Carrera V, Cuadri AA, García-Morales M, Partal P. (2014) Influence of the prepolymer weight and free isocyanate content on the rheology of polyurethane modified bitumens. *European Polymer Journal*, 57: 151-159.

Casey D, McNally C, Gibney A, Gilchrist MD. (2008) Development of a recycled polymer modified binder for use in stone mastic asphalt. *Resources Conservation and Recycling*, 52:1167-1174.

Chen JJ, Thomas JJ, Taylor H, Jennings HM. (2004) Solubility and structure of calcium silicate hydrate, *Cement and Concrete Research*, 34:1499-1519.

Chevali V, Kandare E. (2016) Rigid biofoam composites as eco-efficient construction materials. *Biopolymers and Biotech Admixtures for Eco-Efficient Construction Materials*, 275-304.



Ciudad A, Lacasta AM, Haurie L, Formosa J, Chimenos J.M. (2011) Improvement of passive fire protection in a gypsum panel by adding inorganic fillers: Experiment and theory. *Applied Thermal Engineering*, 31:3971-3978.

Communication from the commission to the European Parliament, the Council, the European Economic and Social Committee and the Committee of the Regions. "A resource-efficient Europe – Flagship initiative under the Europe 2020 Strategy".

Corinaldesi V, Mazzoli A, Moriconi G. (2011) Mechanical behaviour and thermal conductivity of mortars containing waste rubber particles. *Materials and Design*, 32:1646-1650.

Courard L. (2002) Evaluation of thermodynamic properties of concrete substrates and cement slurries modified with admixtures, *Materials Structures*, 35:149-155.

Cregut M, Bedas M, Durand MJ, Thouand G. (2013) New insights into polyurethane biodegradation and realistic prospects for the development of a sustainable waste recycling process. *Biotechnology Advances*, 31:1634-1647.

Czarnecki C. (2010) Polymer-cement concretes, *Cement-Wapno-Beton*, 15:63-85.

Davis RW, Young JF. (1975) Hydration and strength development in tricalcium silicate pastes seeded with afwillite. *Journal American Ceramic Society*, 58:67-70.

M del Río M, F. Hernández Olivares. (2004) Lightened blaster: alternative solutions to cellular solids addition. *Materiales de Construcción*, 54:65-76.

Directive 2008/98/CE of European Parliament and Council of 19th November 2008 about wastes.

Dong X, Wang S, Gong C, Lu L. (2014) Effects of aggregate gradation and polymer modifiers on properties of cement-EPS/vitrified microsphere mortar. *Construction Building Materials* 73: 255-260.

Dulsang N, Kasemsiri P, Posi P, Hiziroglu S, Chindaprasirt P. (2016) Characterization of an environment friendly lightweight concrete containing ethyl vinyl acetate waste. *Materials and Design*, 96:350-356.

Dunstetter F, de Noirfontaine MN, Courtial M. (2006) Polymorphism of tricalcium silicate, the major compound of Portland cement clinker 1.



Structural data: review and unified analysis. *Cement and Concrete Research*, 36:39-53.

Eve S, Gomina M, Hamel J, Orange G. (2006) Investigation of the setting of polyamide fibre/latex-filled plaster composites. *Journal of European Ceramic Society*, 26:41-46.

Ferrández V, Bond T, García-Alcocel E, Cheeseman CR. (2014) Lightweight mortars containing expanded polystyrene and paper sludge ash. *Construction and Building Materials*, 61:285-292.

Fraj AB, Kismi M, Mounanga P. (2010) Valorization of coarse rigid polyurethane foam waste in lightweight aggregate concrete. *Construction and Building Materials*, 24:1069-1077.

Gadea J, Rodríguez A, Campos PL, Garabito J, Calderón V. (2010) Lightweight mortar made with recycled polyurethane foam. *Cement Concrete Composites*, 32:672-677.

Gaspar Tebar D, Muñoz Plaza M. (1991) Acción del CO<sub>2</sub> sobre un cemento portland: influencia sobre las características química y fisicomecánicas. *Materiales de Construcción*, 611:37-53.

Glasser FP, Hong SY. (2003) Thermal treatment of C-S-H gel at 1 bar H<sub>2</sub>O pressure up to 200 °C. *Cement Concrete Research*, 33:271-279.

Grangeat P. (2002) *La Tomographie*, Hermès Science, Traité IC2, Paris.

Gueit E, Darque-Ceretti E, Tintillier P, Horgnies M. (2012) Surfactant-induced growth of a calcium hydroxide coating at the concrete surface. *Journal of Coating Technology Research*, 9:337-346.

Guide for structural lightweight aggregate concrete. (1987) ACI Manual of Concrete Practice, Part 1 Farmington Hills: American Concrete Institute.

Gutiérrez-González S, Gadea J, Rodríguez A, Junco C, Calderón V. (2012) Lightweight plaster materials with enhanced thermal properties made with polyurethane foam wastes. *Construction and Building Materials*, 28:653-658.

Hamilton HR, Benmokrane B, Dolan W, Sprinkel MM. (2009) Polymer materials to enhance performance of concrete in civil infrastructure. *Journal of Macromolecular Science, Part C: Polymer Reviews*, 49:1-24.

He JJ, Jiang L, JH Suna, Lo S. (2016) Thermal degradation study of pure rigid polyurethane in oxidative and non-oxidative atmospheres. *Journal of Analytical and Applied Pyrolysis*, 120: 269-283.



Hong SY, Glasser FP. (2004) Phase relations in the CaO–SiO<sub>2</sub>–H<sub>2</sub>O system to 200°C at saturated steam pressure, *Cement Concrete Research*, 34:1529-1534.

Horgnies M, Gutiérrez-González S, Rodríguez A, Calderón V. (2014) Effects of the use of polyamide powder wastes on the microstructure and macroscopic properties of masonry mortars. *Cement Concrete Composites*, 52:64-72.

Hornain H. (1976) Carbonatación del Concreto. RILEM. Wexham-Springs. Inglaterra.

Howard GT, Norton WN, Burks T. (2012) Growth of *Acinetobacter* generic P7 on polyurethane and the purification and characterization of a polyurethanase enzyme. *Biodegradation*, 23:561-73.

Huang Y, Bird RN, Heidrich O. (2007) A review of the use of recycled solid waste materials in asphalt pavements. *Resources, Conservation and Recycling*, 52: 58-73.

Iucolano F, Liguori B, Caputo D, Colangelo F, Cioff R. (2013) Recycled plastic aggregate in mortars composition: effect on physical and mechanical properties. *Materials and Design*, 52:916-922.

Izquierdo MA, Navarro FJ, Martínez-Boza FJ, Gallegos C. (2012) Bituminous polyurethane foams for building applications: Influence of bitumen hardness. *Construction and Building Materials*, 30: 706-713.

Junco C, Gadea J, Rodríguez A, Gutiérrez-González S, Calderón V. (2012) Durability of lightweight masonry mortars made with white recycled polyurethane foam. *Cement Concrete Composites*, 34: 1174-1179.

Kantro DL, Brunauer S, Weise CH. (1959) The ball-mill hydration of tricalcium silicate at room temperature. *Journal of Colloidal Science*, 14:363-376.

Kismi M, Mounanga P. (2012) Comparison of short and long-term performances of lightweight aggregate mortars made with polyurethane foam waste and expanded polystyrene beads. *MATEC Web of Conferences*, 2, article number 02019. *Proceedings on 2nd International Seminar on Innovation and Valorization in Civil Engineering and Construction Materials*.

Kismi M, Poullain P, Mounanga P. (2012) Transient Thermal Response of Lightweight Cementitious Composites Made with Polyurethane Foam Waste. *International Journal Thermophysics*, 1-20.



Kjellsen KO, Justnes H. (2004) Revisiting the microstructure of hydrated tricalcium silicate—a comparison to Portland cement. *Cement Concrete Composites*, 26:947-956.

Kong X, Emmerling S, Pakusch J, Rueckel M, Nieberle, J. (2015) Retardation effect of styrene-acrylate copolymer latexes on cement hydration. *Cement Concrete Research*, 75:23-41.

Kowalczyk K, Spychaj T, Krala G. (2015) High-build alkyd urethane coating materials with a partially solvolyzed waste polyurethane foam. *Polymer Engineering Science*, 55: 2174-2183.

Kusachi I, Henmi C, Henmi K. (1989) Afillite and jennite from Fuka, Okayama Prefecture, Japan. *Mineralogical Journal*, 14: 279-292.

Lachowski EE, Hong SY, Glasser FP. (1997) Crystallinity in C-S-H gels: Influence of preparation and cure conditions, 2nd International RILEM Workshop on Hydration and Setting, 11-13.

Le Chatelier H. (1900) Sur les changements de volume qui accompagnent le durcissement des bétons. *Bull. Soc. Encourag. Ind. Natl*, 5: 54-57.

Lushnikova N, Dvorkin L. (2016) Sustainability of gypsum products as a construction material, in *Sustainability of Construction Materials*. Woodhead Publishing Series in Civil and Structural Engineering, 643-681.

Manso JM, Rodríguez A, Aragón A, González JJ. (2011). The durability of masonry mortars made with ladle furnace slag. *Construction and Building Materials*, 25, 3508-3519.

Maycock JN, Skalny J, Kalyoncu RS. (1974) Thermal decomposition of cementitious hydrates, R.S. Porter and J.F. Johnson Eds., *Analytical Calorimetry*, New York & London 697-711.

Molero C, de Lucas A, Rodriguez JF. (2008) Influence of the use of recycled polyols obtained by glycolysis on the preparation and physical properties of flexible polyurethane. *Journal of Applied Polymer Science*, 109:617–626.

Molero C, Mitova V, Troev K, Rodriguez JF. (2010) Kinetics and mechanism of the chemical degradation of flexible polyurethane foam wastes with dimethyl H-phosphonate with different catalysts. *Journal of Macromolecular Science, Part A: Pure and Applied Chemistry*, 47: 983-990.



Moody KM. (1952) Thermal decomposition of afwillite. *Mineralogical Magazine*, 29:838-840.

Moreno El. (1999) Carbonation of blended cement concretes, University of South Florida.

Mounanga P, Gbongbon W, Poullain P, Turcry P. (2008) Proportioning and characterization of lightweight concrete mixtures made with rigid polyurethane foam wastes. *Cement Concrete Composites*, 30: 806-814.

Odler I. (2003) The BET-specific surface area of hydrated Portland cement and related materials, *Cement and Concrete Research*, 33:1049-2056.

Ohama Y, Nishimura T, Hachisuka H. (1980) Strength properties of steel fiber reinforced polystyrene-impregnated concrete. *Proceedings - Computer Networking Symposium*, 3, 151-158.

Ohama Y. (2010) Concrete-polymer composites-the past, present and future. *Key Engineering Materials*, 466, 1-14 and International Congress on Polymers in Concrete. ICPIC Madeira (Portugal).

Ohama Y. (1998) Polymer-based admixtures. *Cement Concrete Composites*, 20(2-3): 189-212.

Oprea S. (2010) Synthesis and properties of polyurethane elastomers with castor oil as crosslinker. *Journal of the American Oil Chemists Society*, 87, 313-320.

Peng JH, Chen MF, Zhang JX. (2002) Study on waste expanded polystyrene as lightweight aggregate for thermal insulating mortar. *Jianzhu Cailiao Xuebao/Journal Building Materials*, 5 (2):166.

Petch HE, Sheppard N, Megaw HD. (1956) The infra-red spectrum of afwillite,  $\text{Ca}_3(\text{SiO}_3\text{OH})_2\cdot\text{H}_2\text{O}$ , in relation to the proposed hydrogen positions. *Acta Crystallographica*, 9:29-34.

Plastics The facts 2016. An analysis of European plastics production, demand and waste data. Brussels, Belgium.

Poulikakos LD, Papadaskalopoulou C, Hofko B, Gschösser F, Cannone Falchetto A, Bueno M, Arraigada M, Sousa J, Ruiz R, Petit C, Loizidou M, Partl MN. (2017) Harvesting the unexplored potential of European waste materials for road construction. *Resources, Conservation and Recycling*, 116: 32-44.



Reis JML, Carneiro EP. (2012) Evaluation of PET waste aggregates in polymer mortars. *Construction Building Materials*, 27 (1): 107-11.

Reis JML, Motta EP. (2014) Mechanical behavior of piassava fiber reinforced castor oil polymer mortars. *Composite Structures*, 111:468-472.

Richardson IG. (2008) The calcium silicate hydrates. *Cement and Concrete Research*, 38:137-158.

Rocco JAFF, Lima JES, Lourenço VL, Batista NL, Botelho EC, Iha, K. (2012) Dynamic mechanical properties for polyurethane elastomers applied in elastomeric mortar. *Journal Applied Polymer Science*, 126(4): 1461-1467

Ruiz-Herrero JL, Velasco Nieto D, López-Gil A, Arranz A, Fernández A, Lorenzana A, Merino S, De Saja JA, Rodríguez-Pérez MA. (2016) Mechanical and thermal performance of concrete and mortar cellular materials containing plastic waste. *Construction Building Materials*, 104: 298-310.

Saikia N, de Brito J. (2012) Use of plastic waste as aggregate in cement mortar and concrete preparation: A review. *Construction and Building Materials* 34: 385-401.

Saito F, Mi G, Hanada M. (1997) Mechanochemical synthesis of hydrated calcium silicates by room temperature grinding. *Solid State Ionics*, 101-103: 37-43.

Seligmann P, Greening NR. (1964) Studies of the early hydration reactions of Portland cement by X-ray diffraction. *Highway Research Record*, 62:80-105.

Serhat BM, Kahraman E. (2011) Modifications in the properties of gypsum construction element via addition of expanded macroporous silica granulates. *Construction and Building Materials*, 25:3327-3333.

Siddique R, Khati J, Kaur I. (2008) Use of recycled plastic in concrete: A review. *Waste Management*, 28: 1835-1852.

Singh B, Gupta M, Kumar L. (2006) Bituminous polyurethane network: preparation, properties and end use. *Journal of Applied Polymer Science*, 101: 217-226.

Taylor HFW. (1997) *Cement Chemistry*, 2nd Ed. Thomas Telford Edition Publishing, London.

Theiner Y, Hofstetter G. (2012) Evaluation of the effects of drying shrinkage on the behavior of concrete structures strengthened by overlays. *Cement Concrete Research*, 42: 1286-1297.



Thomas JJ, Chen JJ, Allen AJ, Jennings HM. (2004) Effects of decalcification on the microstructure and surface area of cement and tricalcium silicate pastes. *Cement Concrete Research*, 34: 2297-2307.

Van Gemert D, Czarnecki L, Maultzsch M, Schorn H, Beeldens A, Lukowski P, Knapen E. (2005) Cement concrete and concrete-polymer composites: Two merging worlds: A report from 11th ICPI Congress in Berlin, 2004. *Cement Concrete Composites*, 27 (9-10): 926-933.

Verdolotti L, Di Maio E, Lavorgna M, Iannace S, Nicolais L. (2008) Polyurethane–cementbased foams: Characterization and potential uses. *Journal Applied Polymer Science*, 107(1): 1-8.

Wang R, Meyer C. (2012) Performance of cement mortar made with recycled high impact polystyrene. *Cement Concrete Composites*, 34 (9):975-981.

Weygand E. (1996) "Properties and applications of recycled polyurethanes," in *Recycling and Recovery of Plastics*, J. Brandrup, M. Bittner, M. Menges, and W. Michaeli, Eds., Hanser, Munich, 683.

Whinfield and Dickson. (1949) Improvements Relating to the Manufacture of Highly Polymeric Substances, British Patent 578,079, 1941; Polymeric Linear Terephthalic Esters, U.S. Patent 2,465,319.

Wu JW, Sung WF, Chu HS. (1999) Thermal conductivity of polyurethane foams. *International Journal Heat Mass Transfer*, 42:2211-2217.

Yanga W, Dongb Q, Liu S, Xie H, Liu L, Li J. (2012) Recycling and disposal methods for polyurethane foam wastes. *Procedia Environmental Sciences* 16:167-175.

Yildirim Y. (2007) Polymer modified asphalt binders. *Construction and Building Materials*, 21:66-72.

Zhu P, Cao ZB, Chen Y, Zhang XJ, GR Qian, Chu YL, Zhou M. (2014) Glycolysis recycling of rigid waste polyurethane foam from refrigerators, *Environmental Technology*, 35:21, 2676-2684.



**Anexo 2**

---

**Producción científica**





## PRODUCCIÓN CIENTÍFICA RELACIONADA CON ESTA TESIS DOCTORAL

### Artículos internacionales

Título: **The effects of seeding C<sub>3</sub>S pastes with afwillite.**

Revista: Cement and Concrete Research. Volume 89, Novembre 2016,  
Pages 145-157.

Autores: Matthieu Hognies, Lingjie Fei, Raquel Arroyo, Jeffrey J. Chen,  
Ellis M. Gartnera.

Título: **Lightweight structural mortars made with polyurethane waste and non-ionic surfactant.**

Revista: Cement and Concrete Composites.

Autores: Raquel Arroyo, Matthieu Hognies, Carlos Junco, Verónica Calderón.

Estado: En revisión (Enviado en Febrero de 2016).

### Patentes de invención

Denominación: **Mortero estructural aligerado y de baja porosidad fabricado con residuos de poliuretano.**

Inventores: Verónica Calderón Carpintero, Carlos Junco Petrement, Ángel Rodríguez Saiz, Sara Gutiérrez González, Jesús Gadea Sainz, Raquel Arroyo Sanz.

Número de solicitud: **PCT/ES2016/070582** Fecha de solicitud: **29/07/2016**

Denominación: **Mortero de cal para construcción y rehabilitación fabricado con residuos siderúrgicos.**

Inventores: Verónica Calderón Carpintero, Juan García Cuadrado, Raúl Zarzosa Tartílan, Ángel Rodríguez Saiz, Sara Gutiérrez González, Raquel Arroyo Sanz.

Número de solicitud: **P 2014 00 382** Fecha de solicitud: **13/05/2014**

Número de patente: **ES 2 551 248-B2** Fecha de concesión: **17/04/2016**

Denominación: **Procedimiento de obtención de morteros de cal con residuo de poliamida en polvo.**

Inventores: Raquel Arroyo Sanz, Verónica Calderón Carpintero, Sara Gutiérrez González, Ángel Rodríguez Saiz; Carlos Junco Petrement, Jesús Gadea Sainz.

Número de solicitud: **P 2013 00 847** Fecha de solicitud: **16/09/2013**

Número de patente: **ES 253 1463-B2** Fecha de concesión: **11/08/2015**



### **Congresos nacionales e internacionales**

5th International Congress on Polymers in Concrete (Singapore). Oral communication. 2015

XIV Reunión del Grupo Especializado de Polímeros (GEP) de las Reales Sociedades Españolas de Química y Física, Póster, 2016.

Jornadas de Doctorandos de la Universidad de Burgos, comunicación oral. 2014

### **Estancia de investigación predoctoral**

Estancia en el Centre de Reserche LafargeHolcim de Lyon (Francia) durante 8 meses.